Supporting Information

Adducts of Lewis acidic stibanes with phosphane chalcogenides

Jonas Krieft, Hannah Koch, Beate Neumann, Hans-Georg Stammler, Jan-Hendrik Lamm, Andreas Mix and Norbert W. Mitzel*

*Corresponding Author

Chair of Inorganic and Structural Chemistry, Center for Molecular Materials CM_2

Faculty of Chemistry, Bielefeld University

Universitätsstraße 25, 33615 Bielefeld (Germany)

E-mail: mitzel@uni-bielefeld.de

Table of Contents

Experimental Procedures

General Information

All operations with air- and moisture-sensitive substances were performed under conventional Schlenk techniques or in a glove box using argon as inert gas. Volatile compounds were handled in a vacuum line. All solvents (*n*-hexane, *n*-pentane, benzene-d_6 dried over Na/K alloy; dichloromethane over calcium hydride; cyclopentane, dichloromethane-d_2 and toluene-d_8 dried over molecular sieves, diethyl ether over $LiAlH_4$) were distilled and degassed prior use.

Chemicals were purchased from commercial sources and were used without further purification if not noted otherwise [antimony trichloride (≥99 %), 2-bromomesitylene (99 %), *n*-butyllithium (1.6 m in hexanes), hydrogen chloride (99.8 %), magnesium (99 %), 1-bromo-3,5-bis(trifluoromethyl)benzene (98 %), tri-*n*-butyltin hydride (97 %)]. Trimesitylstibane,[1] di-chloromesitylstibane,[1] and di-*tert*-butylphosphane oxide[2] were prepared according to literature. Di-*tert*-butylphosphane sulphide was synthesised analogously to di-*tert*-butylphosphane oxide,[2] starting from di-*tert*-butylchlorophosphane and hydrogen sulphide. The synthesis of $(F_5C_2)_2SbCl$ presented here is slightly modified due to the use of an alternative reactant to that described in the literature.[3] For the syntheses of **6** and **7** we used the $(F_5C_2)_2SbCl$: toluene (1:1) mixture as described in the literature.[3]

NMR spectra were recorded on a Bruker Avance III 500, Bruker Avance III 500 HD or Bruker Avance NEO 600 spectrometer at ambient temperature, if not noted otherwise. NMR spectroscopic chemical shifts were referenced to the residual proton or carbon peaks of the solvent (CD_2Cl_2: ^{1}H: 5.32 ppm, ^{13}C: 54.0 ppm; C_6D_6: ^{1}H: 7.16 ppm, ^{13}C: 128.1 ppm; $C_6D_5(CD_3)$: ^{1}H: 2.09 ppm (CD_3), ^{13}C: 20.4 ppm (CD_3)) or externally (^{19}F: $CFCl_3$, ^{31}P: 85% H_3PO_4 in H_2O). Elemental analyses were carried out by a co-worker of the University of Bielefeld using a HEKATECH EURO Element Analyser. IR spectroscopic measurements were performed on a Bruker-Alpha-FT-IR spectrometer; the gaseous probes were measured in a gas chamber with KBr windows. SC-XRD was performed on a Rigaku Supernova diffractometer using Mo-Kα radiation.

Syntheses

Mes_3Sb:

Trimesitylstibane was synthesised according to literature[1] (yield: 17.9 g, 37.3 mmol, 75 %).

Analytical data:

^{1}H NMR (500 MHz, C_6D_6): δ [ppm] = 6.74 (s, 2H, *m*-C**H**), 2.41 (s, 6H, *o*-C**H**$_3$), 2.10 (s, 3H, *p*-C**H**$_3$).

^{13}C{^{1}H} NMR (126 MHz, C_6D_6): δ [ppm] = 145.0 (s, *i*-**C**), 138.0 (s, *p*-**C**), 137.1 (s, *o*-**C**), 129.5 (s, *m*-**C**H), 25.6 (m, *o*-**C**H$_3$), 20.9 (s, *p*-**C**H$_3$).

Elemental analysis calcd (%) for $C_{27}H_{33}Sb$ (M_r = 479.32): C 67.66, H 6.94; found: C 67.63, H 7.04.

$MesSbCl_2$ (1):

Dichloromesitylstibane was synthesised according to literature[1] (yield: 22.7 g, 72.8 mmol, 81 %).

Analytical data:

^{1}H NMR (500 MHz, C_6D_6): δ [ppm] = 6.74 (s, 2H, *m*-C**H**), 2.41 (s, 6H, *o*-C$\mathbf{H}_3$), 2.10 (s, 3H, *p*-C$\mathbf{H}_3$).

^{13}C{^{1}H} NMR (126 MHz, C_6D_6): δ [ppm] = 147.9 (s, *i*-**C**), 144.9 (s, *o*-**C**), 141.9 (s, *p*-**C**), 130.7 (s, *m*-**C**H), 22.6 (m, *o*-**C**H_3), 21.1 (s, *p*-**C**H_3).

Elemental analysis calcd (%) for $C_9H_{11}Cl_2Sb$ (M_r = 311.85): C 34.66, H 3.56; found: C 34.66, H 3.68.

$(F_5C_2)_2Sb(Mes)$ (2):

CAUTION: Caution and sufficient safety measures against explosions are advised when handling ethereal solutions of pentafluoroethyllithium. They may decompose violently when warmed to temperatures higher than −40 °C.

A solution of *n*-butyllithium (96.0 mmol, 60.0 mL, 1.6 m in hexanes) in diethyl ether (300 mL) was degassed at −78 °C. At the same temperature pentafluoroethane (110 mmol) was condensed into the reaction flask and stirred for 2.5 h. Dichloromesitylstibane (13.1 g, 42.0 mmol) in diethyl ether (75 mL) was added dropwise. The mixture was allowed to reach room temperature overnight. The solvent was removed under reduced pressure. The resulting residue was suspended in *n*-pentane (50 mL) and filtrated inertly. The solvent was removed under reduced pressure. Distillation of the colourless liquid at 100 °C under vacuum (10^{-3} mbar) yielded bis(pentafluoroethyl)mesitylstibane (17.6 g, 36.7 mmol, 87 %). A single-crystal suitable for X-ray diffraction experiments was grown in-situ on the diffractometer.

Analytical data:

^{1}H NMR (500 MHz, CD_2Cl_2): δ [ppm] = 7.06 (s, 2H, *m*-C**H**), 2.58 (s, 6H, *o*-C$\mathbf{H}_3$), 2.31 (s, 3H, *p*-C$\mathbf{H}_3$).

^{13}C{^{19}F} NMR (126 MHz, CD_2Cl_2): δ [ppm] = 146.5 (q, $^2J_{C,H}$ = 6 Hz, *o*-C), 142.9 (q, $^2J_{C,H}$ = 6 Hz, *p*-C), 132.0 (m, *i*-C), 130.5 (ddm, $^1J_{C,H}$ = 153 Hz, $^4J_{C,H}$ = 11 Hz, $^4J_{C,H}$ = 5 Hz, *m*-**C**H), 121.8 (m, **C**F_2), 120.4 (m, **C**F_3), 26.3 (m, *o*-**C**H_3), 21.4 (qt, $^1J_{C,H}$ = 127 Hz, $^3J_{C,H}$ = 5 Hz, *p*-**C**H_3).

^{19}F NMR (471 MHz, CD_2Cl_2): δ [ppm] = −83.2 (m, C$\mathbf{F}_3$), −106.4/−107.2 (m, AB-spin system, C$\mathbf{F}_2$, broad).

Elemental analysis calcd (%) for $C_{13}H_{11}F_{10}Sb$ (M_r = 478.98): C 32.60, H 2.31; found: C 32.77, H 2.43.

$(F_5C_2)_2SbCl$ (3):

Gaseous hydrogen chloride (70 mmol) was condensed onto degassed (3 × freeze-pump-thaw cycles) bis(pentafluoroethyl)-mesitylstibane (16.8 g, 35.1 mmol). After the reaction mixture was stirred at 120 °C for 3 d, the excess of HCl was removed. Fractionated distillation with a Vigreux column yielded chlorobis(pentafluoroethyl)stibane (8.63 g, 21.8 mmol, 62 %). A single-crystal suitable for X-ray diffraction experiments was grown in-situ on the diffractometer. Due to its volatility no elemental analysis was carried out.

Analytical data:

$^{13}C\{^1H\}$ NMR (126 MHz, CD_2Cl_2): δ [ppm] = 126.4 (tq, $^1J_{F,C}$ = 317 Hz, $^2J_{F,C}$ = 46/45 Hz, **C**F_2), 120.3 (m, **C**F_3).

$^{13}C\{^{19}F\}$ NMR (126 MHz, CD_2Cl_2): δ [ppm] = 126.4 (s, **C**F_2), 120.4 (s, **C**F_3).

^{19}F NMR (471 MHz, CD_2Cl_2): δ [ppm] = −81.3 (s, C**F**$_3$), −111.8/−112.3 (m, AB-spin system C**F**$_2$, broad).

IR (gaseous): $\tilde{\nu}$ [cm^{-1}] = 1320 (s), 1216 (s), 1153 (s), 1095 (s), 919 (s), 739 (s), 604 (m).

$(Fxyl)_2Sb(Mes)$ (4):

To a suspension of magnesium (0.80 g, 33 mmol) in THF (40 mL) a solution of 1-bromo-3,5-bis(trifluoromethyl)benzene (9.6 g, 33 mmol) in THF (20 mL) was added dropwise at room temperature. After stirring at ambient temperature for 1.5 h, a solution of dichloromesitylstibane (4.2 g, 13 mmol) in THF (20 mL) was added slowly. The colourless suspension was stirred overnight. The solvent was removed under reduced pressure. The resulting residue was suspended in *n*-pentane (50 mL) and filtered inertly. The solvent was removed under reduced pressure and the residue was dried in vacuum. After sublimation in vacuum (100 °C), 3,5-bis[bis(trifluoromethyl)phenyl]mesitylstibane (7.7 g, 12 mmol, 92 %) was obtained as pale yellow, crystalline solid. This yielded crystals suitable for X-ray diffraction experiments.

Analytical data:

^1H NMR (500 MHz, C_6D_6): δ [ppm] = 7.81 (s, 4H, *o*-**H**$_{Fxyl}$), 7.66 (s, 2H, *p*-**H**$_{Fxyl}$), 6.65 (s, 2H, *m*-**H**$_{Mes}$), 1.97 (s, 9H, *o*-C**H**$_3$ and *p*-C**H**$_3$).

$^{13}C\{^1H\}$ NMR (126 MHz, C_6D_6): δ [ppm] = 145.3 (s, *o*-**C**$_{Mes}$), 141.0 (s, *i*-**C**$_{Fxyl}$), 140.9 (s, *i*-**C**$_{Mes}$), 135.3 (d, $^3J_{F,C}$ = 4 Hz, *o*-**C**$_{Fxyl}$), 132.1 (q, ($^2J_{F,C}$ = 33 Hz, *m*-**C**$_{Fxyl}$), 130.2 (s, *m*-**C**$_{Mes}$), 123.8 (d, $^1J_{F,C}$ = 273Hz, **C**F_3), 122.8 (sept, $^3J_{F,C}$ = 4 Hz, *p*-**C**$_{Fxyl}$), 26.4 (m, *o*-**C**$_{Mes}$), 20.9 (m, *p*-**C**$_{Mes}$).

^{19}F NMR (471 MHz, C_6D_6): δ [ppm] = −63.0 (s).

Elemental analysis calcd (%) for $C_{25}H_{17}F_{12}Sb$ (M_r = 667.15): C 45.01, H 2.57; found: C 44.72, H 2.62.

$(Fxyl)_2SbCl$ (5):

Gaseous hydrogen chloride (29 mmol) was condensed onto a degassed (3 × freeze-pump-thaw cycles) solution of 3,5-bis[bis-(trifluoromethyl)phenyl]mesitylstibane (7.7 g, 12 mmol) in dichloromethane (50 mL). After the reaction mixture was stirred at 120 °C for 3 h. All volatile components were removed in vacuum. After distillation in vacuum (150 °C), chlorobis(3,5-bis(tri-fluoromethyl)phenyl)stibane (6.3 g, 11 mmol, 90 %) was obtained as colourless undercooled melt.

Analytical data:

^{1}H NMR (500 MHz, C_6D_6): δ [ppm] = 7.66 (m, 4H, *o*-$\mathbf{H}_{Fxyl}$), 7.59 (s, 2H, *p*-$\mathbf{H}_{Fxyl}$).

^{13}C{^{1}H} NMR (126 MHz, C_6D_6): δ [ppm] = 147.3 (s, *i*-$\mathbf{C}_{Fxyl}$), 134.0 (d, $^3J_{F,C}$ = 4 Hz, *o*-$\mathbf{C}_{Fxyl}$), 132.3 (q, $^2J_{F,C}$ = 33 Hz, *m*-$\mathbf{C}_{Fxyl}$), 124.1 (sept, $^3J_{F,C}$ = 3 Hz, *p*-$\mathbf{C}_{Fxyl}$), 123.6 (d, $^1J_{F,C}$ = 273 Hz, $\mathbf{C}F_3$).

^{19}F NMR (471 MHz, C_6D_6): δ [ppm] = −62.8 (s).

Elemental analysis calcd (%) for $C_{16}H_6ClF_{12}Sb$ (M_r = 583.41): C 32.94, H 1.04; found: C 33.33, H 1.07.

$(F_5C_2)_2(Cl)Sb(O)P(H)(t\mathrm{Bu})_2$ (6):

To a solution of di-*tert*-butylphosphane oxide (325 mg, 2.00 mmol) in *n*-hexane (30 mL), a solution of chlorobis(pentafluoro-ethyl)stibane: toluene (1:1, 1.14 g, 2.33 mmol) in *n*-hexane (15 mL) was added. The mixture was stirred for 30 min at room temperature. The volatile compounds were removed under reduced pressure. After sublimation in vacuum (80 °C) **6** (1.01 g, 1.81 mmol, 90 %) was obtained as colourless solid. After recrystallisation from *n*-hexane single crystals of **6**, suitable for X-ray diffraction, were obtained.

Analytical data:

^{1}H NMR (600 MHz, CD_2Cl_2): δ [ppm] = 6.03 (d, $^1J_{P,H}$ = 447 Hz, 1H, P**H**), 1.27 (d, $^3J_{P,H}$ = 16 Hz, 18H, C($C\mathbf{H}_3$)$_3$).

^{13}C{^{1}H} NMR (151 MHz, CD_2Cl_2): δ [ppm] = 126.6 (tq, $^1J_{F,C}$ = 317 Hz, $^2J_{F,C}$ = 42 Hz, $\mathbf{C}F_2$), 121.1 (qt, $^1J_{F,C}$ = 285 Hz, $^2J_{F,C}$ = 30 Hz, $\mathbf{C}F_3$), 34.7 (d, $^1J_{P,C}$ = 57 Hz, $\mathbf{C}(CH_3)_3$), 25.9 (m, C($\mathbf{C}H_3$)$_3$).

^{19}F NMR (565 MHz, CD_2Cl_2): δ [ppm] = −81.1 (s, $C\mathbf{F}_3$), −112.2 (s, $C\mathbf{F}_2$).

^{31}P{^{1}H} NMR (243 MHz, CD_2Cl_2): δ [ppm] = 71.6 (s).

Elemental analysis calcd (%) for $C_{12}H_{19}ClF_{10}OPSb$ (M_r = 557.45): C 25.86, H 3.44; found: C 25.86, H 3.46.

$(F_5C_2)_2(Cl)Sb(S)P(H)(tBu)_2$ (7):

To a solution of di-*tert*-butylphosphane sulphide (183 mg, 1.03 mmol) in *n*-hexane (10 mL), a solution of chlorobis(penta-fluoroethyl)stibane : toluene (1:1, 660 mg, 1.35 mmol) in *n*-hexane (3 mL) was added. The mixture was stirred for 1.5 h at room temperature. The volatile compounds were removed under reduced pressure. After sublimation in vacuum (80 °C) **7** (466 mg, 813 µmol, 81 %) was obtained as colourless solid. After recrystallisation from *n*-hexane single crystals of **7**, suitable for X-ray diffraction, were obtained.

Analytical data:

^{1}H NMR (600 MHz, CD_2Cl_2): δ [ppm] = 5.77 (d, $^1J_{P,H}$ = 420 Hz, 1H, P**H**), 1.34 (d, $^3J_{P,H}$ = 17 Hz, 18H, C(C**H**$_3$)$_3$).

^{13}C{^{1}H} NMR (151 MHz, CD_2Cl_2): δ [ppm] = 126.0 (tq, $^1J_{F,C}$ = 319 Hz, $^2J_{F,C}$ = 44 Hz, **C**F$_2$), 120.7 (qt, $^1J_{F,C}$ = 286 Hz, $^2J_{F,C}$ = 29 Hz, **C**F$_3$), 36.8 (d, $^1J_{P,C}$ = 40 Hz, **C**(CH$_3$)$_3$), 27.7 (m, $^2J_{P,C}$ = 2 Hz, C(**C**H$_3$)$_3$).

^{19}F NMR (565 MHz, CD_2Cl_2): δ [ppm] = −80.7 (s, C**F**$_3$), −109.6 (s, C**F**$_2$).

^{31}P{^{1}H} NMR (243 MHz, CD_2Cl_2): δ [ppm] = 72.3 (s).

Elemental analysis calcd (%) for $C_{12}H_{19}ClF_{10}PSSb$ (M_r = 573.51): C 25.13, H 3.34, S 5.59; found: C 25.52, H 3.44, S 5.61.

$(Fxyl)_2(Cl)Sb(O)P(H)(tBu)_2$ (8):

To a solution of di-*tert*-butylphosphane oxide (32 mg, 0.20 mmol) in *n*-pentane (3 mL), a solution of chlorobis(3,5-bis(tri-fluoromethyl)phenyl)stibane (0.12 g, 0.21 mmol) in *n*-pentane (2 mL) was added. The mixture was stirred for 30 min at room temperature. The solvent was removed under reduced pressure. After sublimation in vacuum (100 °C) **8** (97 mg, 0.13 mmol, 66 %) was obtained as colourless solid. After recrystallisation from cyclopentane, single crystals of **8**, suitable for X-ray diffraction, were obtained.

Analytical data:

^{1}H NMR (600 MHz, CD_2Cl_2): δ [ppm] = 8.35 (m, 4H, *o*-H), 7.88 (m, 2H, *p*-H), 5.85 (d, $^1J_{P,H}$ = 436 Hz, 1H, P**H**), 1.13 (d, $^3J_{P,H}$ = 16 Hz, 18H, C(C**H**$_3$)$_3$).

^{13}C{^{1}H} NMR (151 MHz, CD_2Cl_2): δ [ppm] = 152.1 (s, *i*-**C**$_{Fxyl}$), 135.7 (q, $^3J_{F,C}$ = 4 Hz, *o*-**C**$_{Fxyl}$), 131.6 (q, $^2J_{F,C}$ = 33 Hz, *m*-**C**$_{Fxyl}$), 124.2 (qt, $^1J_{F,C}$ = 273 Hz, **C**F$_3$), 123.4 (m, *p*-**C**$_{Fxyl}$) 34.3 (d, $^1J_{P,C}$ = 58 Hz, **C**(CH$_3$)$_3$), 25.8 (d, $^2J_{P,C}$ = 2 Hz, C(**C**H$_3$)$_3$).

^{19}F NMR (565 MHz, CD_2Cl_2): δ [ppm] = −63.1 (s).

^{31}P{^{1}H} NMR (243 MHz, CD_2Cl_2): δ [ppm] = 70.2 (s).

Elemental analysis calcd (%) for $C_{24}H_{25}ClF_{12}OPSb$ (M_r = 745.63): C 38.66, H 3.38; found: C 38.52, H 3.23.

$(Fxyl)_2(Cl)Sb(S)P(H)(tBu)_2$ (9):

To a solution of di-*tert*-butylphosphane sulphide (36 mg, 0.20 mmol) in *n*-pentane (3 mL), a solution of chlorobis(3,5-bis(trifluoromethyl)phenyl)stibane (0.12 g, 0.21 mmol) in *n*-pentane (2 mL) was added. The mixture was stirred for 30 min at room temperature. The solvent was removed under reduced pressure. After sublimation in vacuum (80 °C) **9** (0.12 g, 0.16 mmol, 78 %) was obtained as colourless solid. After recrystallisation from *n*-hexane single crystals of **9**, suitable for X-ray diffraction, were obtained.

Analytical data:

^{1}H NMR (600 MHz, CD_2Cl_2): δ [ppm] = 8.28 (m, 4H, *o*-H), 7.93 (m, 2H, *p*-H), 5.69 (d, $^1J_{P,H}$ = 420 Hz, 1H, P**H**), 1.27 (d, $^3J_{P,H}$ = 17 Hz, 18H, C(C**H**$_3$)$_3$).

^{13}C{^{1}H} NMR (151 MHz, CD_2Cl_2): δ [ppm] = 149.2 (s, *i*-**C**$_{Fxyl}$), 136.0 (q, $^3J_{F,C}$ = 4 Hz, *o*-**C**$_{Fxyl}$), 132.1 (q, $^2J_{F,C}$ = 33 Hz, *m*-**C**$_{Fxyl}$), 124.1 (sept, $^3J_{F,C}$ = 4 Hz, *p*-**C**$_{Fxy}$), 124.0 (qt, $^1J_{F,C}$ = 273 Hz, **C**F$_3$), 36.6 (d, $^1J_{P,C}$ = 40 Hz, **C**(CH$_3$)$_3$), 27.6 (d, $^2J_{P,C}$ = 2 Hz, C(**C**H$_3$)$_3$).

^{19}F NMR (565 MHz, CD_2Cl_2): δ [ppm] = −63.2 (s).

^{31}P{^{1}H} NMR (243 MHz, CD_2Cl_2): δ [ppm] = 74.2 (s).

Elemental analysis calcd (%) for $C_{24}H_{25}ClF_{12}PSSb$ (M_r = 761.69): C 37.85, H 3.31, S 4.21; found: C 38.68, H 3.30, S 3.94.

$(F_5C_2)SbH$ (10):

Chlorobis(pentafluoroethyl)stibane (3.1 g, 7.8 mmol) was stirred with tri-*n*-butyltin hydride (2.5 g, 8.6 mmol) at −30 °C for 30 min. The volatile bis(pentafluoroethyl)stibane (2.7 g, 7.5 mmol, 96 %) was condensed in a separate tube under reduced pressure. The colourless liquid slowly decomposes by temperatures above −30 °C. A single-crystal suitable for X-ray diffraction experiments was grown *in-situ* on the diffractometer. Due to its high volatility no elemental analysis was carried out.

Analytical data:

^{1}H NMR (600 MHz, CD_2Cl_2): δ [ppm] = 8.11 (m, $^3J_{F,H}$ = 14 Hz/11 Hz, $^4J_{F,H}$ = 3 Hz, Sb**H**).

^{13}C{^{19}F} NMR (151 MHz, CD_2Cl_2): δ [ppm] = 121.0 (m), 119.3 (m).

^{19}F NMR (565 MHz, CD_2Cl_2): δ [ppm] = −82.0 (m, C**F**$_3$), −99.0/−102.1 (m, AB-spin system C**F**$_2$, broad).

IR (gaseous): $\tilde{\nu}$ [cm^{-1}] = 1919 (m), 1320 (s), 1217 (s), 1137 (m), 1090 (m), 923 (s), 739 (s).

Reaction of (F_5C_2)SbH (10) with di-*tert*-butylphosphane oxide:

A solution of bis(pentafluoroethyl)stibane (40 mg, 0.11 mmol) in C_6D_6 was dropped into a solution of di-*tert*-butylphosphane oxide (16 mg, 0.10 mmol) in C_6D_6 in a Young NMR tube. After shaking, the mixture started to turn black. NMR spectra indicate the formation of $(F_5C_2)_2Sb(H)O(H)P(tBu)_2$, which seems to decompose. The progressive formation of black precipitate can be seen macroscopically and the formation of pentafluoroethane via ^{19}F NMR, wherein a second species starts to form. Isolation attempts failed. After drying, the residue was suspended again in C_6D_6, filtered and again NMR spectra of the filtrate were recorded. The data obtained do not allow a precise statement to be made about the type of the product of conversion. The mixture slowly decomposes further.

A second batch with precooled (−30 °C) toluene-d_8 solutions was made. Even with strictly cooling till and while recording NMR spectra at −30 °C, a black precipitate arose. The NMR spectra indicate the formation of the same product of conversion like at room temperature. This batch showed the same workup behaviour as mentioned above.

Diffusion NMR experiments were made, but do not lead to clear results (see below).

Analytical data of the mixture:

^{1}H NMR (600 MHz, C_6D_6): δ [ppm] = 7.96 (m, 1H, Sb**H**), 5.52 (d, $^1J_{P,H}$ = 429 Hz, 1H, P**H**), 0.84 (d, $^3J_{P,H}$ = 15 Hz, 18H, C(C**H**$_3$)$_3$).

^{13}C{^{1}H} NMR (126 MHz, C_6D_6): δ [ppm] = 122.9 (m, **C**F_2), 120.9 (m, **C**F_3), 33.4 (d, $^1J_{P,C}$ = 60 Hz, **C**$(CH_3)_3$), 25.4 (s, C(**C**H_3)$_3$).

^{13}C{^{19}F} NMR (151 MHz, C_6D_6): δ [ppm] = 122.9 (s, **C**F_2), 120.9 (m, **C**F_3).

^{19}F NMR (565 MHz, C_6D_6): δ [ppm] = −83.1 (s, C**F**$_3$), −104.2/−106.0 (m, AB-spin system, C**F**$_2$).

^{31}P{^{1}H} NMR (202 MHz, C_6D_6): δ [ppm] = 63.2 (s).

Reaction of (F_5C_2)SbH (10) with di-*tert*-butylphosphane sulphide:

A solution of bis(pentafluoroethyl)stibane (48 mg, 0.13 mmol) in C_6D_6 was dropped in a solution of di-*tert*-butylphosphane sulphide (21 mg, 0.12 mmol) in C_6D_6 in a Young NMR tube. After shaking, the mixture started to turn black. NMR spectra do not indicate the formation of an adduct. The resonances of the phosphorus precursor undergo no shift due to the mixing of bis(pentafluoroethyl)stibanes and di-*tert*-butylphosphane sulphide. Nevertheless, the mixture became darker with time. After drying, the residue was suspended again in C_6D_6, filtered and again NMR spectra of the filtrate were recorded. The NMR data show only the resonances of the reactant di-*tert*-butylphosphane sulphide.

Analogue to the cooled second batch of bis(pentafluoroethyl)stibane and di-*tert*-butylphosphane oxide, we performed a second batch for this conversion. Again, no reaction was mentioned.

For completeness, the NMR spectra before workup are shown below.

NMR spectroscopic data

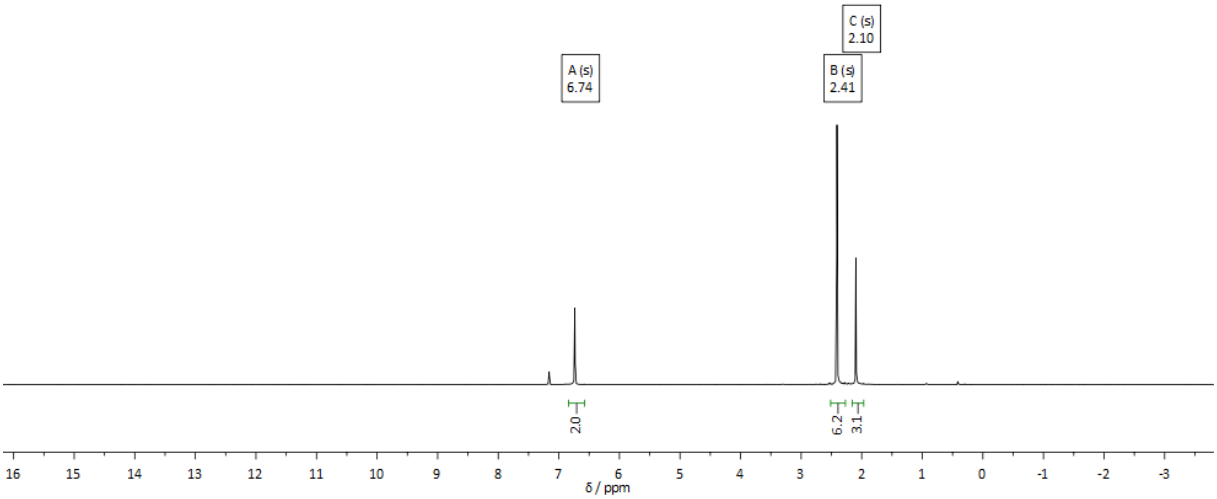

Figure S1 ^{1}H NMR spectrum of Mes_3Sb in C_6D_6.

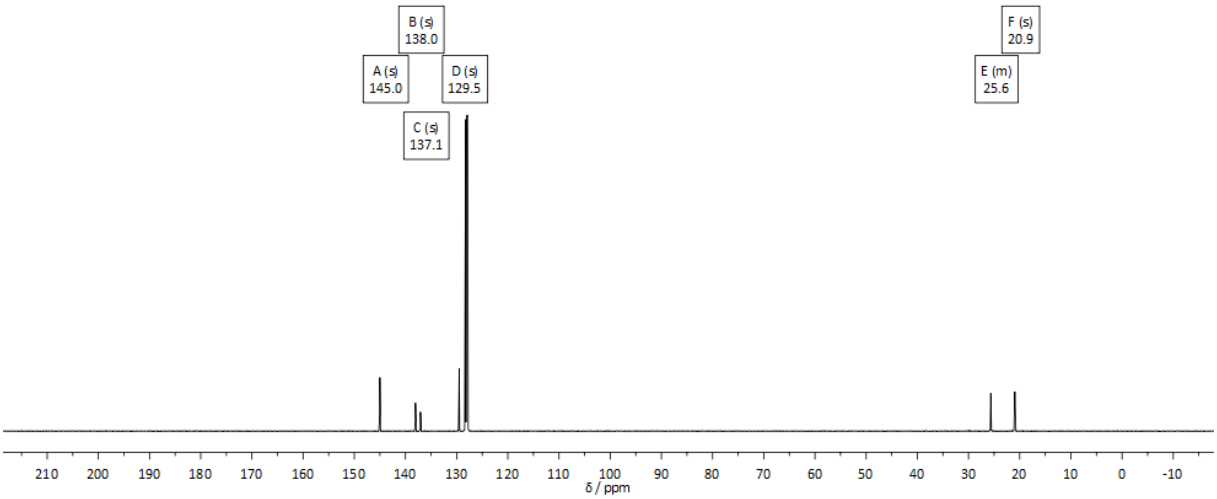

Figure S2 $^{13}C\{^{1}H\}$ NMR spectrum of Mes_3Sb in C_6D_6.

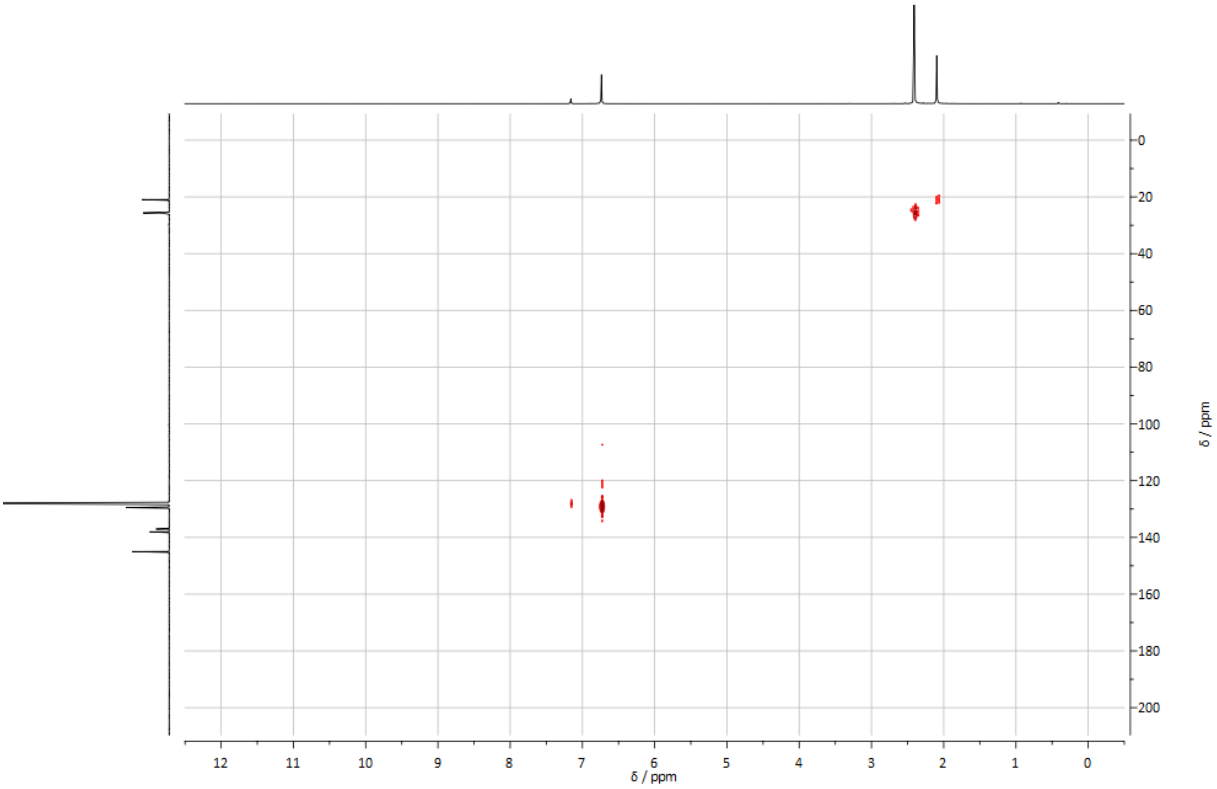

Figure S3 $^{13}C^{1}H$ HMQC NMR spectrum of Mes_3Sb in C_6D_6.

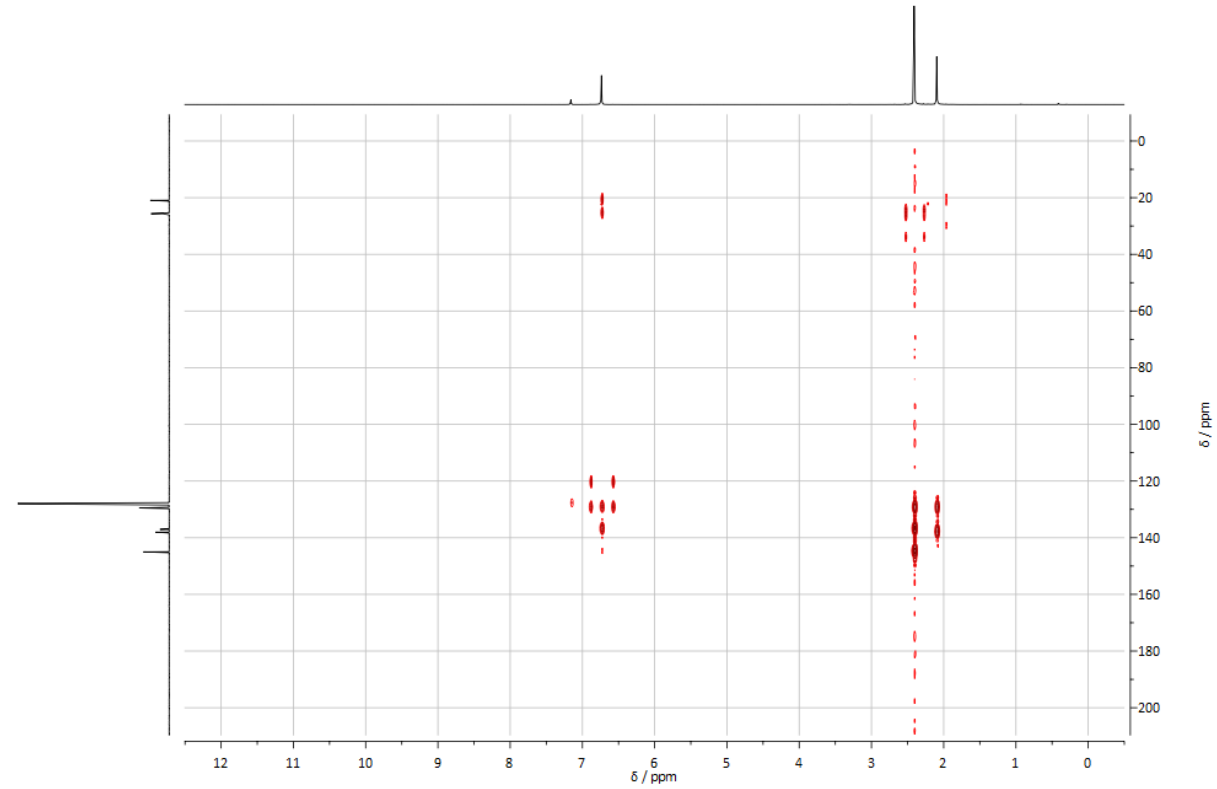

Figure S4 $^{13}C^{1}H$ HMQC NMR spectrum of Mes_3Sb in C_6D_6.

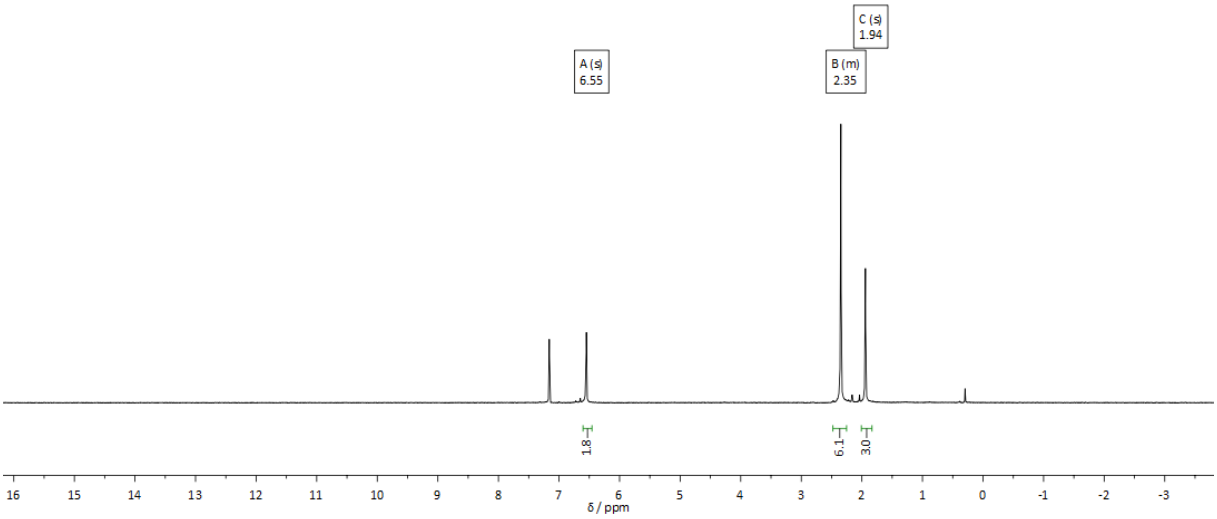

Figure S5 ^{1}H NMR spectrum of **1** in C_6D_6.

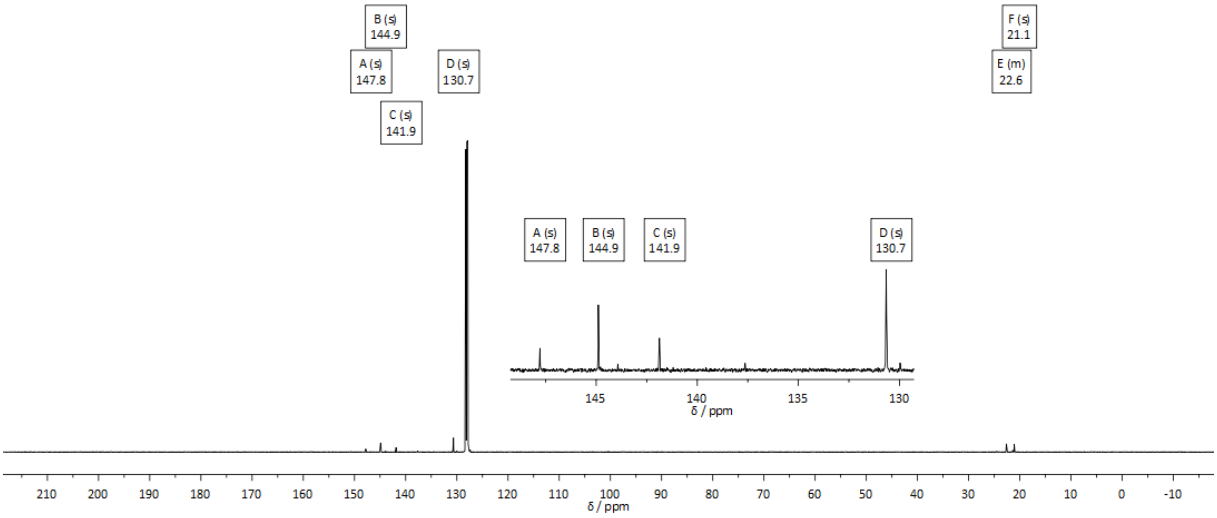

Figure S6 $^{13}C\{^{1}H\}$ NMR spectrum of **1** in C_6D_6.

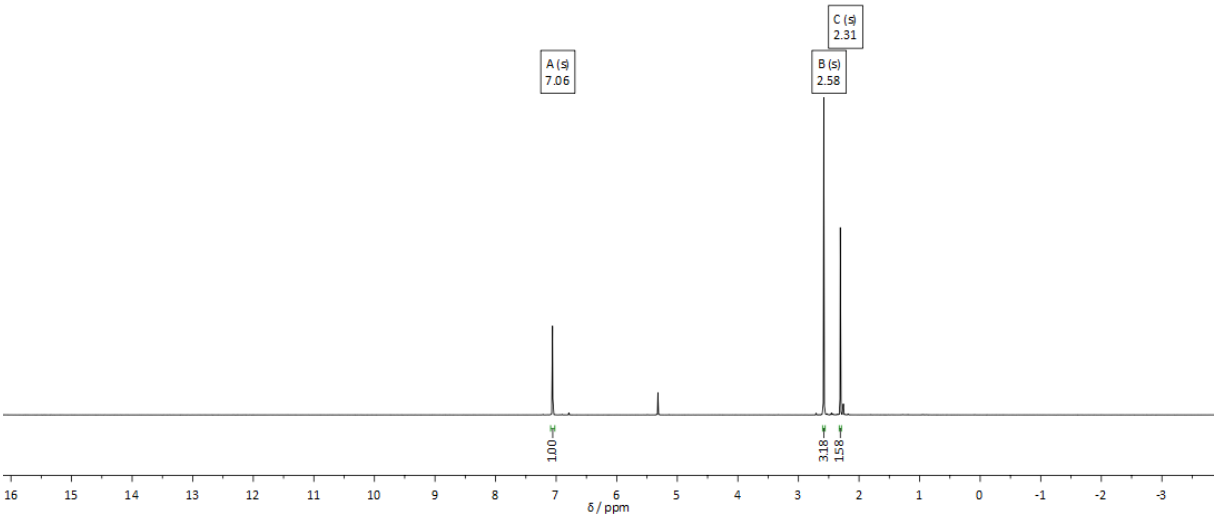

Figure S7 ^{1}H NMR spectrum of **2** in CD_2Cl_2.

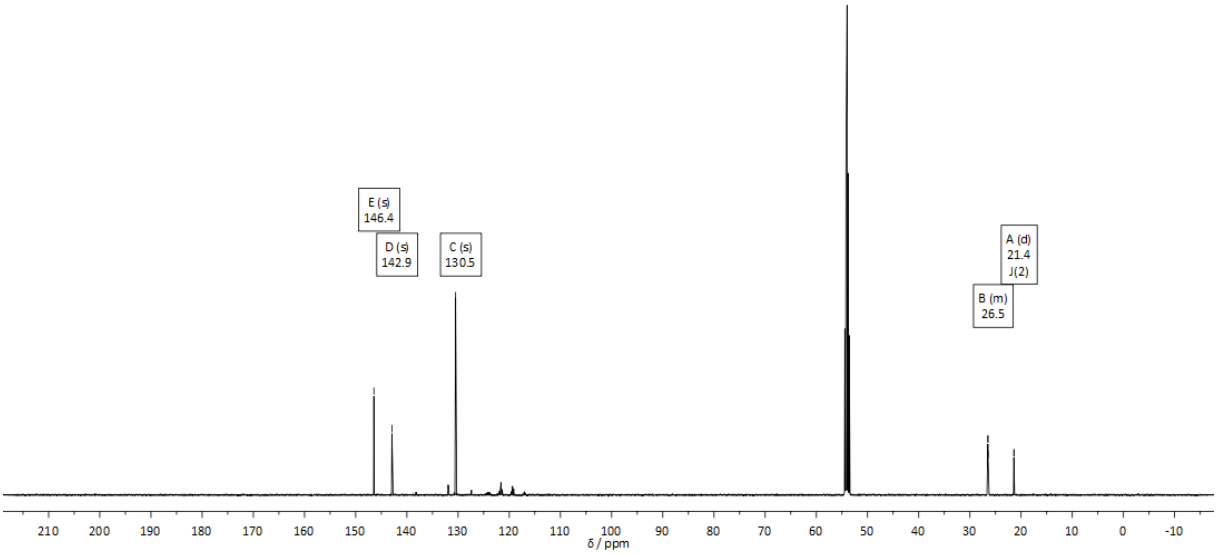

Figure S8 $^{13}C\{^{1}H\}$ NMR spectrum of **2** in CD_2Cl_2.

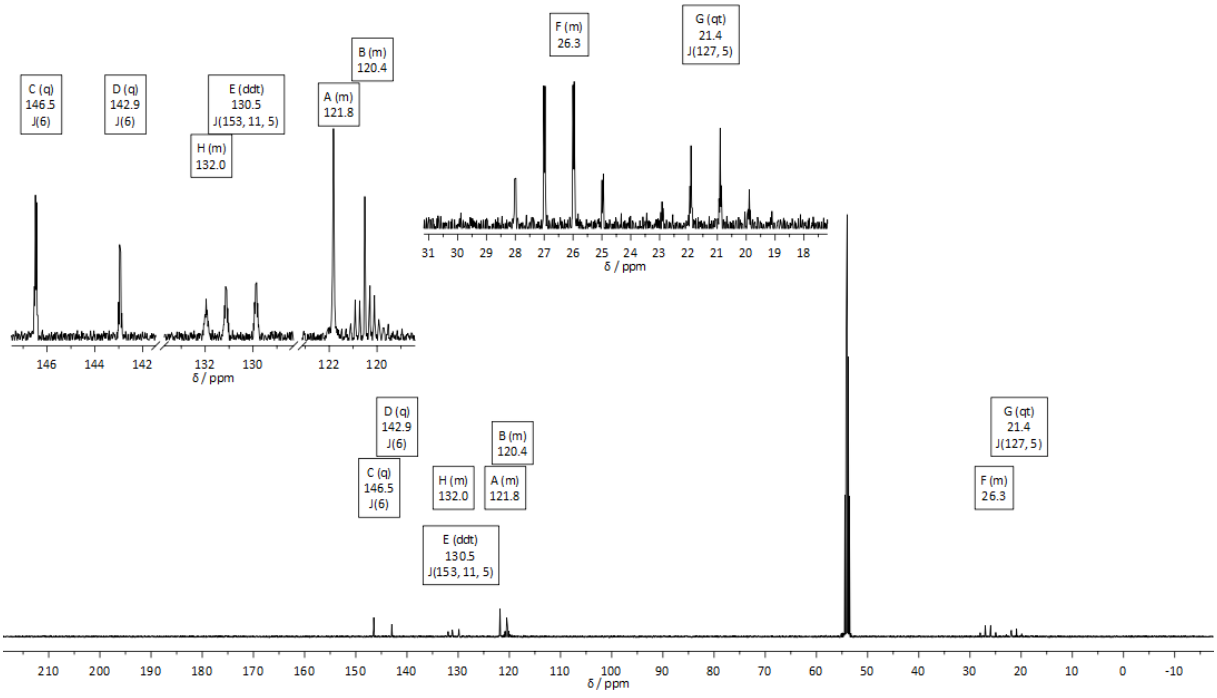

Figure S9 $^{13}C\{^{19}F\}$ NMR spectrum of **2** in CD_2Cl_2.

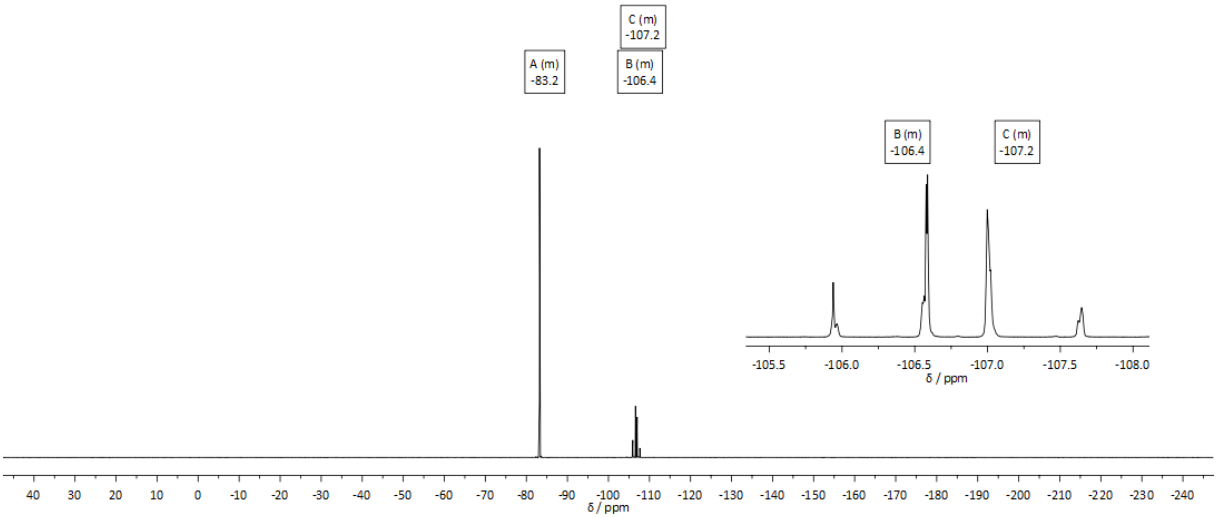

Figure S10 ^{19}F NMR spectrum of **2** in CD_2Cl_2.

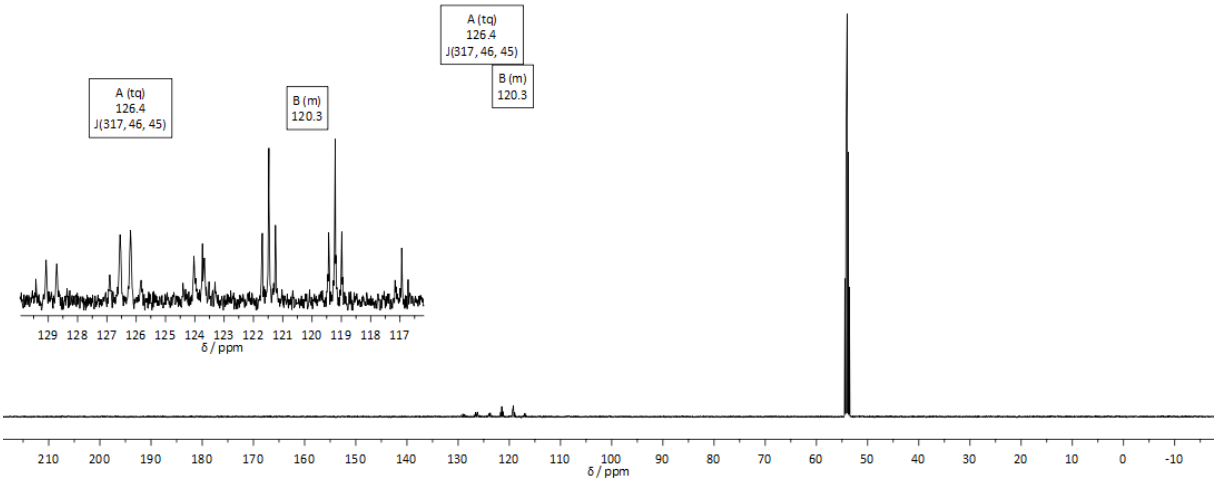

Figure S11 $^{13}C\{^{1}H\}$ NMR spectrum of **3** in CD_2Cl_2.

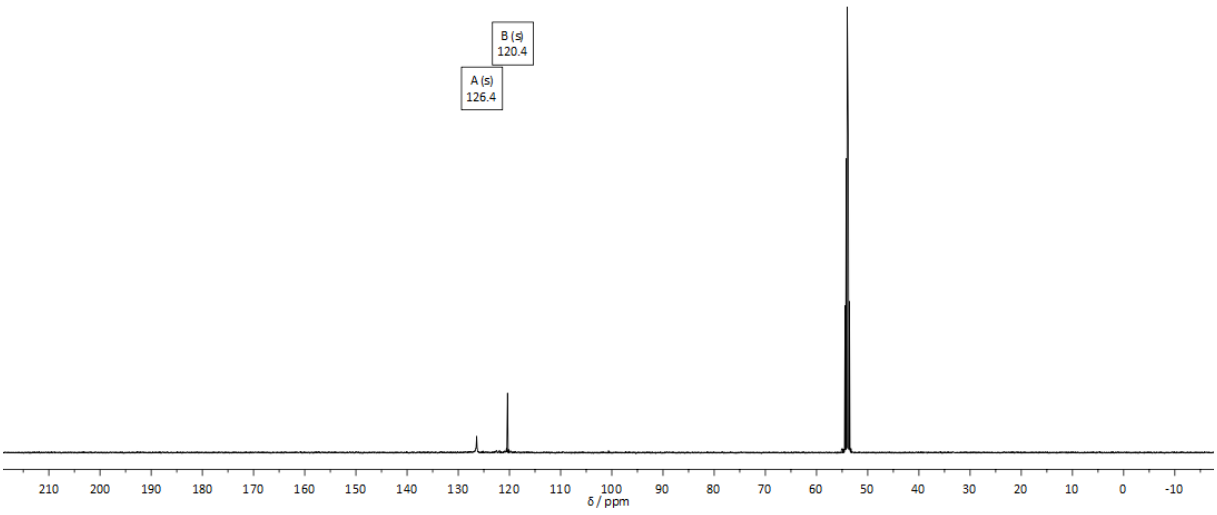

Figure S12 $^{13}C\{^{19}F\}$ NMR spectrum of **3** in CD_2Cl_2.

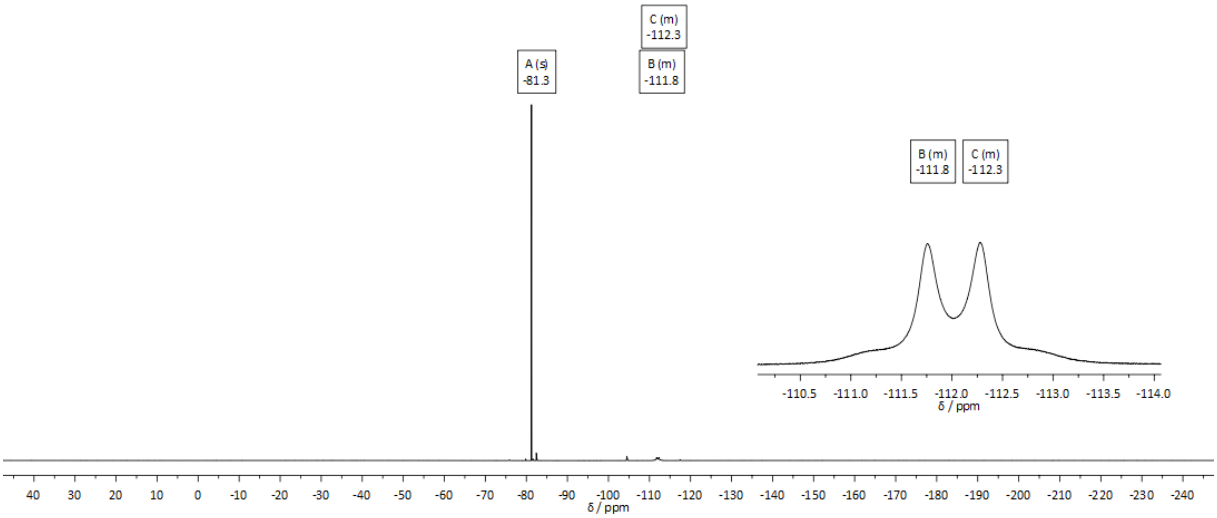

Figure S13 ^{19}F NMR spectrum of **3** in CD_2Cl_2.

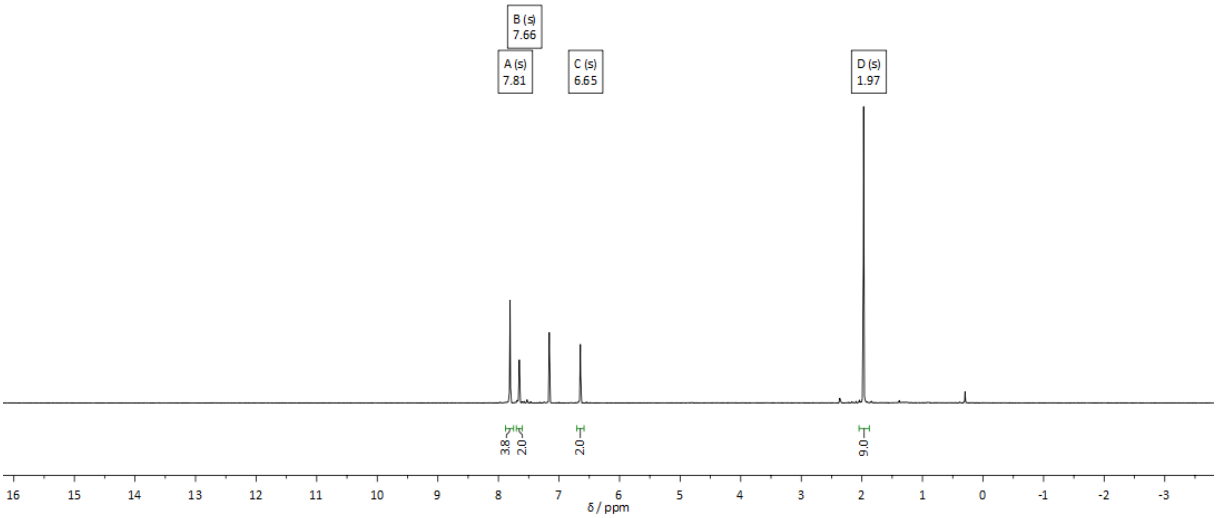

Figure S14 ^{1}H NMR spectrum of **4** in C_6D_6.

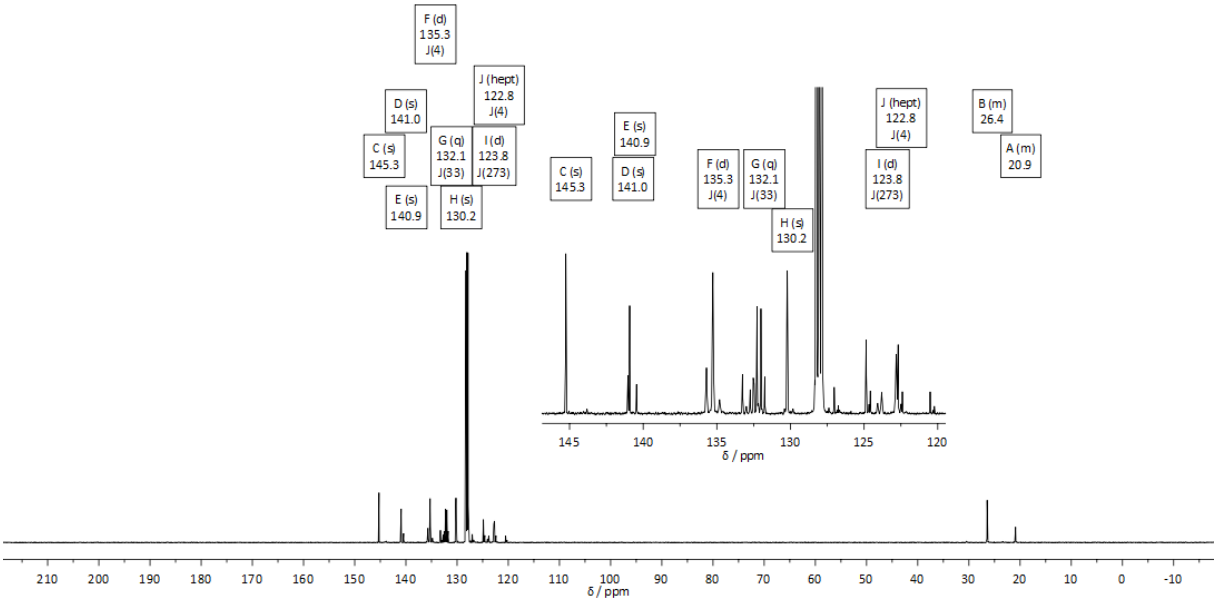

Figure S15 $^{13}C\{^{1}H\}$ NMR spectrum of **4** in C_6D_6.

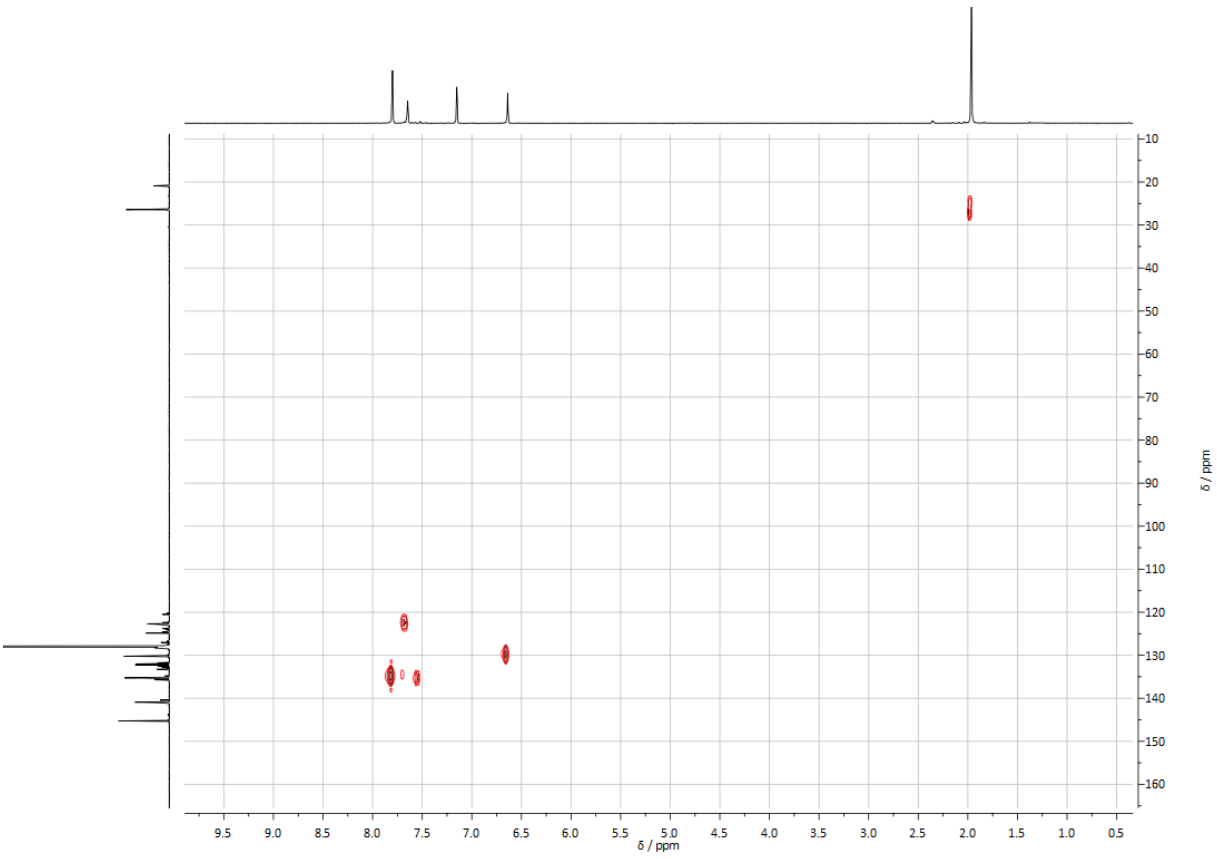

Figure S16 $^{13}C^{1}H$ HMQC NMR spectrum of **4** in C_6D_6.

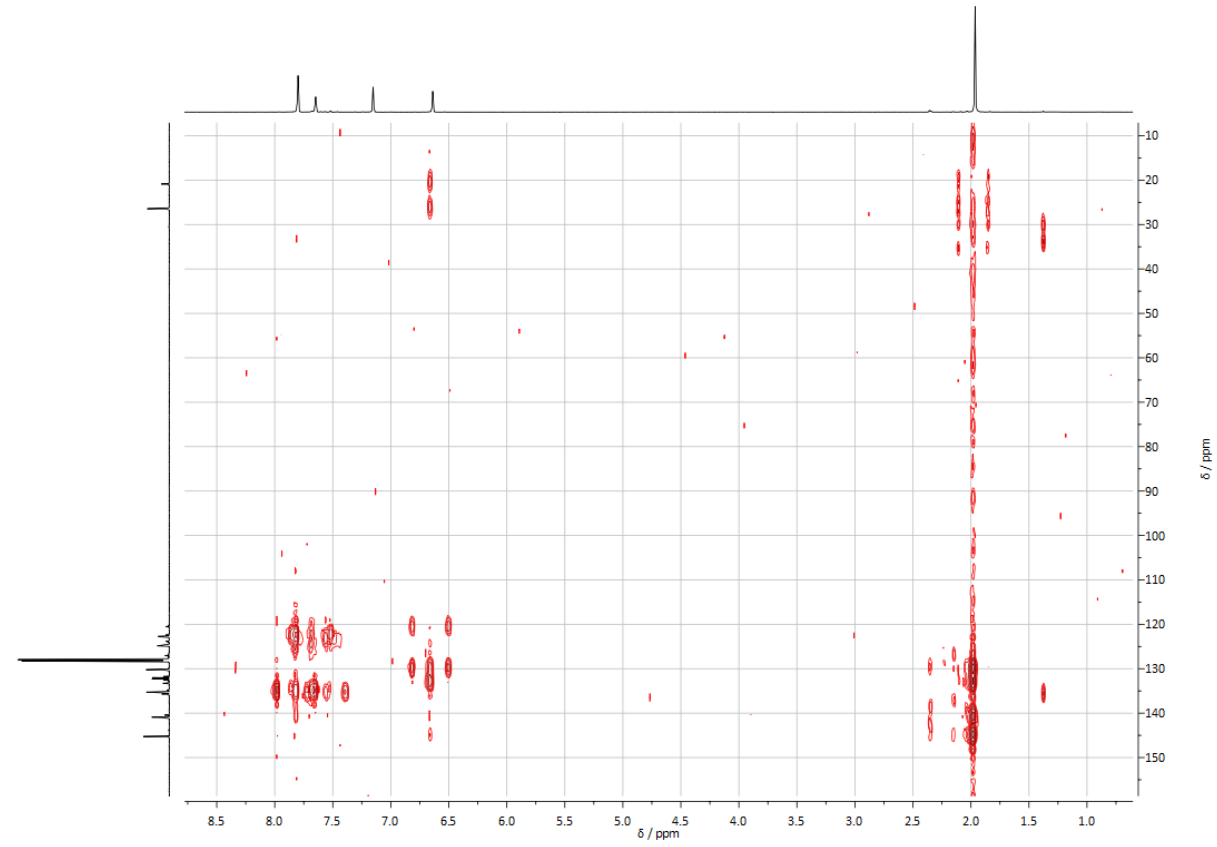

Figure S17 $^{13}C^{1}H$ HMBC NMR spectrum of **4** in C_6D_6.

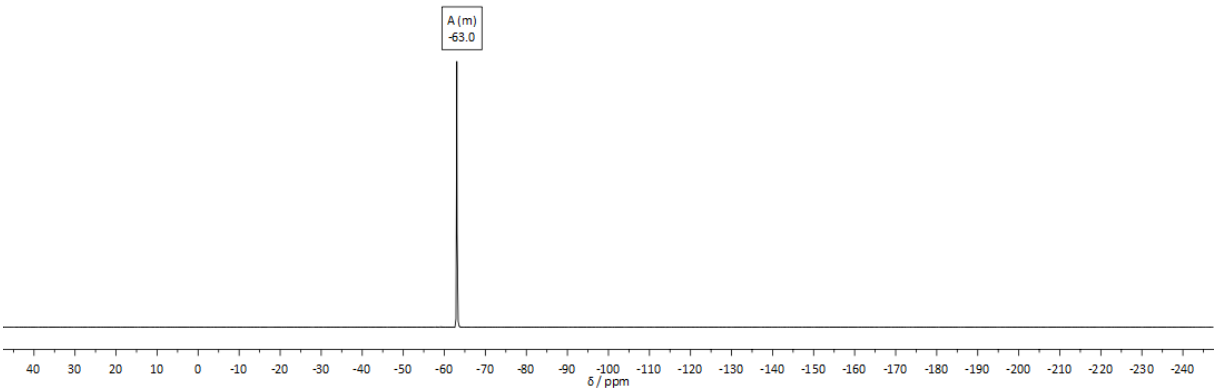

Figure S18 ^{19}F NMR spectrum of **4** in C_6D_6.

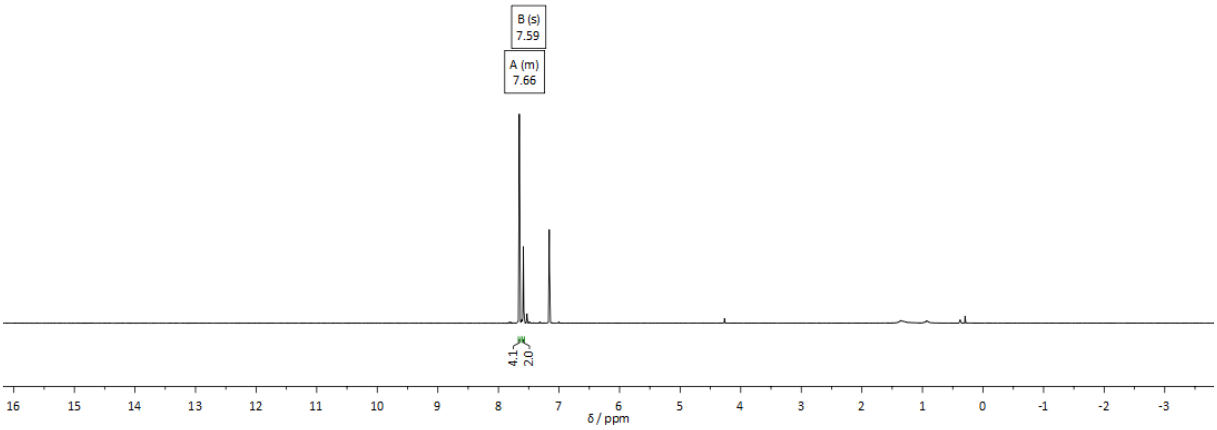

Figure S19 ^{1}H NMR spectrum of **5** in C_6D_6.

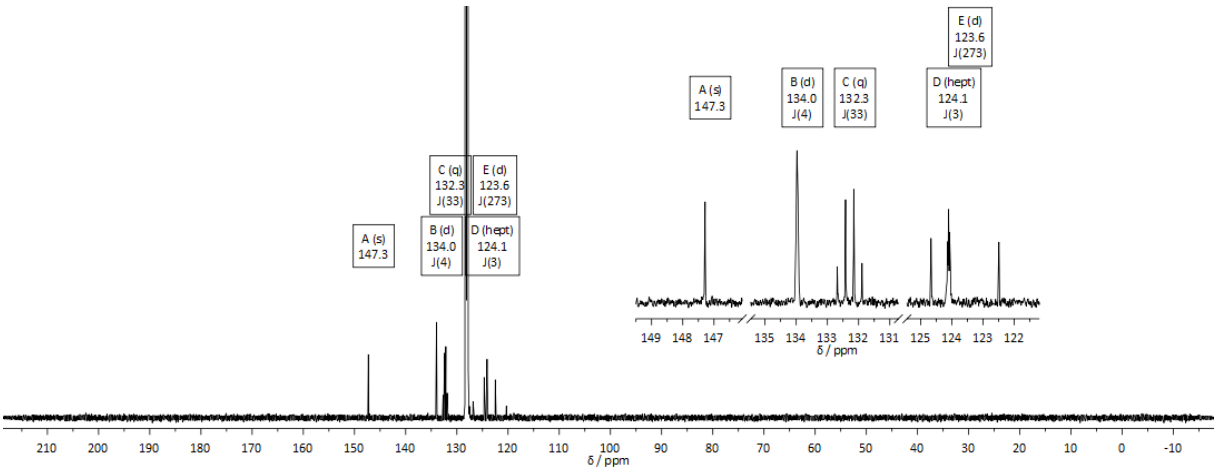

Figure S20 $^{13}C\{^{1}H\}$ NMR spectrum of **5** in CD_2Cl_2.

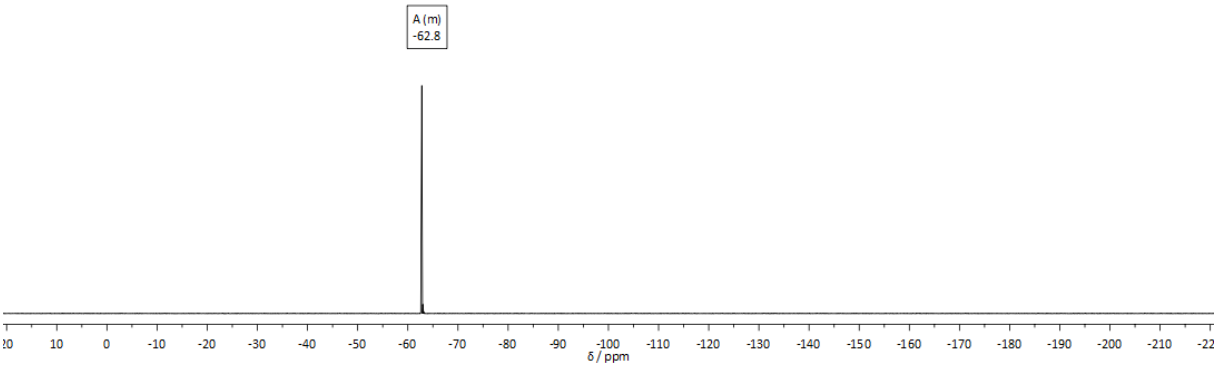

Figure S21 ^{19}F NMR spectrum of **5** in CD_2Cl_2.

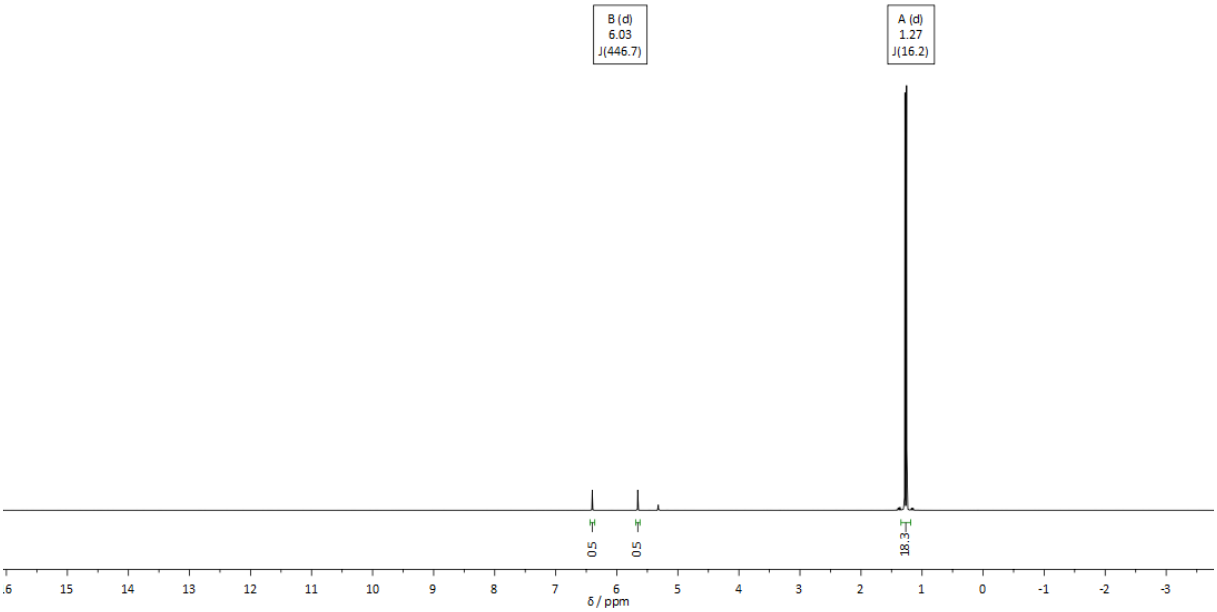

Figure S22 ^{1}H NMR spectrum of **6** in CD_2Cl_2.

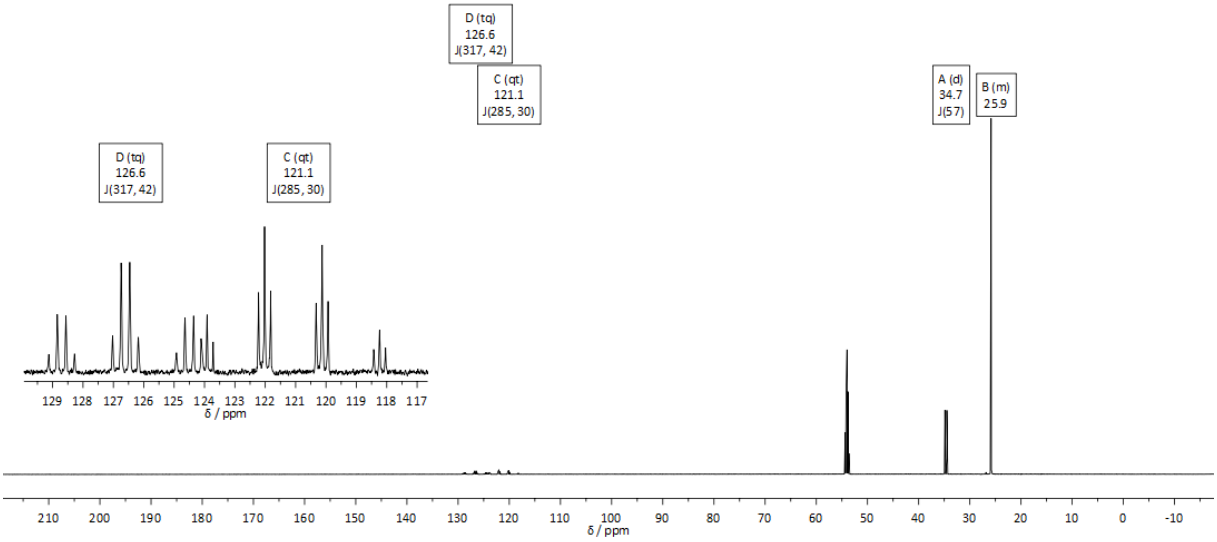

Figure S23 $^{13}C\{^{1}H\}$ NMR spectrum of **6** in CD_2Cl_2.

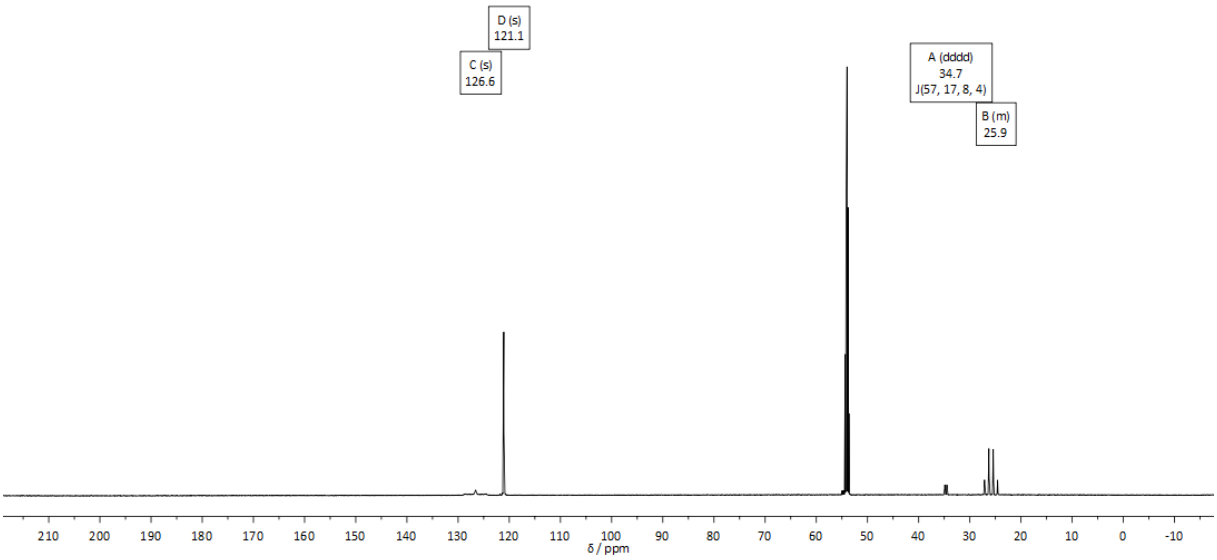

Figure S24 $^{13}C\{^{19}F\}$ NMR spectrum of **6** in CD_2Cl_2.

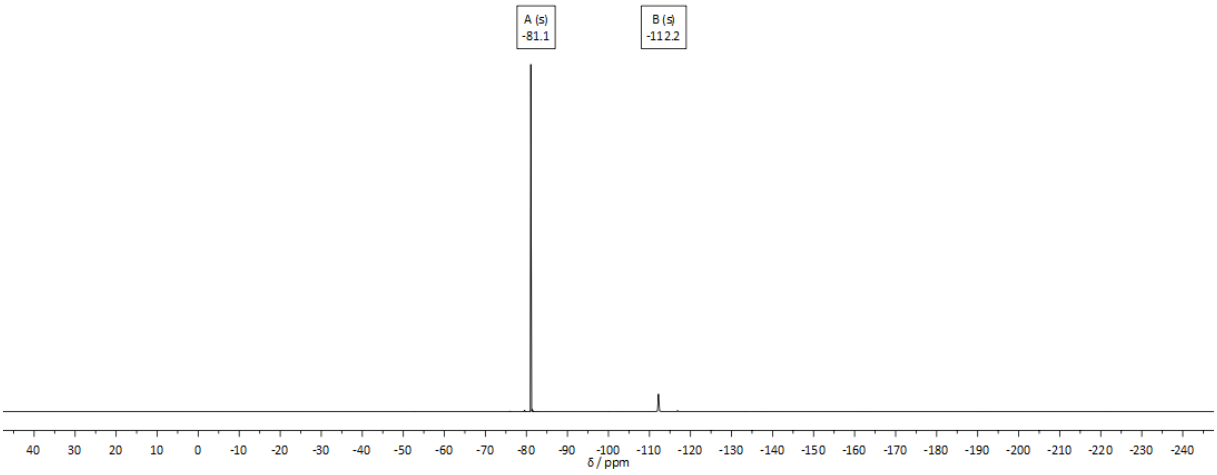

Figure S25 ^{19}F NMR spectrum of **6** in CD_2Cl_2.

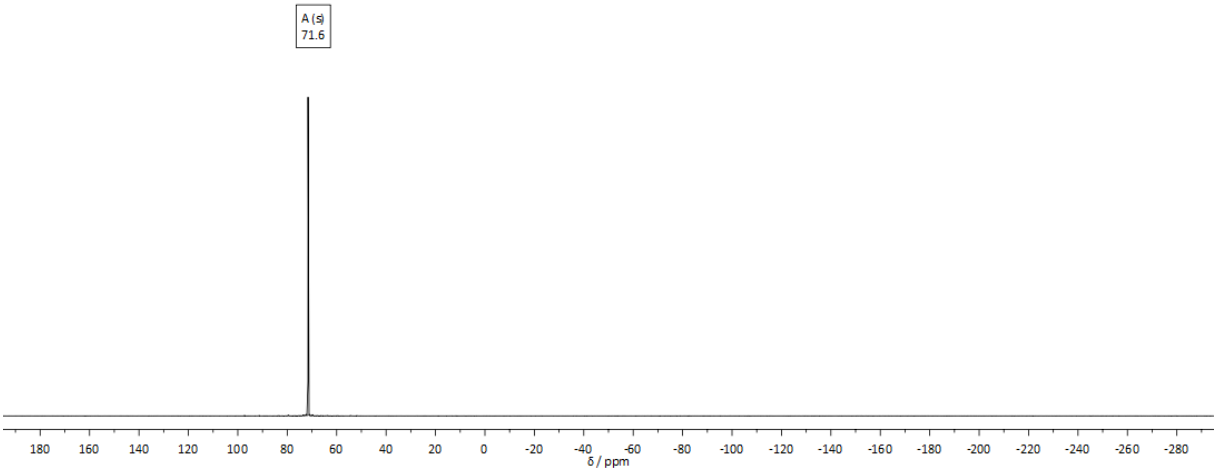

Figure S26 $^{31}P\{^{1}H\}$ NMR spectrum of **6** in CD_2Cl_2.

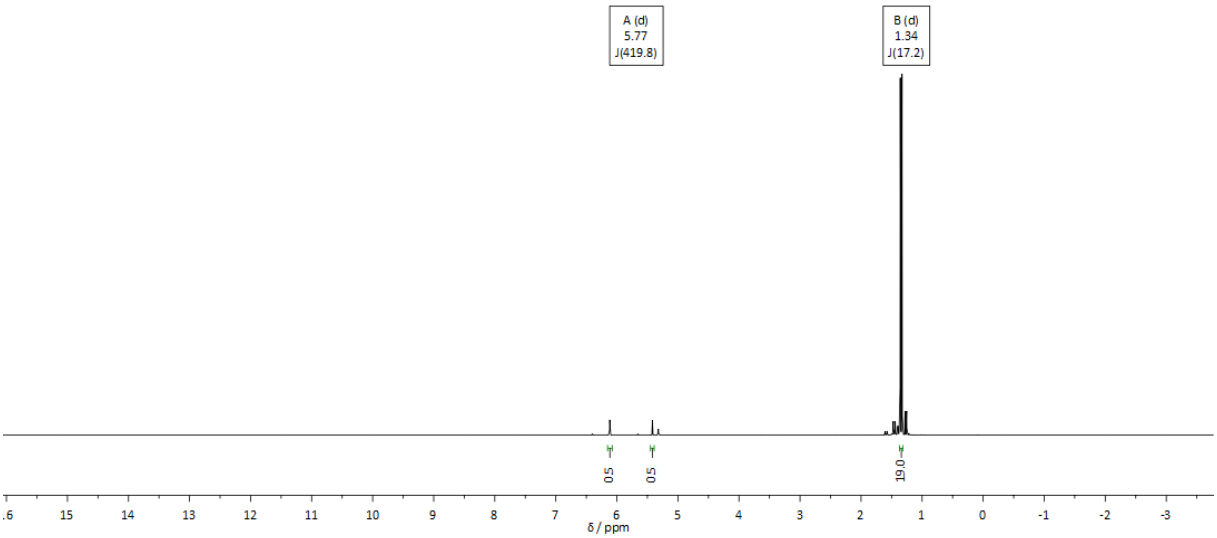

Figure S27 ^{1}H NMR spectrum of **7** in CD_2Cl_2.

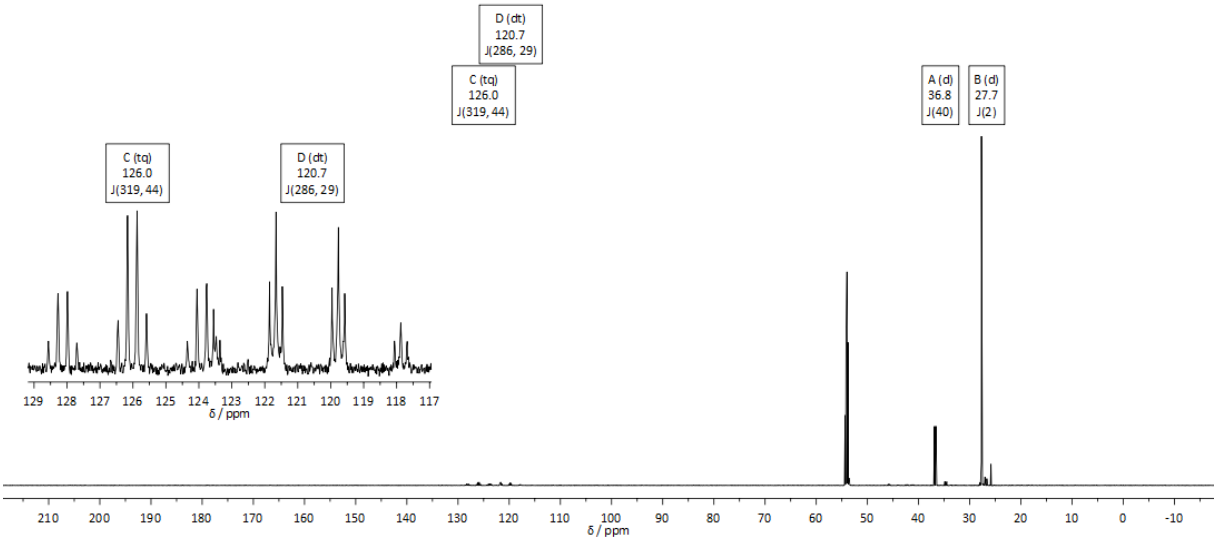

Figure S28 $^{13}C\{^{1}H\}$ NMR spectrum of **7** in CD_2Cl_2.

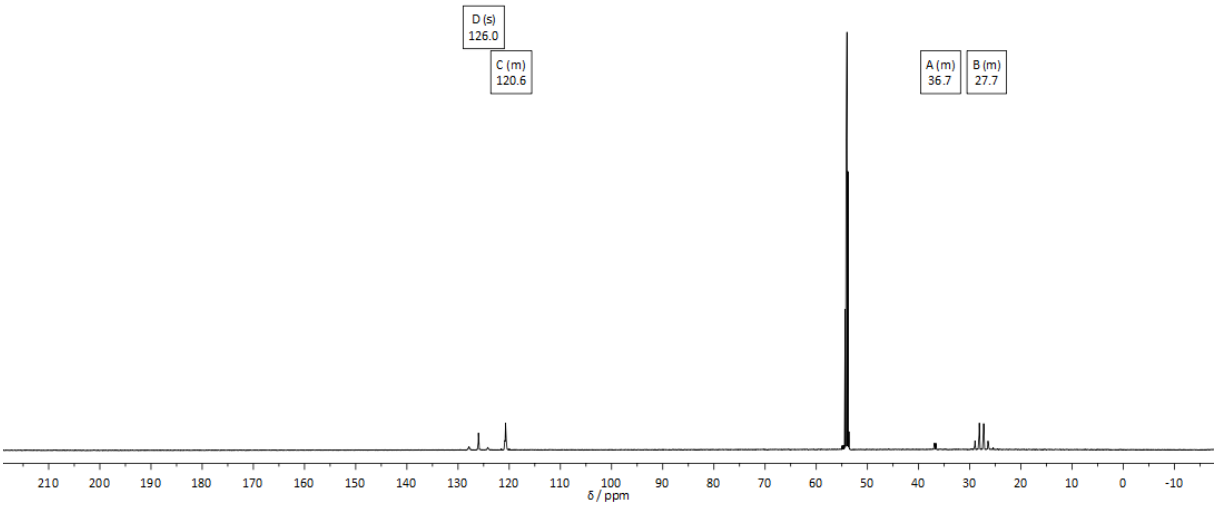

Figure S29 $^{13}C\{^{19}F\}$ NMR spectrum of **7** in CD_2Cl_2.

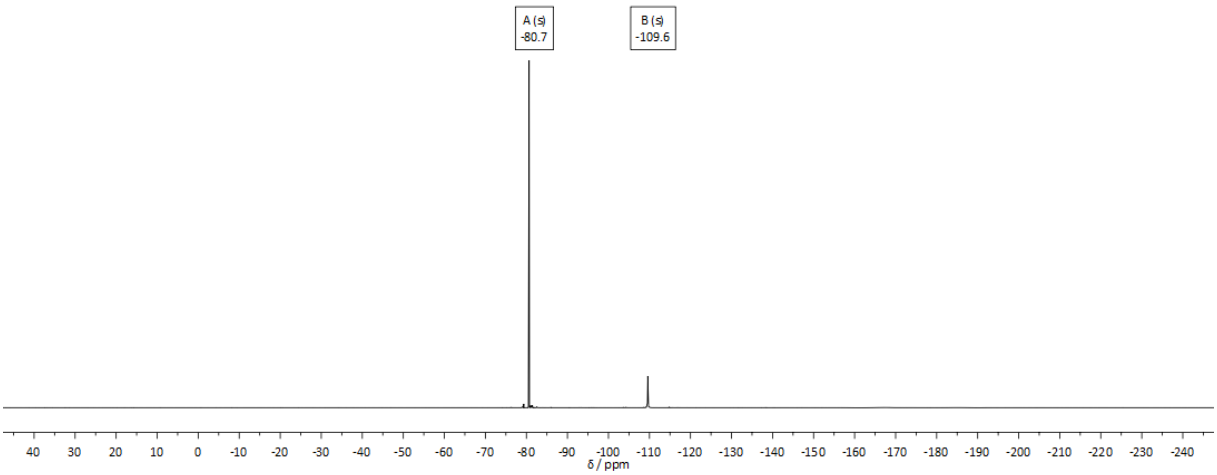

Figure S30 ^{19}F NMR spectrum of **7** in CD_2Cl_2.

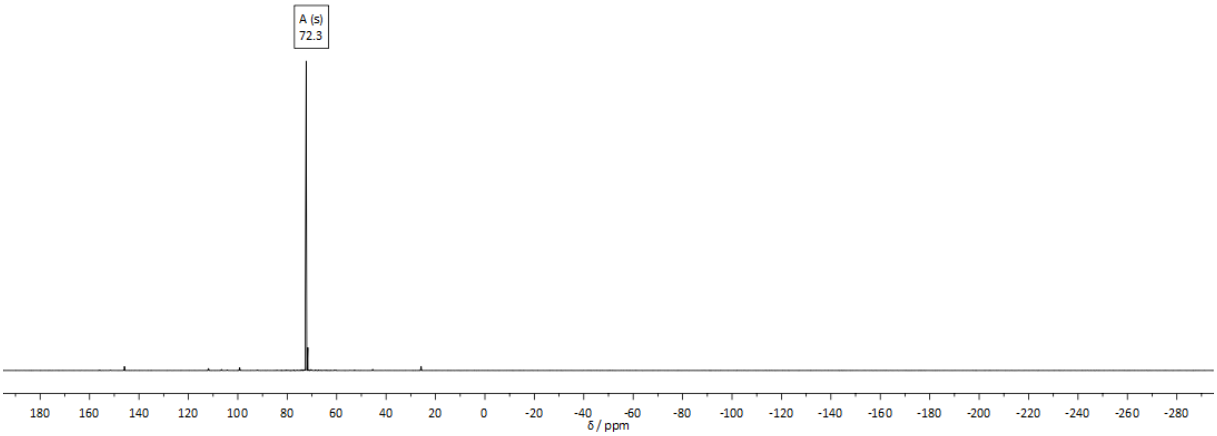

Figure S31 $^{31}P\{^1H\}$ NMR spectrum of **7** in CD_2Cl_2.

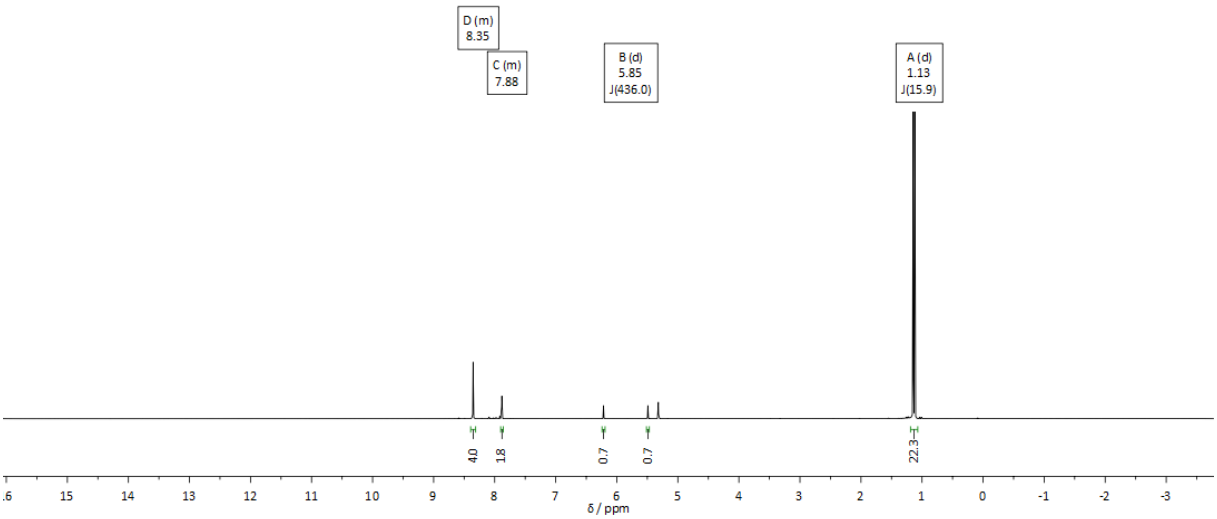

Figure S32 ^1H NMR spectrum of **8** in CD_2Cl_2.

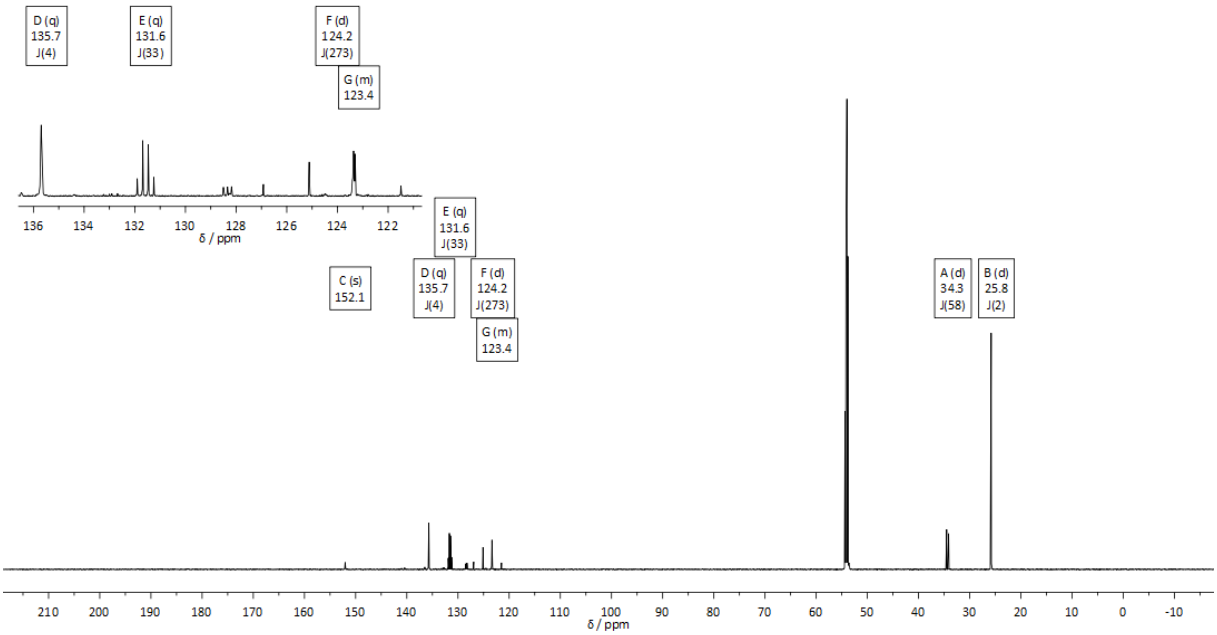

Figure S33 $^{13}C\{^{1}H\}$ NMR spectrum of **8** in CD_2Cl_2.

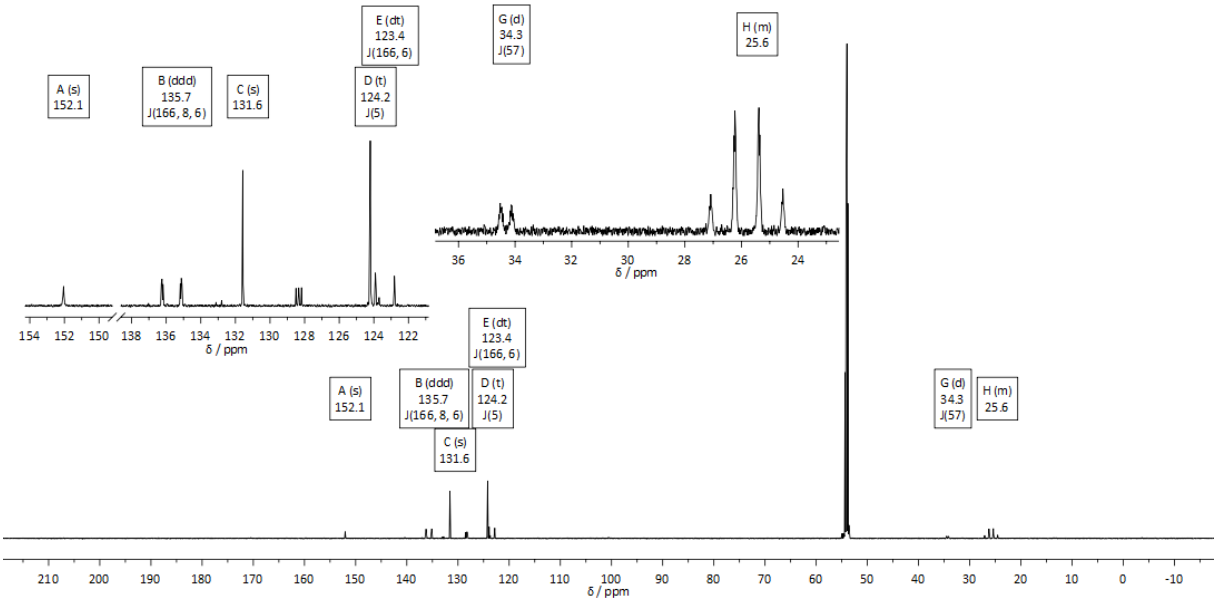

Figure S34 $^{13}C\{^{19}F\}$ NMR spectrum of **8** in CD_2Cl_2.

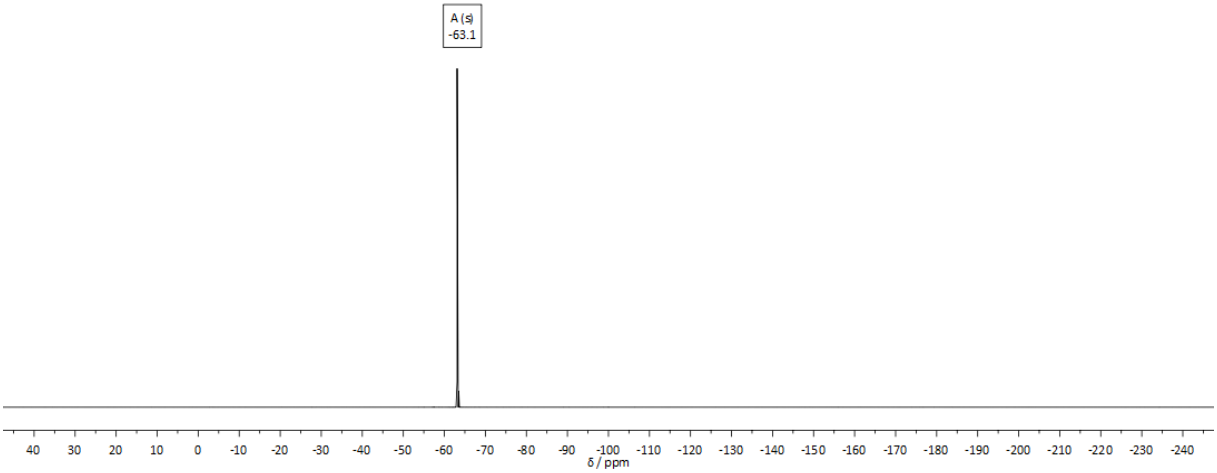

Figure S35 ^{19}F NMR spectrum of **8** in CD_2Cl_2.

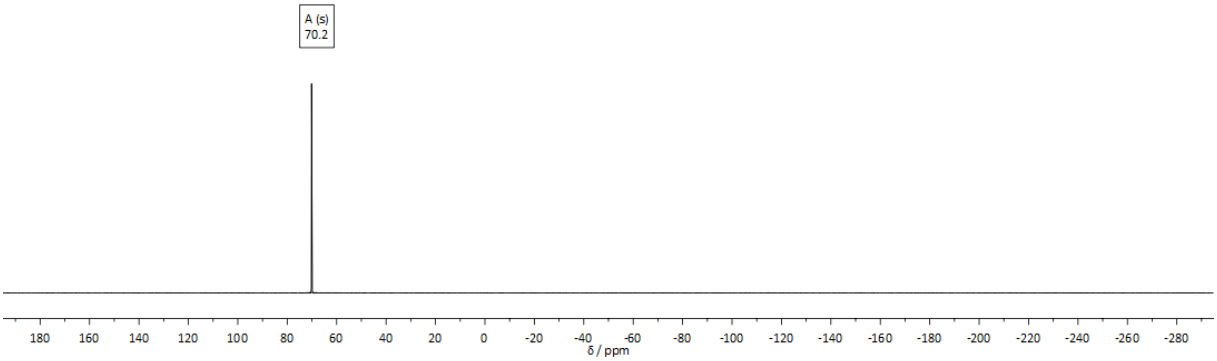

Figure S36 $^{31}P\{^1H\}$ NMR spectrum of **8** in CD_2Cl_2.

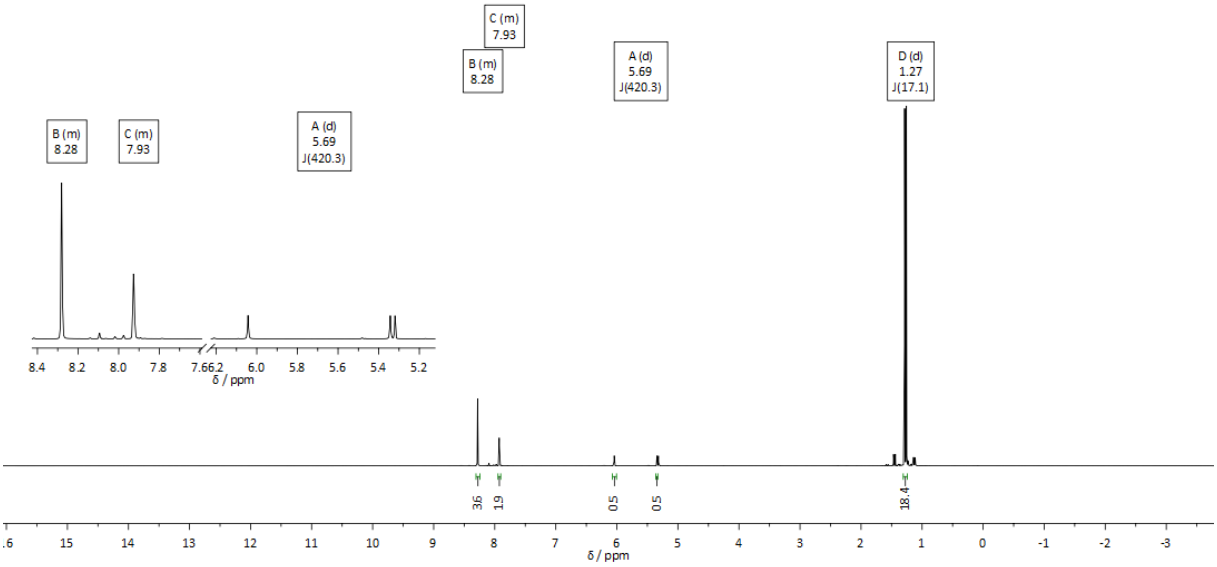

Figure S37 ^1H NMR spectrum of **9** in CD_2Cl_2.

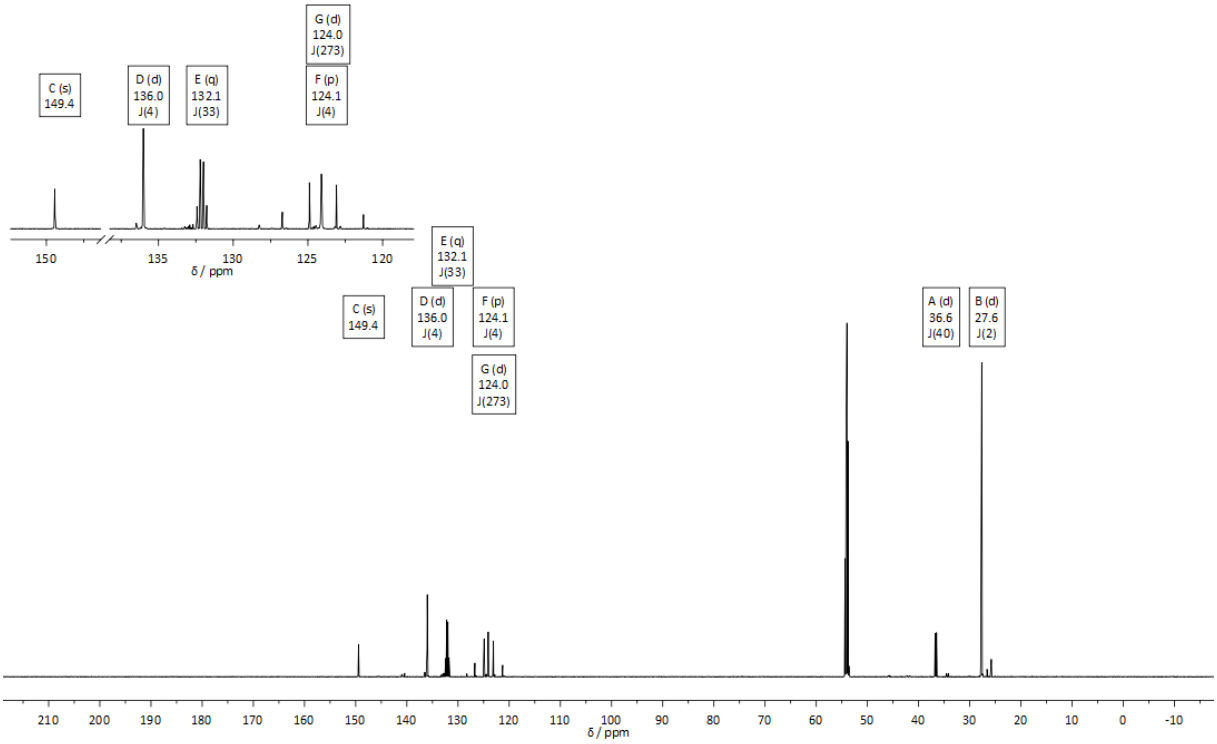

Figure S38 $^{13}C\{^{1}H\}$ NMR spectrum of **9** in CD_2Cl_2.

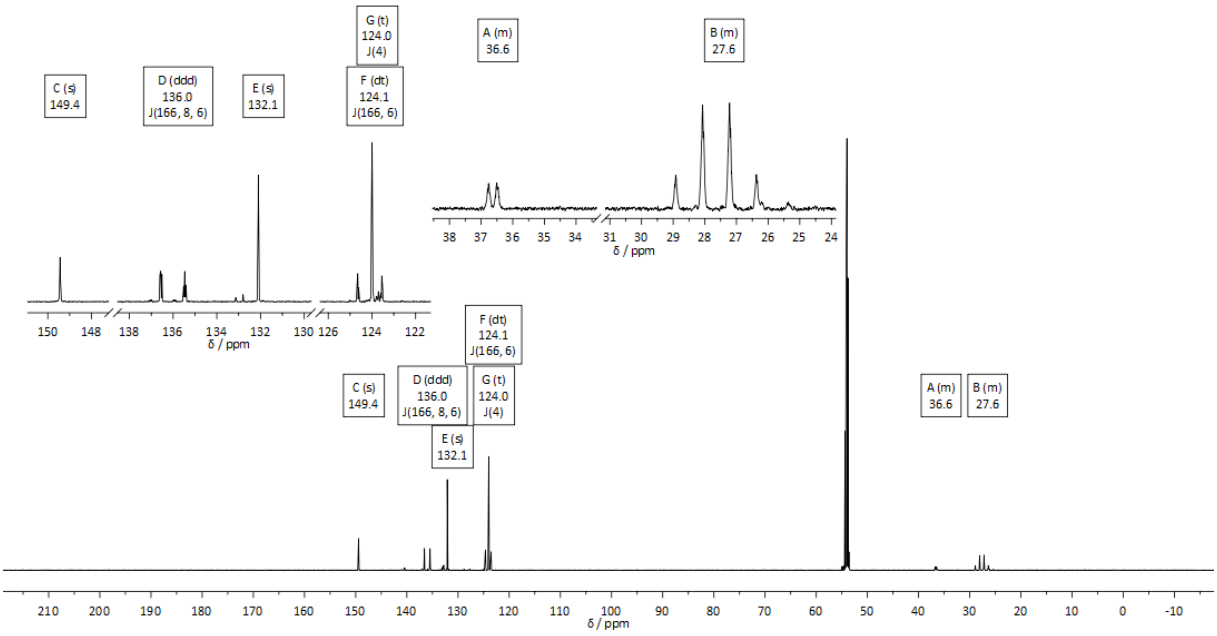

Figure S39 $^{13}C\{^{19}F\}$ NMR spectrum of **9** in CD_2Cl_2.

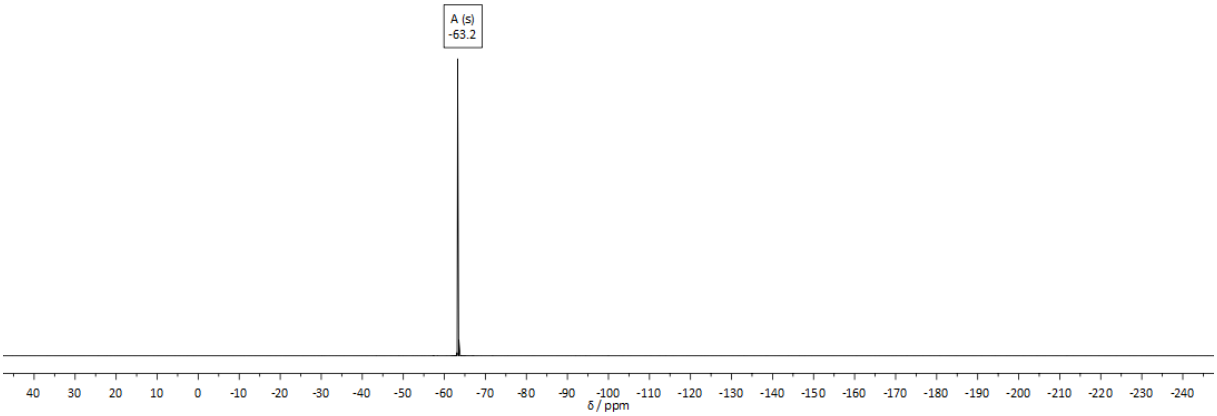

Figure S40 ^{19}F NMR spectrum of **9** in CD_2Cl_2.

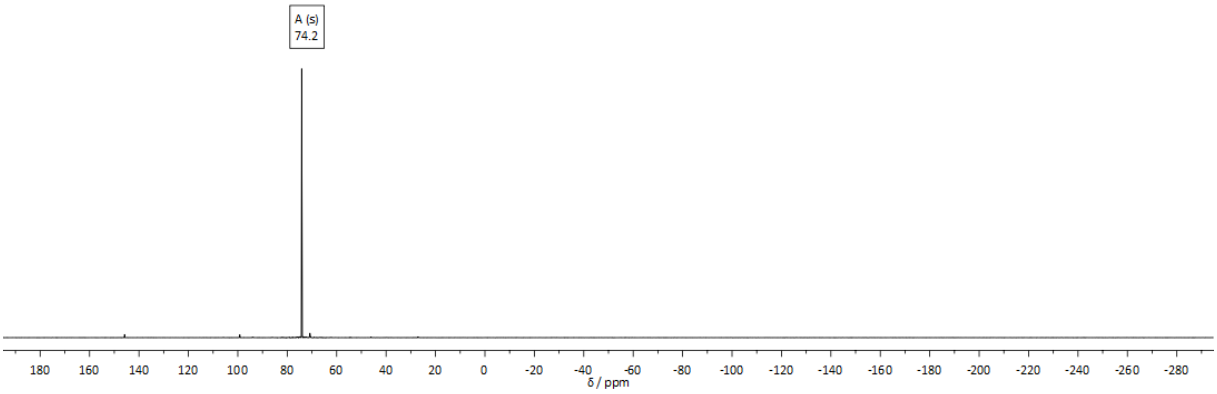

Figure S41 $^{31}P\{^1H\}$ NMR spectrum of **9** in CD_2Cl_2.

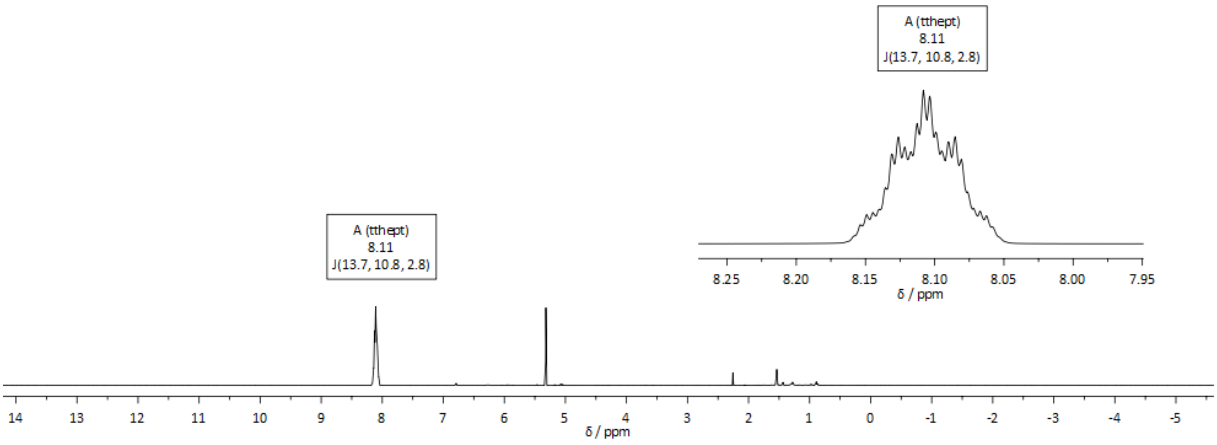

Figure S42 ^1H NMR spectrum of **10** in CD_2Cl_2.

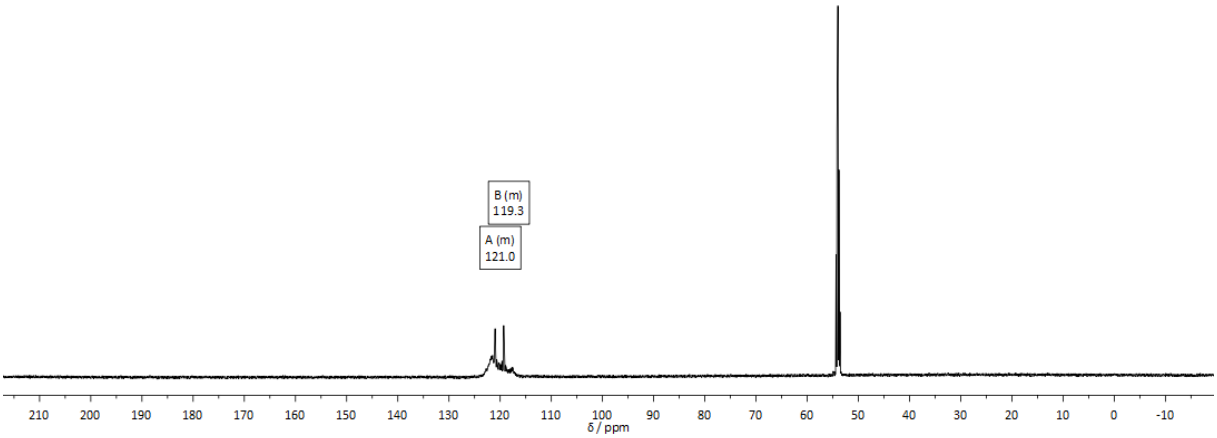

Figure S43 $^{13}C\{^{19}F\}$ NMR spectrum of **10** in CD_2Cl_2.

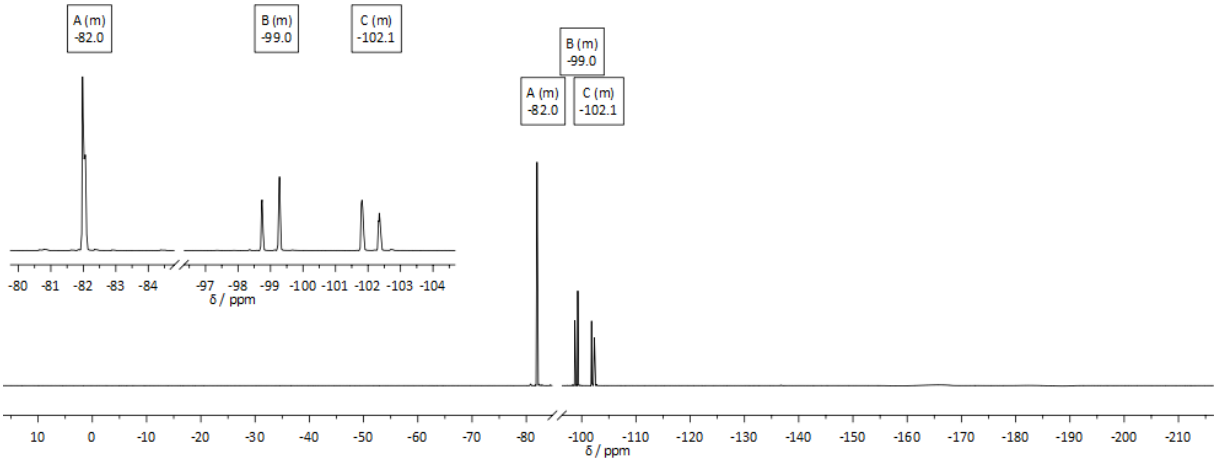

Figure S44 ^{19}F NMR spectrum of **10** in CD_2Cl_2.

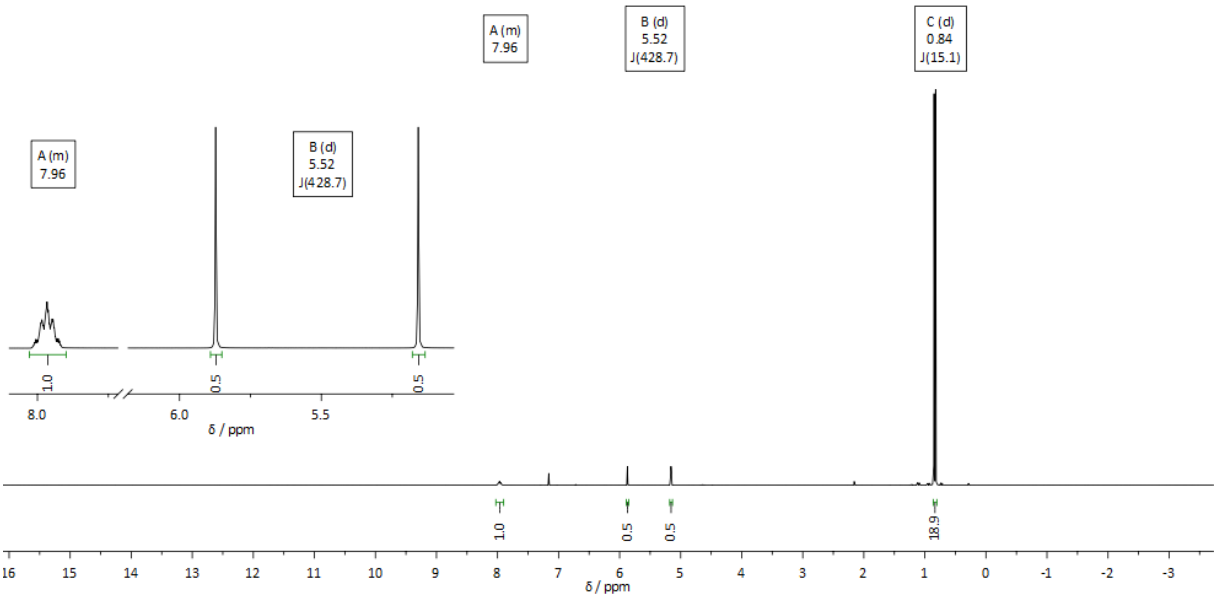

Figure S45 ^{1}H NMR spectrum of the conversion of bis(pentafluoroethyl)stibane (**10**) and di-*tert*-butylphoshane oxide in C_6D_6.

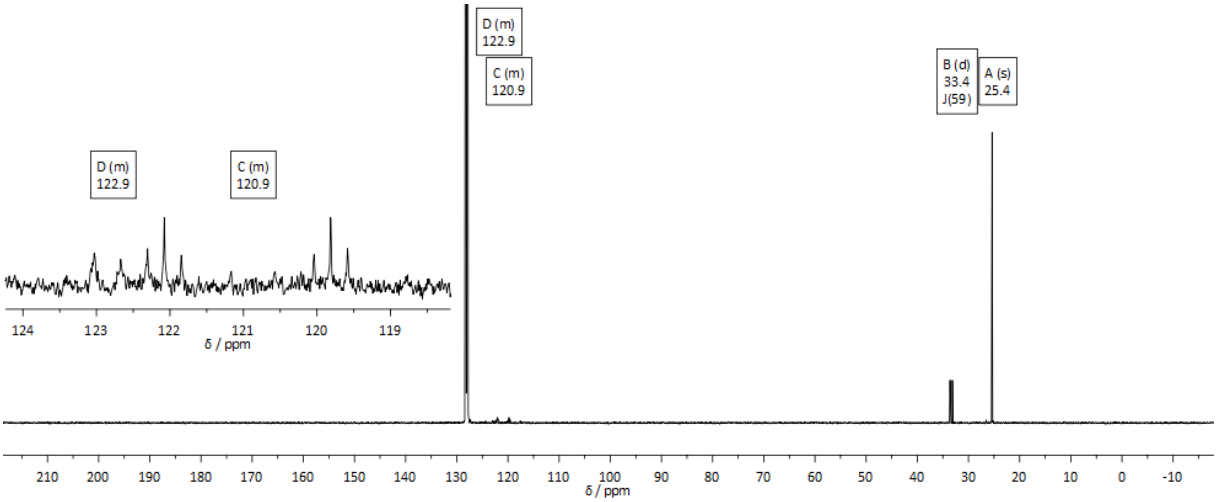

Figure S46 $^{13}C\{^{1}H\}$ NMR spectrum of the conversion of bis(pentafluoroethyl)stibane (**10**) and di-*tert*-butylphoshane oxide in C_6D_6.

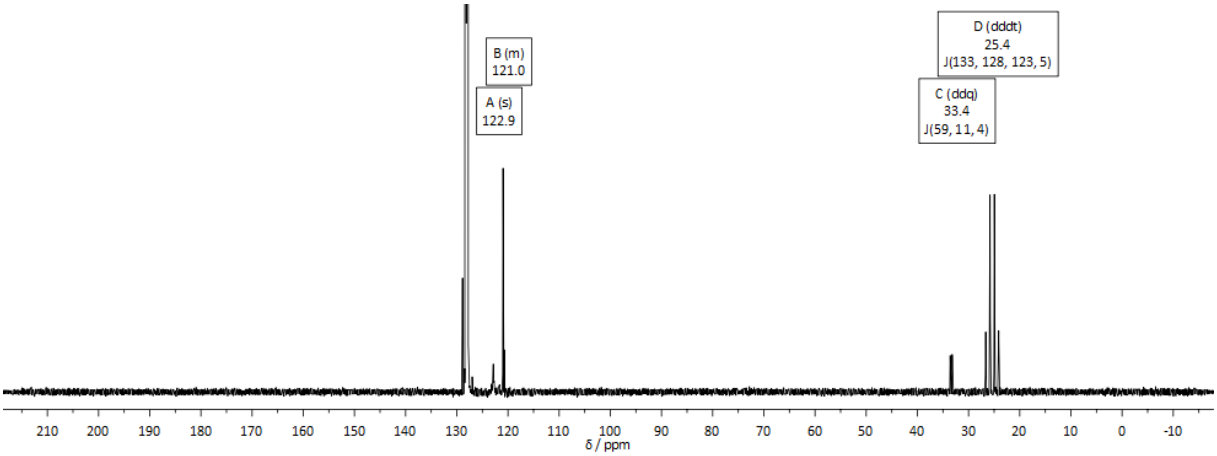

Figure S47 $^{13}C\{^{19}F\}$ NMR spectrum of the conversion of bis(pentafluoroethyl)stibane (**10**) and di-*tert*-butylphoshane oxide in C_6D_6.

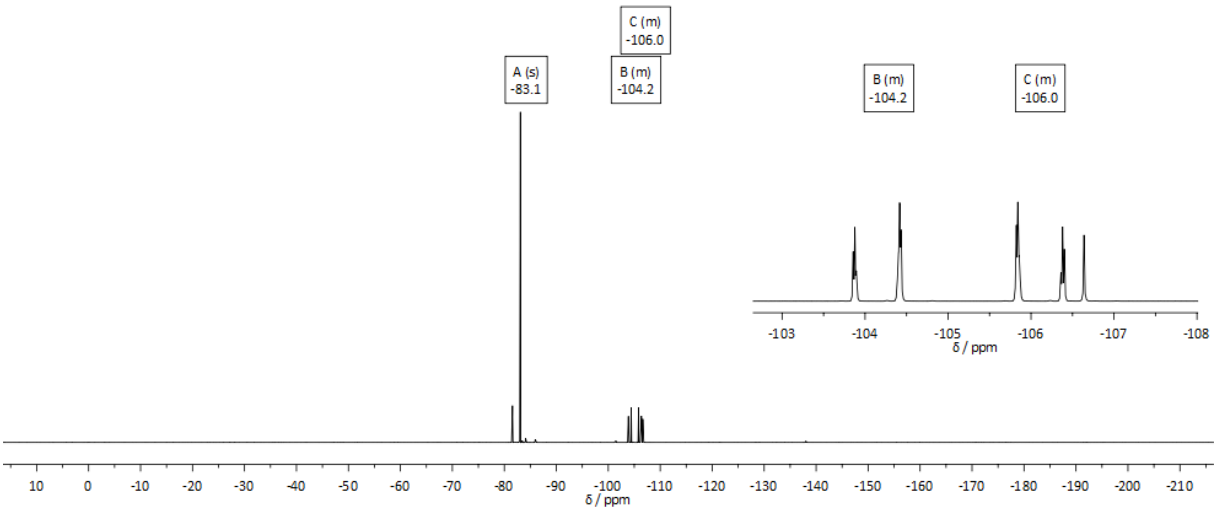

Figure S48 ^{19}F NMR spectrum of the conversion of bis(pentafluoroethyl)stibane (**10**) and di-*tert*-butylphoshane oxide in C_6D_6.

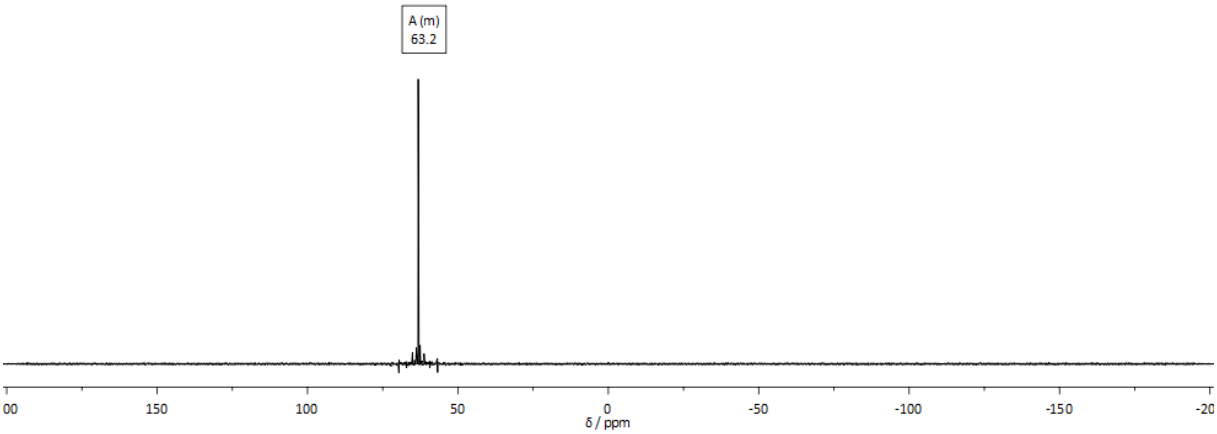

Figure S49 $^{31}P\{^{1}H\}$ NMR spectrum of the conversion of bis(pentafluoroethyl)stibane (**10**) and di-*tert*-butylphoshane oxide in C_6D_6.

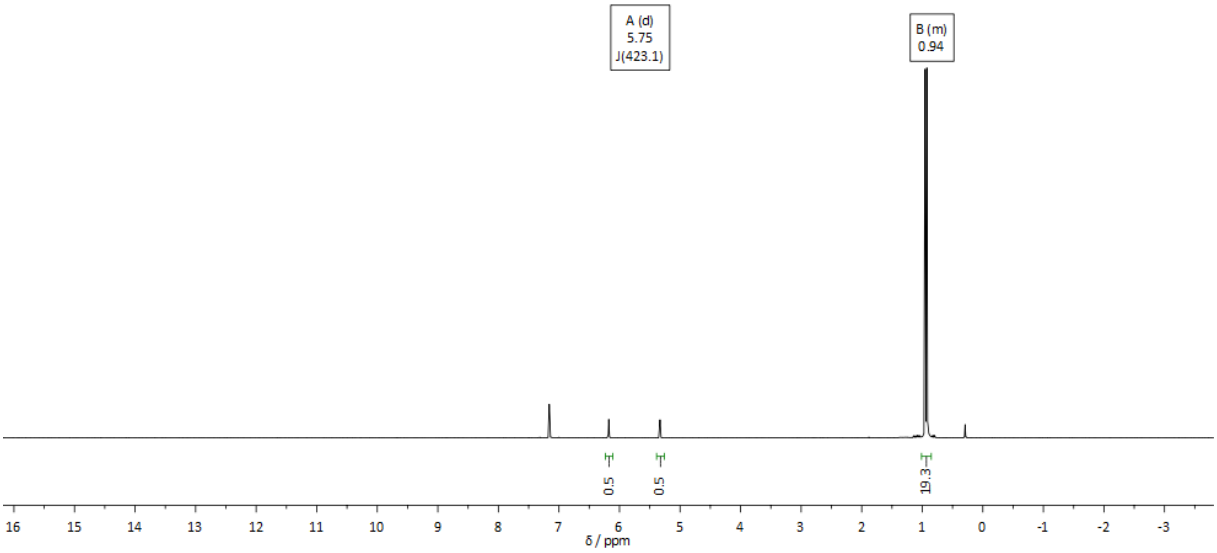

Figure S50 ^{1}H NMR spectrum of the crude product of the workup of the conversion of bis(pentafluoroethyl)stibane (**10**) and di-*tert*-butylphoshane oxide in C_6D_6.

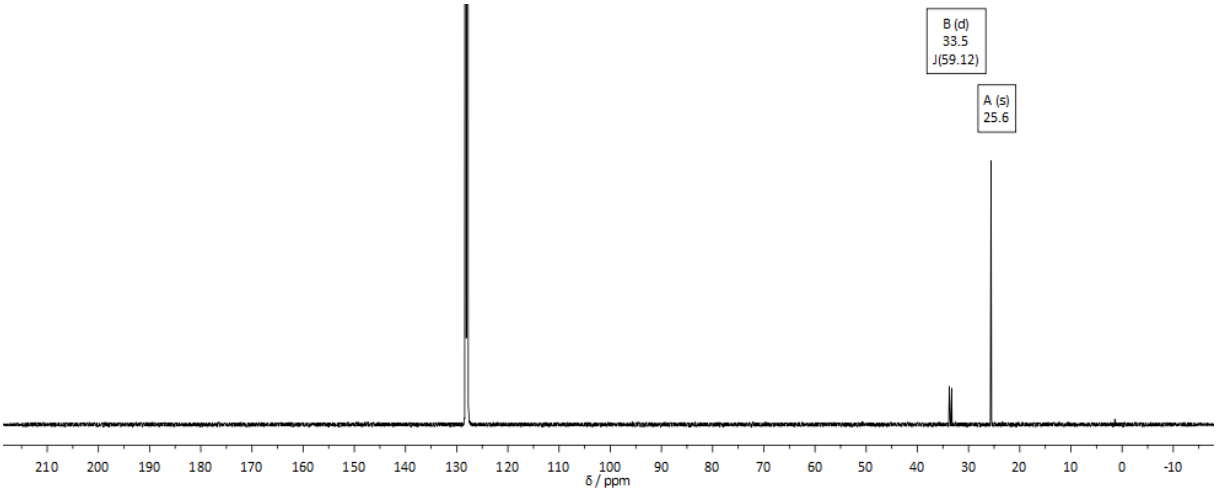

Figure S51 $^{13}C\{^{1}H\}$ NMR spectrum of the crude product of the workup of the conversion of bis(pentafluoroethyl)stibane (**10**) and di-*tert*-butylphoshane oxide in C_6D_6.

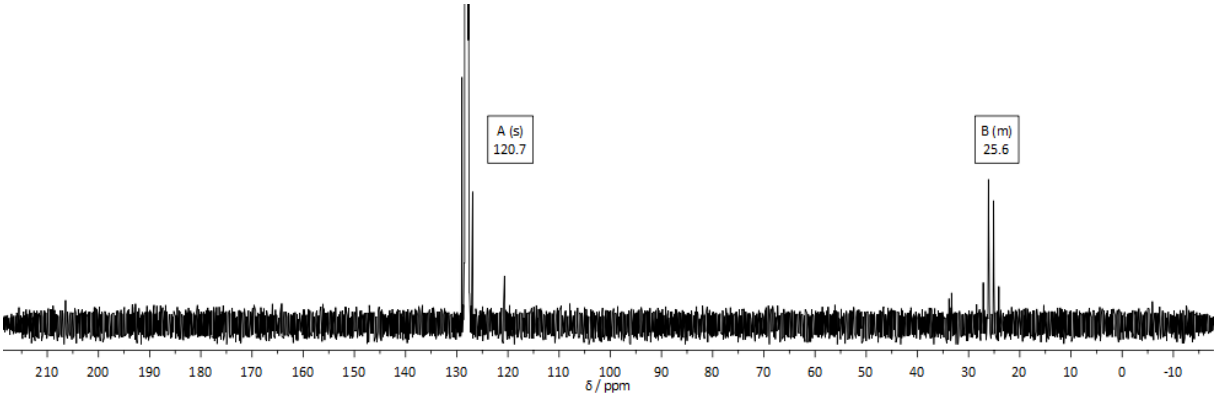

Figure S52 $^{13}C\{^{19}F\}$ NMR spectrum of the crude product of the workup of the conversion of bis(pentafluoroethyl)stibane (**10**) and di-*tert*-butylphoshane oxide in C_6D_6.

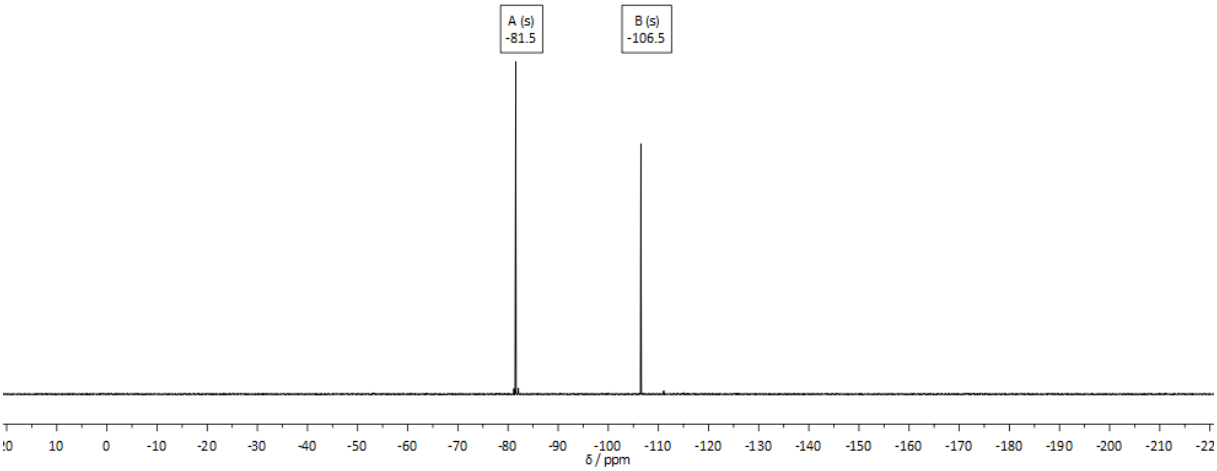

Figure S53 ^{19}F NMR spectrum of the crude product of the workup of the conversion of bis(pentafluoroethyl)stibane (**10**) and di-*tert*-butylphoshane oxide in C_6D_6.

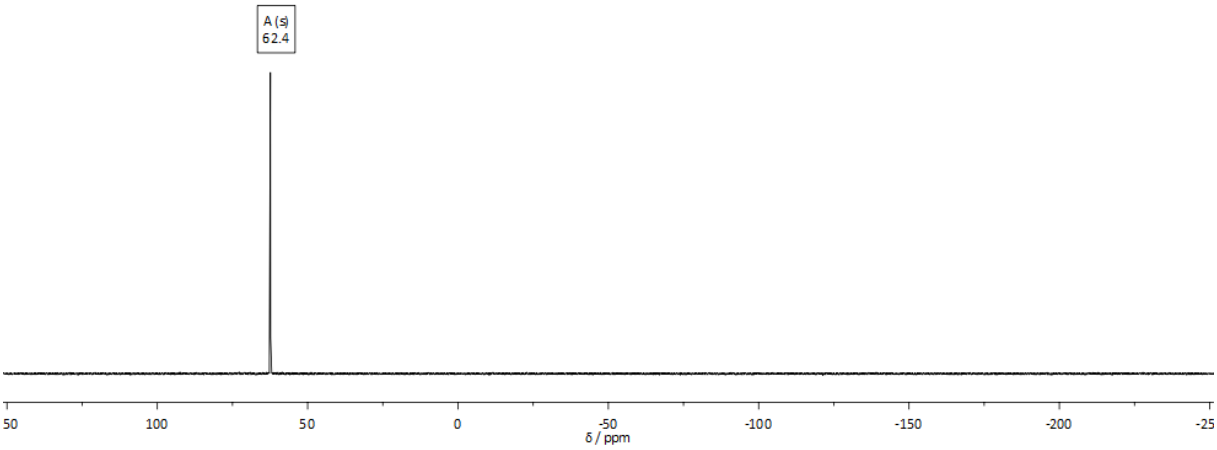

Figure S54 $^{31}P\{^{1}H\}$ NMR spectrum of the crude product of the workup of the conversion of bis(pentafluoroethyl)stibane (**10**) and di-*tert*-butylphoshane oxide in C_6D_6.

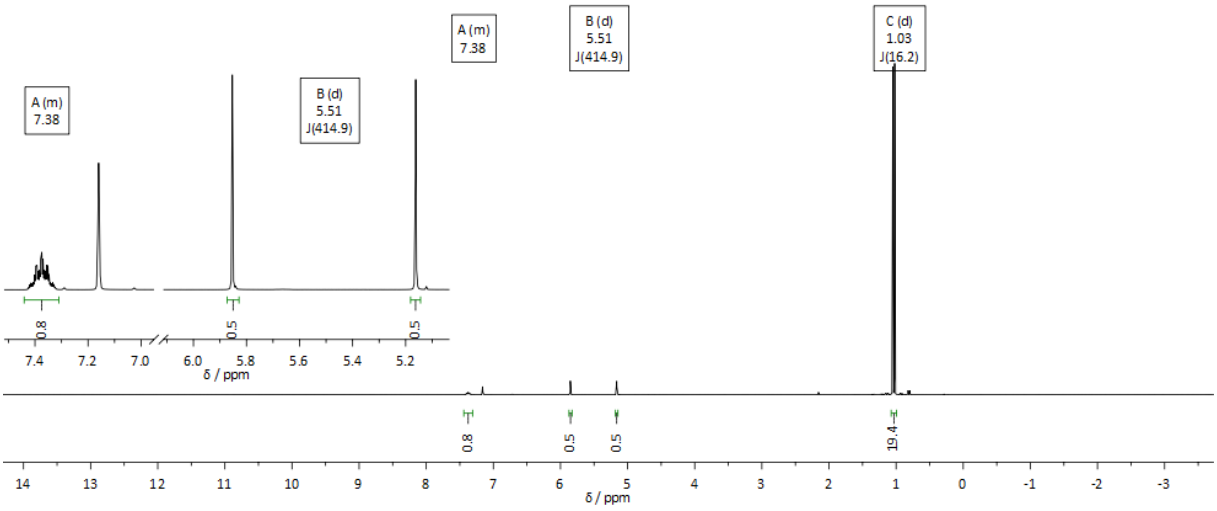

Figure S55 ^{1}H NMR spectrum of the conversion of bis(pentafluoroethyl)stibane and di-*tert*-butylphoshane sulphide in C_6D_6.

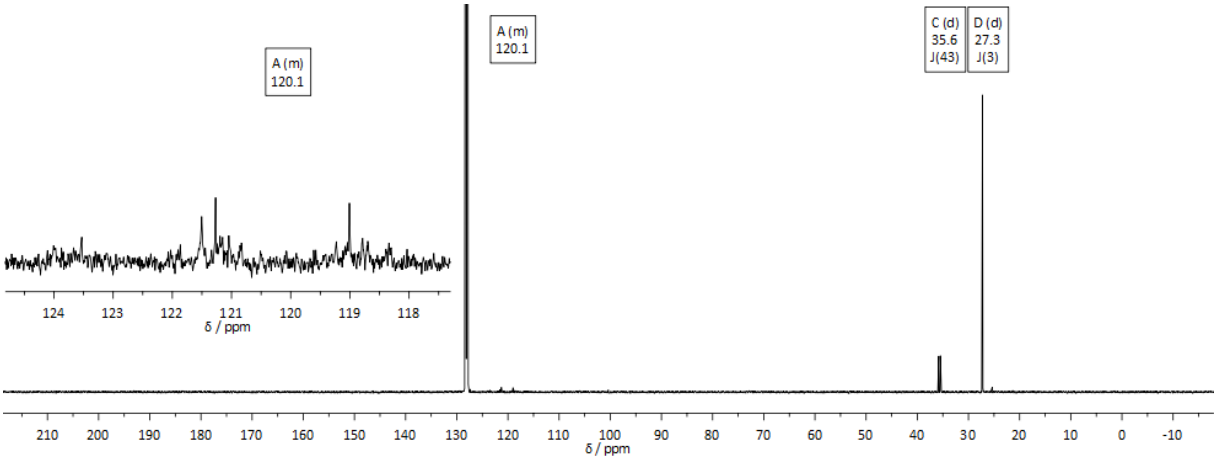

Figure S56 ^{13}C{^{1}H} NMR spectrum of the conversion of bis(pentafluoroethyl)stibane and di-*tert*-butylphoshane sulphide in C_6D_6.

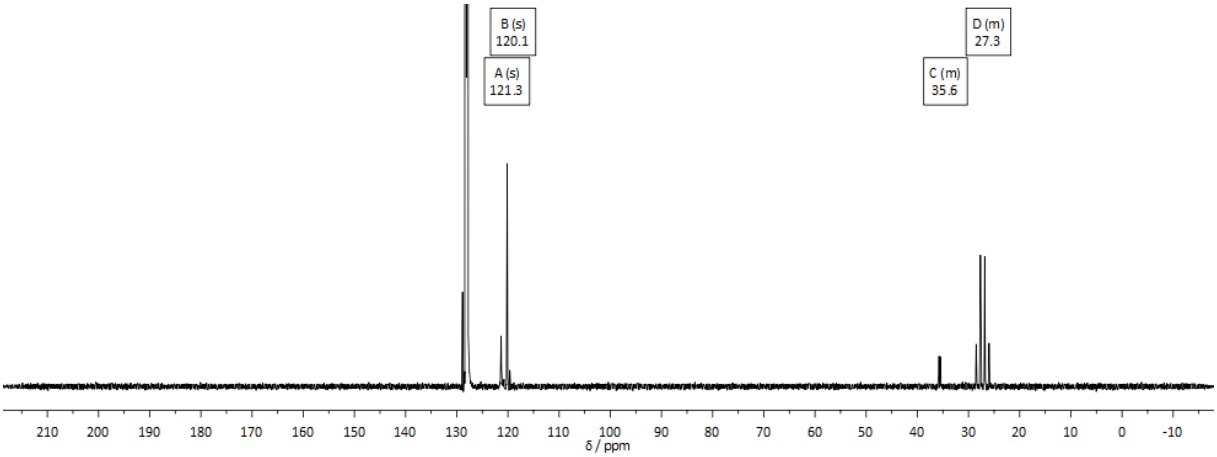

Figure S57 ^{13}C{^{19}F} NMR spectrum of the conversion of bis(pentafluoroethyl)stibane and di-*tert*-butylphoshane sulphide in C_6D_6.

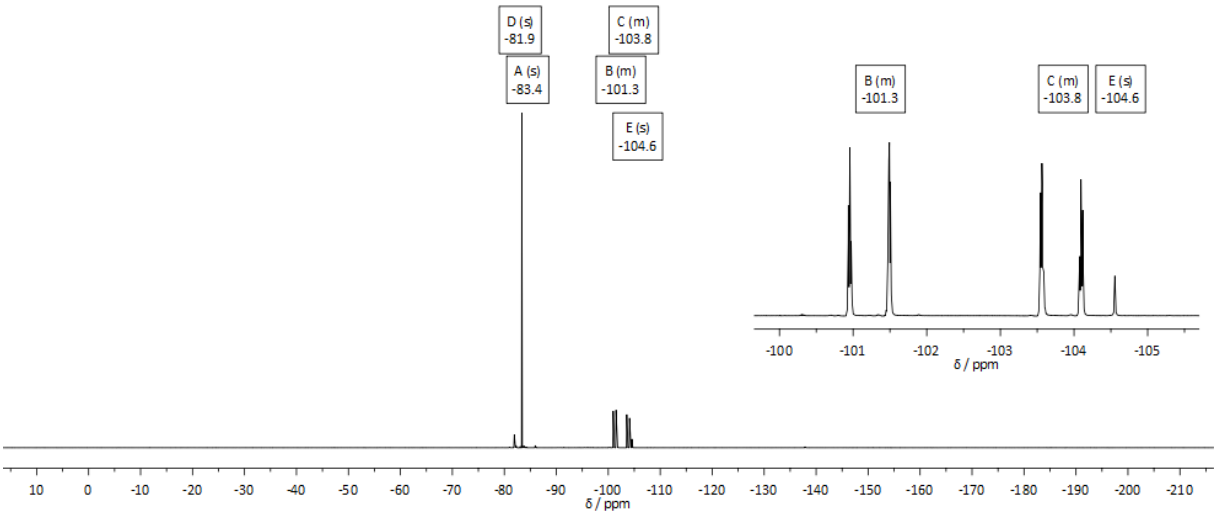

Figure S58 ^{19}F NMR spectrum of the conversion of bis(pentafluoroethyl)stibane and di-*tert*-butylphoshane sulphide in C_6D_6.

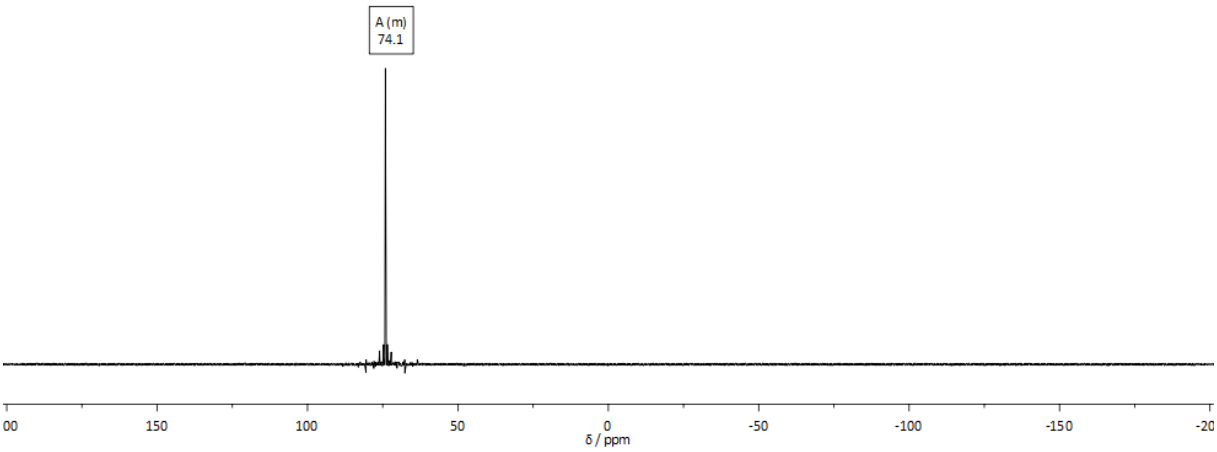

Figure S59 $^{31}P\{^1H\}$ NMR spectrum of the conversion of bis(pentafluoroethyl)stibane and di-*tert*-butylphoshane sulphide in C_6D_6.

Diffusion NMR experiments

Diffusion NMR experiments were performed on a Bruker Avance *NEO* 600 FT NMR spectrometer, operating at a ^{1}H resonance frequency of 600.13 MHz. The instrument was equipped with a 5 mm BBO Prodigy cryoprobe with a *z*-gradient coil providing a maximum gradient strength of 6.57 G mm^{-1} at 10 A. Diffusion data were recorded using the *ledbpgp2s* pulse sequence supplied by the manufacturer. Diffusion coefficients were corrected according to the diffusion coefficient of H_2O (2.299 × 10^{-9} m^2 s^{-1} at 298 K) reported in the literature.[4] The corresponding proportional factor $D_{H2O,lit.}/D_{H2O,est.}$ was determined on a sample of acetone-*d*6 equipped with a capillary containing H_2O. The temperature unit of the instrument was calibrated according to the instrument manufacturer's manual using the temperature dependence of the proton chemical shift difference of methanol. To obtain stable temperature conditions, the sample was held in the magnet for at least one hour prior to data collection. Proton diffusion data were collected at 293 K with 16k data points and a spectral width of 5880 Hz (^{1}H) and 32k data points and a spectral width of 16670 Hz (^{19}F), respectively. The relaxation delay was set to 5 s.
The diffusion delay time (big delta, Δ) was set to 50 ms. The gradient duration time (small delta, $\delta/2$) was set to 1100 µs. The gradient strength within the diffusion experiments was increased linearly in 16 steps. The diffusion data were analysed using the *T*1/*T*2 module which is part of the Bruker *TopSpin*® software package.
The standard deviation of the experimentally determined gradient-strength dependent signal intensities from the fitted decay function was ≤ 3.62 × 10^{-3}. DOSY-Plots were generated using the Bruker *TopSpin*® software.

The hydrodynamic radii have been calculated by the Stokes-Einstein (SE) equation, (eq. 1)[5] and the hydrodynamic volume have been calculated by equation for a spherical volume (eq. 2):

$$D = \frac{k_B T}{c f_s \pi \eta r_H} \quad r_H = \frac{k_B T}{c f_s \pi \eta D} \qquad \text{(eq. 1)} \qquad V_H = \frac{4}{3}\pi r_H^3 \qquad \text{(eq. 2)}$$

D = diffusion constant, k_B = Boltzmann constant, T = temperature, η = viscosity, r_H = hydrodynamic radius, V_H = hydrodynamic volume

The *c*-factor was calculated according to Chen *et al*. (eq. 3):[6]

$$c = \frac{6}{1+0.695\left(\frac{r_{solvent}}{r_{solute}}\right)^{2.234}} \qquad \text{(eq. 3)}$$

$r_{solvent}$ = *van der Waals* radius of the solvent, r_{solute} = *van der Waals* radius of the solute

Van der Waals radii of molecules have been calculated using a method reported by Abraham et *al*. (eq. 4):[7]

$$V_{vdW}\,[\text{Å}] = \sum all\ atom\ contributions\ - 5.92N_b\ - 14.7R_A\ - 3.8R_{NR} \qquad \text{(eq. 4)}$$

N_b = number of bonds, R_A = number of aromatic rings, R_{NR} = number of non-aromatic rings

Table S1 Atom contributions used for *van der Waals* radii calculations[8]

Atom	r_{vdW} [Å]	V_{vdW} [Å³]
H	1.20	
C	1.77	
O	1.52	
F	1.46	
P	1.90	
Sb	2.47	

Table S2 Viscosity data of benzene[9]

Temperature [K]	Viscosity [Pa s]
293.15	0.0006537

Table S3 Determined diffusion constants (D), hydrodynamic radii (r_H), hydrodynamic volumes (V_H) and calculated van der Waals radii (r_{vdW}) and volumes (V_{vdW}) of **10**, H(O)P*t*Bu$_2$ and a 1:1 mixture of them. r_{vdW} of C_6D_6 = 2.69 Å

Probe	D [m² s]	r_H [m]	V_H [Å³]	r_{vdW} [Å]	V_{vdW} [Å³]
10 (from ^{19}F)	$1.24\cdot10^{-9}$	$3.59\cdot10^{-10}$	194.39	3.63	200.46
H(O)P*t*Bu$_2$ (from ^{1}H)	$1.41\cdot10^{-9}$	$3.14\cdot10^{-10}$	129.90	3.66	204.83
10 + H(O)P*t*Bu$_2$ (from ^{19}F)	$1.13\cdot10^{-9}$	$3.51\cdot10^{-10}$	181.76	4.57	399.37
10 + H(O)P*t*Bu$_2$ (from ^{1}H)	$1.04\cdot10^{-9}$	$3.81\cdot10^{-10}$	232.50		

Samples for DOSY NMR experiments were freshly prepared by dissolving 10 mg of **10** and 10 mg of H(O)P*t*Bu$_2$ and a mixture of 10 mg **10** and 4 mg of H(O)P*t*Bu$_2$ in C_6D_6 respectively

The overall error in the calculated diffusion coefficients can be estimated to be ≤ ±5%. Deviations from the SE law are expected for small molecules with radii in the range of that of the solvent exhibiting non-spherical molecular structures. Although methods have been reported to describe the hydrodynamic behaviour of such compounds by using a factor *c* adapted to the size and a factor *f*s depending on the form of the solute, it is difficult to determine the correct factors in this case, since the proportions of the individual species in equilibrium are unknown, especially for open chain and cyclic forms, for which completely different shapes can be expected. Accordingly, we calculated hydrodynamic radii according to the SE law and interpreted the data by comparison with those of suitable reference compounds. The use of reference compounds of very similar shape, treated in exactly the same way as the analyte, lead to a minimum of possible introduced errors in the factor *c*. Although according to eq. 2, the error in V_H increases with respect to r_H, we used V_H to determine the level of aggregation, which facilitates the comparison with reference compounds and it allows the approximation of V_H for the proposed adducts simply by adding the corresponding volumes of the components.

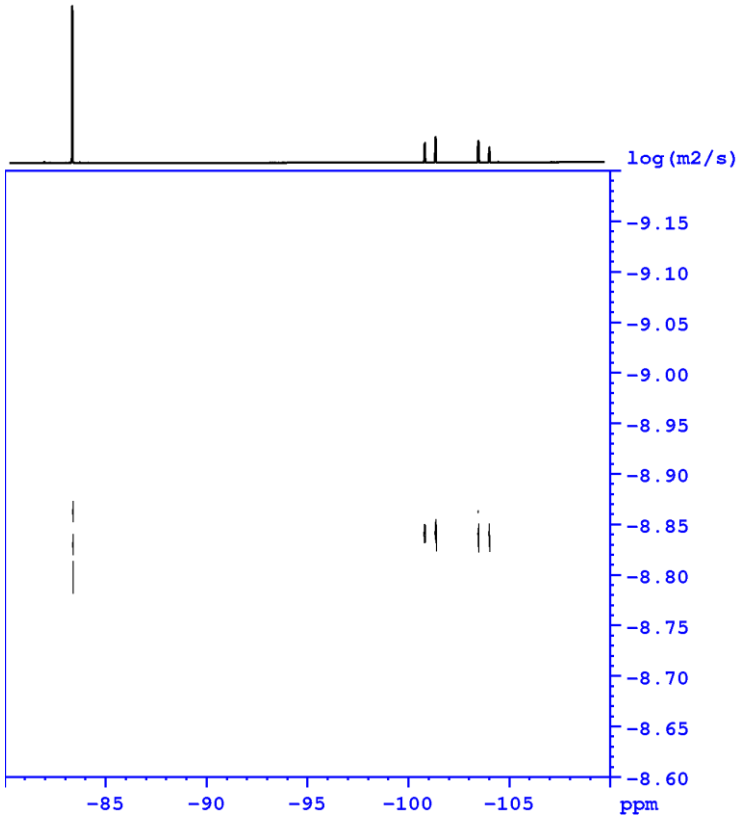

Figure S60 ^{19}F-DOSY-Plot of **10**.

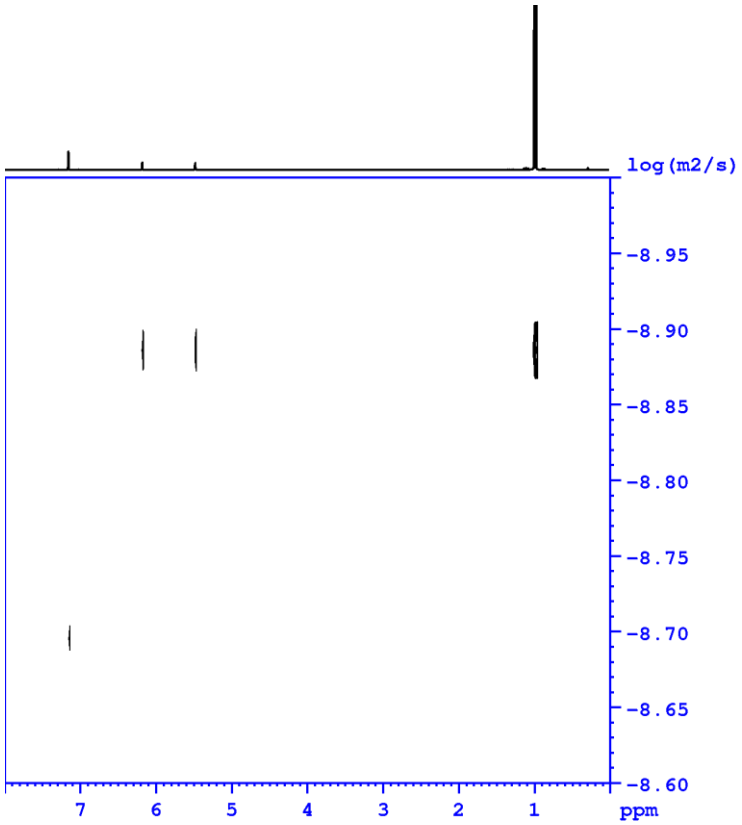

Figure S61 ^{1}H-DOSY-Plot of H(O)P*t*Bu$_2$.

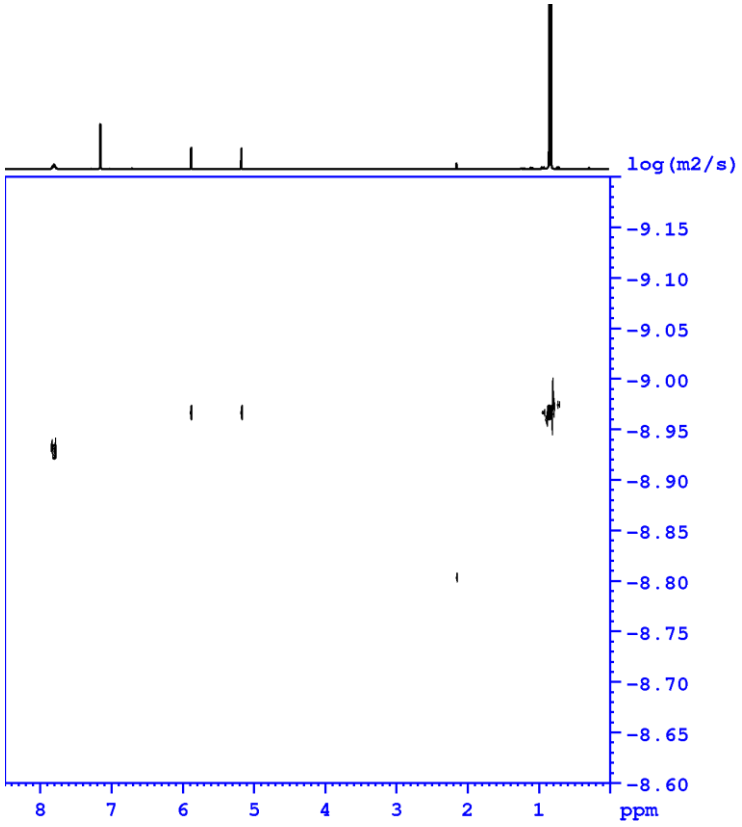

Figure S62 ^{1}H-DOSY-Plot of a 1:1 mixture of **10** and H(O)P*t*Bu$_2$.

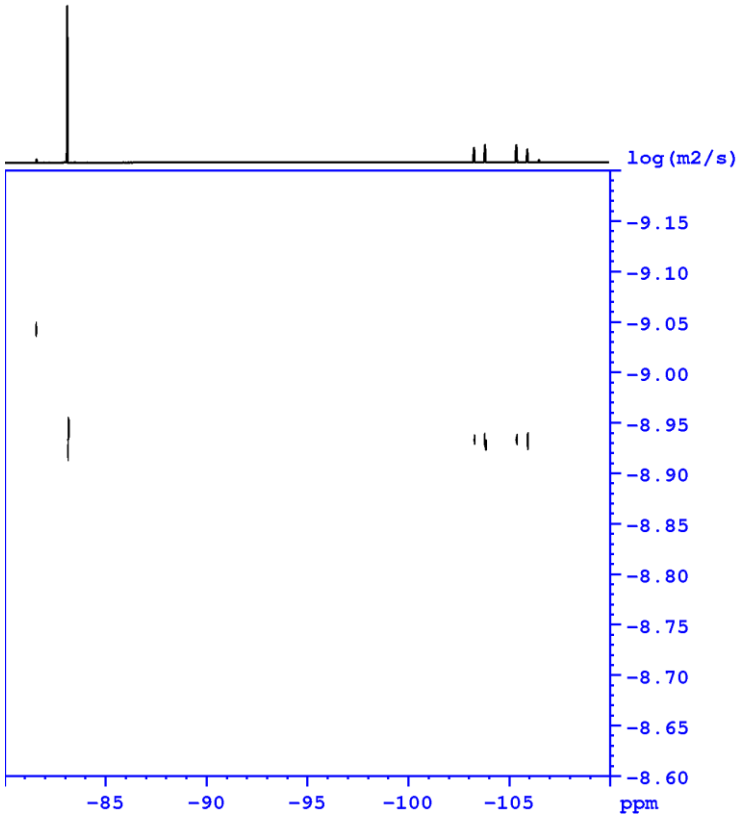

Figure S63 ^{19}F-DOSY-Plot of a 1:1 mixture of **10** and H(O)P*t*Bu$_2$.

Lewis Acidity Tests

We performed Lewis acidity tests with the Gutmann-Beckett method[10] with $OPEt_3$. After addition of $OPEt_3$ to the stibanes **3**, **5** and **10** (1:1 eq. and 1:5 eq.: $OPEt_3$:stibane), we saw a variation of the $^{31}P\{^1H\}$ NMR chemical shift of $OPEt_3$ (52.3 ppm in $CDCl_3$) due to interaction with the corresponding stibane Lewis acids. Based on the chemical shifts of the samples with an excess of Lewis acid, we calculated the acceptor numbers (AN) of the stibanes according to the following literature equation,[10] with $\delta(^{31}P)$ of $OPEt_3$ with hexane = 41 and $\delta(^{31}P)$ of $OPEt_3$ with $SbCl_5$ = 86.14:

$$AN = \left(\delta_{sample} - 41.0\right) \times \left(\frac{100}{86.14 - 41.0}\right).$$

The calculated acceptor numbers are 52.3 for $(F_5C_2)_2SbCl$ (**3**), 52.5 for $(Fxyl)_2SbCl$ (**5**) and 29.8 for $(F_5C_2)_2SbH$ (**10**).

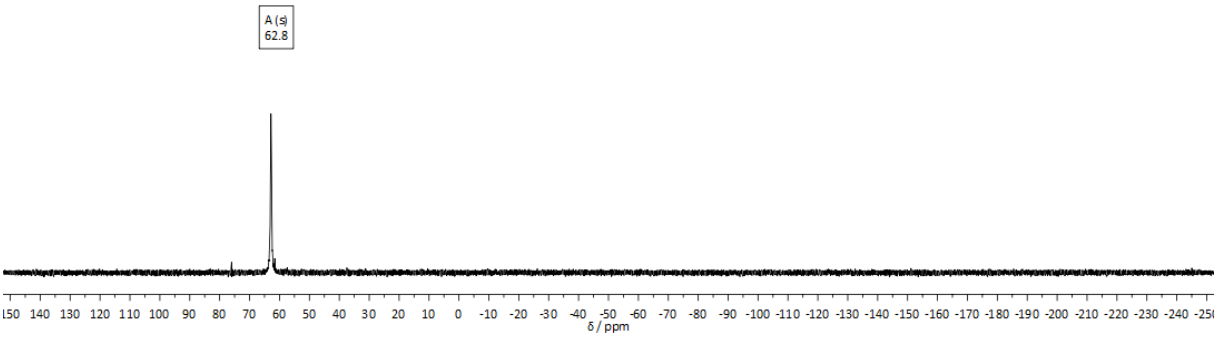

Figure S64 Gutmann-Beckett test in $CDCl_3$ with 1 eq. $OPEt_3$ and 1 eq. $(F_5C_2)_2SbCl$ (**3**).

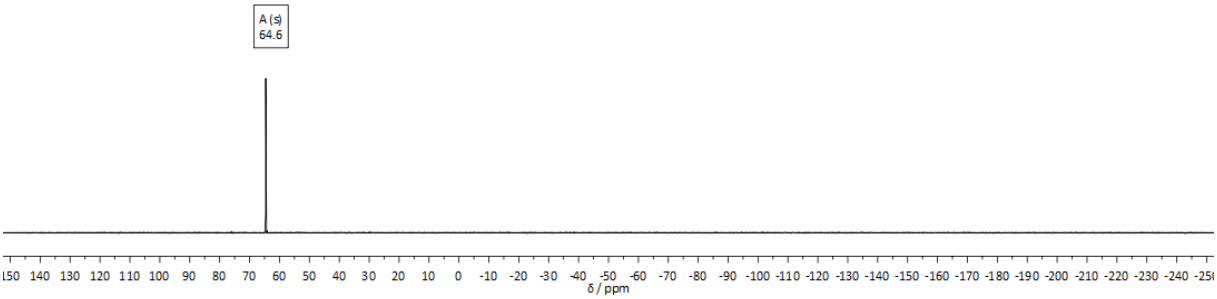

Figure S65 Gutmann-Beckett test in $CDCl_3$ with 1 eq. $OPEt_3$ and 5 eq. $(F_5C_2)_2SbCl$ (**3**).

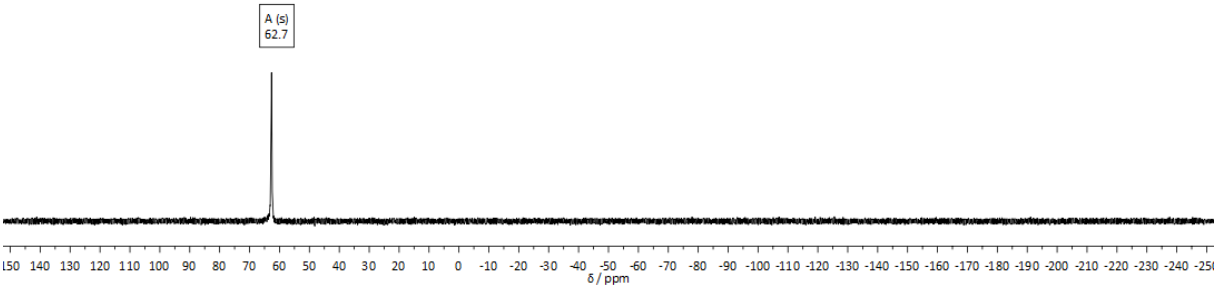

Figure S66 Gutmann-Beckett test in $CDCl_3$ with 1 eq. $OPEt_3$ and 1 eq. $(Fxyl)_2SbCl$ (**5**).

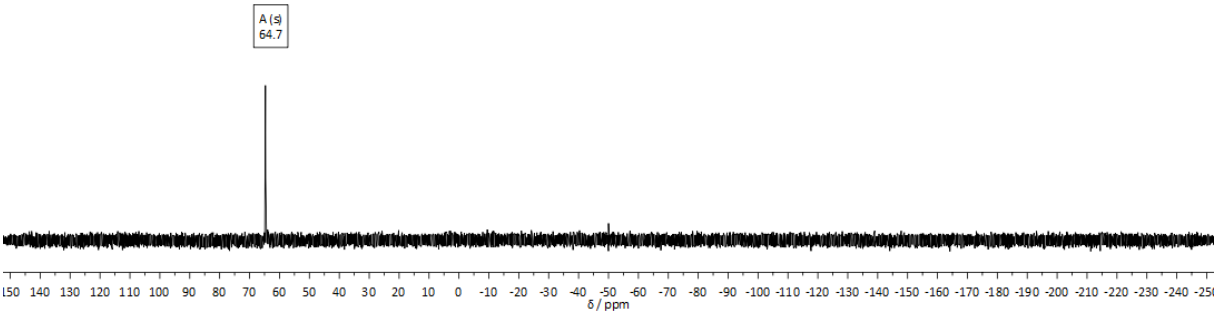

Figure S67 Gutmann-Beckett test in $CDCl_3$ with 1 eq. $OPEt_3$ and 5 eq. $(Fxyl)_2SbCl$ (**5**).

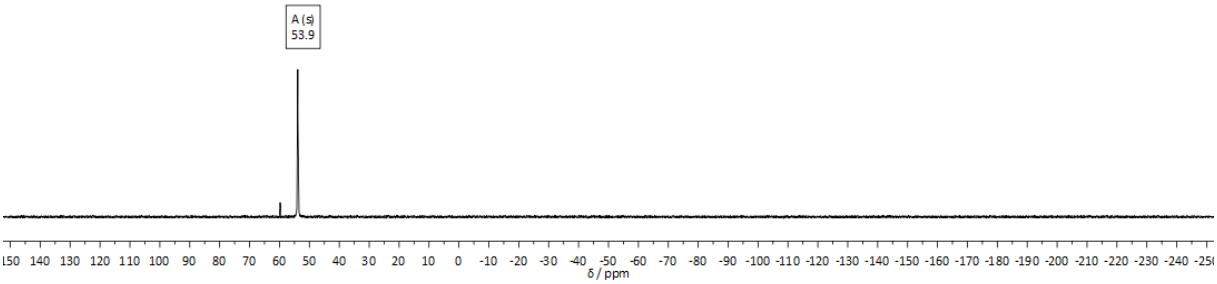

Figure S68 Gutmann-Beckett test in $CDCl_3$ with 1 eq. $OPEt_3$ and 1 eq. $(F_5C_2)_2SbH$ (**10**).

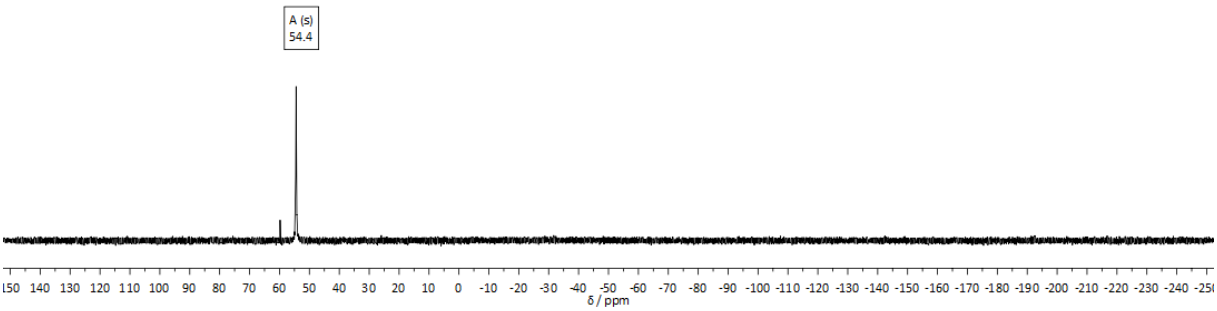

Figure S69 Gutmann-Beckett test in $CDCl_3$ with 1 eq. $OPEt_3$ and 5 eq. $(F_5C_2)_2SbH$ (**10**).

IR Spectroscopy Data

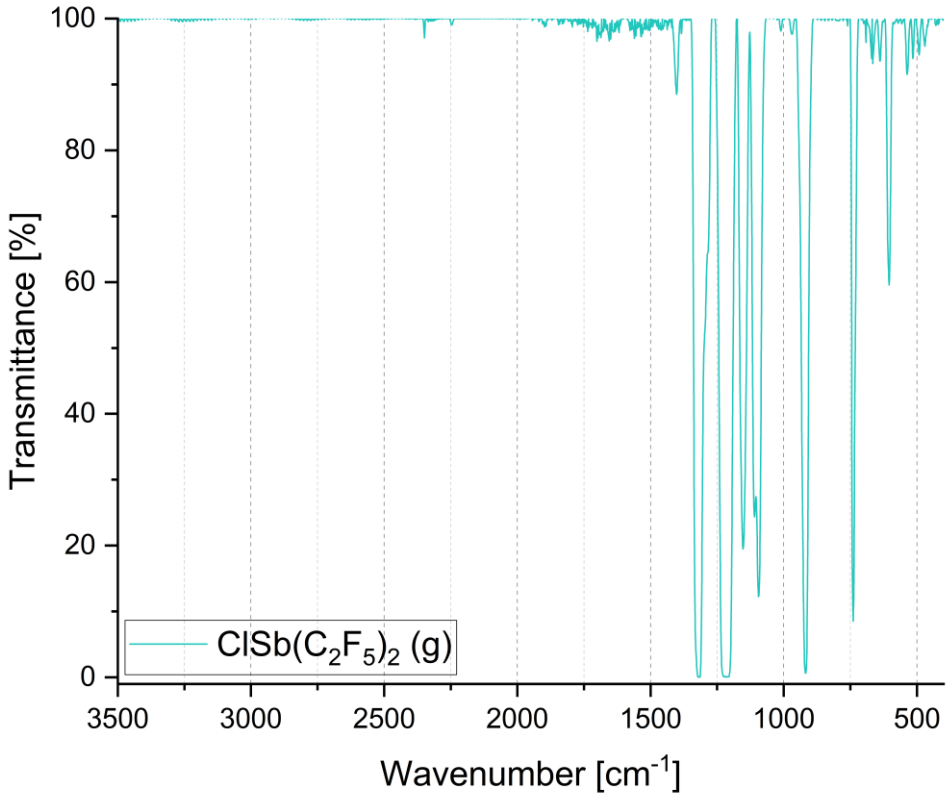

Figure S70 IR spectrum of gaseous $ClSb(C_2F_5)_2$ (**3**).

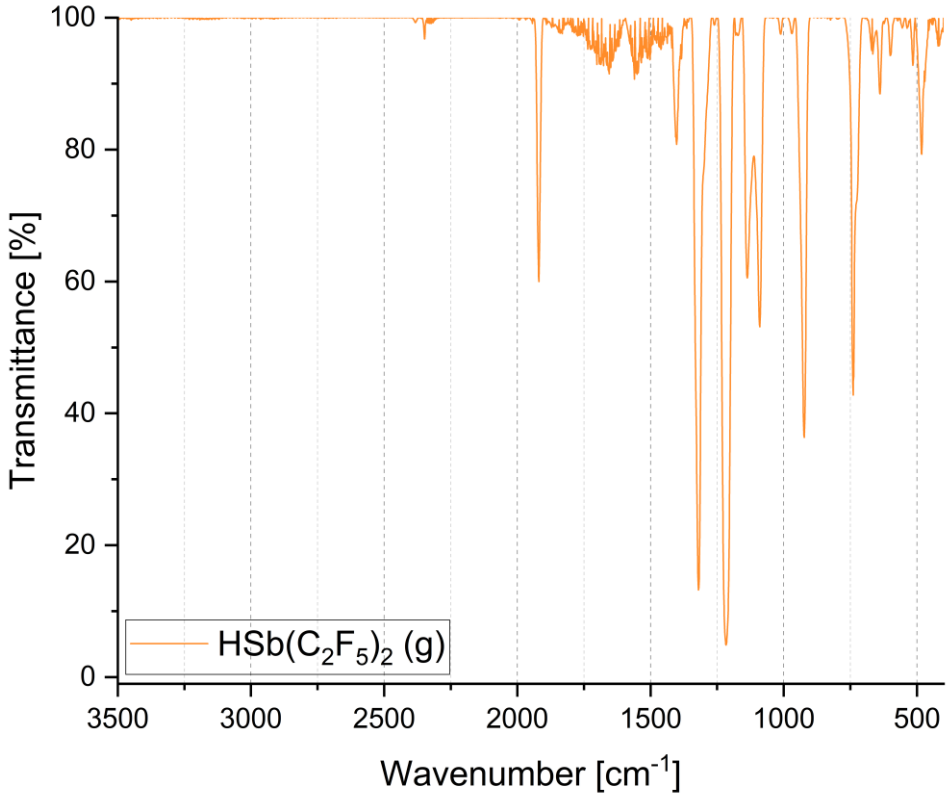

Figure S71 IR spectrum of gaseous $HSb(C_2F_5)_2$ (**10**).

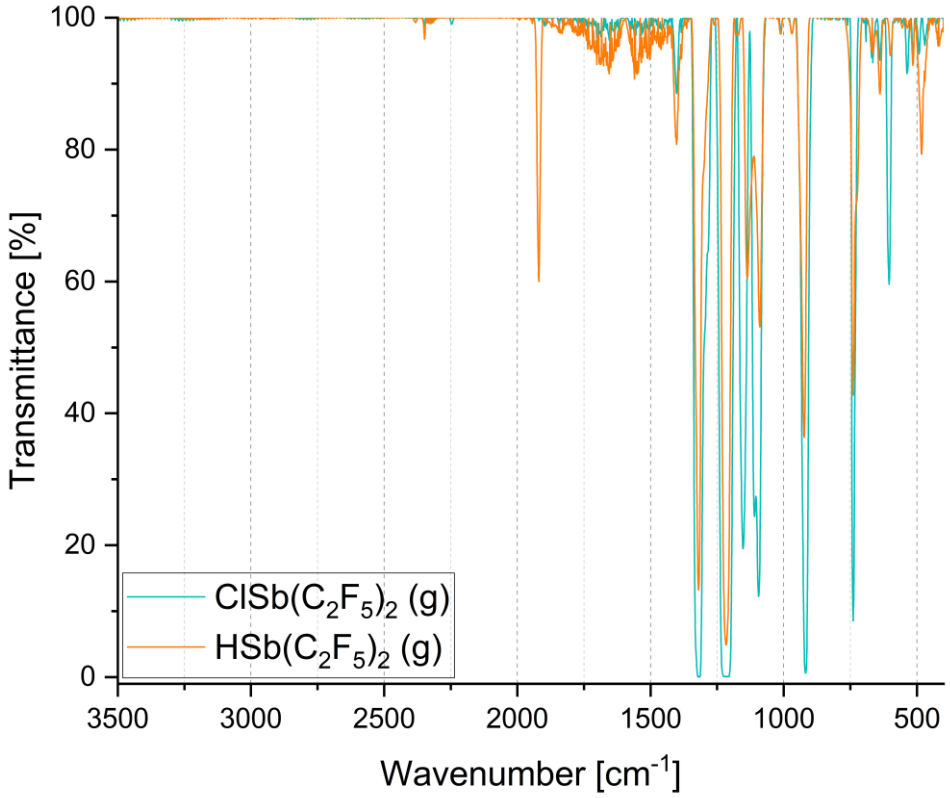

Figure S72 Overlaid IR spectra of gaseous $ClSb(C_2F_5)_2$ (**3**) and gaseous $HSb(C_2F_5)_2$ (**10**).

Crystallographic Data

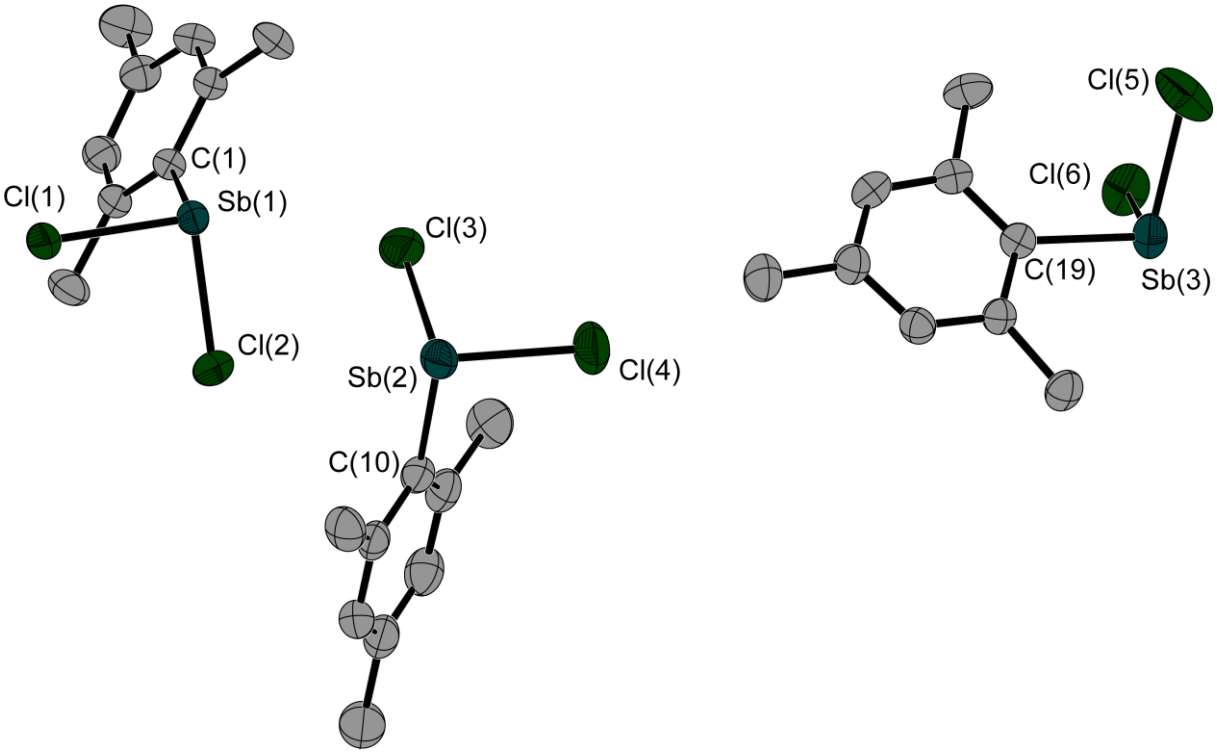

Figure S73 Molecular structure of compound **1** in the solid state with three molecules in the asymmetric unit. Ellipsoids are set at 50 % probability. The hydrogen atoms are omitted for clarity. Selected bond lengths [Å]and angles [°]: Sb(1)–Cl(1) 2.395(1), Sb(1)–Cl(2) 2.381(1), Sb(1)–C(1) 2.150(2), Sb(2)–Cl(3) 2.387(1), Sb(2)–Cl(4) 2.376(1), Sb(2)–C(10) 2.134(3), Sb(3)–Cl(5) 2.381(1), Sb(3)–Cl(6) 2.377(1), Sb(3)–C(19) 2.143(2); Cl(1)–Sb(1)–Cl(2) 92.0(1), Cl(1)–Sb(1)–C(1) 97.5(1), Cl(2)–Sb(1)–C(1) 101.4(1), Cl(3)–Sb(2)–Cl(4) 94.5(1), Cl(3)–Sb(2)–C(10) 101.6(1), Cl(4)–Sb(2)–C(10) 97.0(1), Cl(5)–Sb(3)–Cl(6) 95.3(1), Cl(5)–Sb(3)–C(19) 96.9(1), Cl(6)–Sb(3)–C(19) 100.4(1).

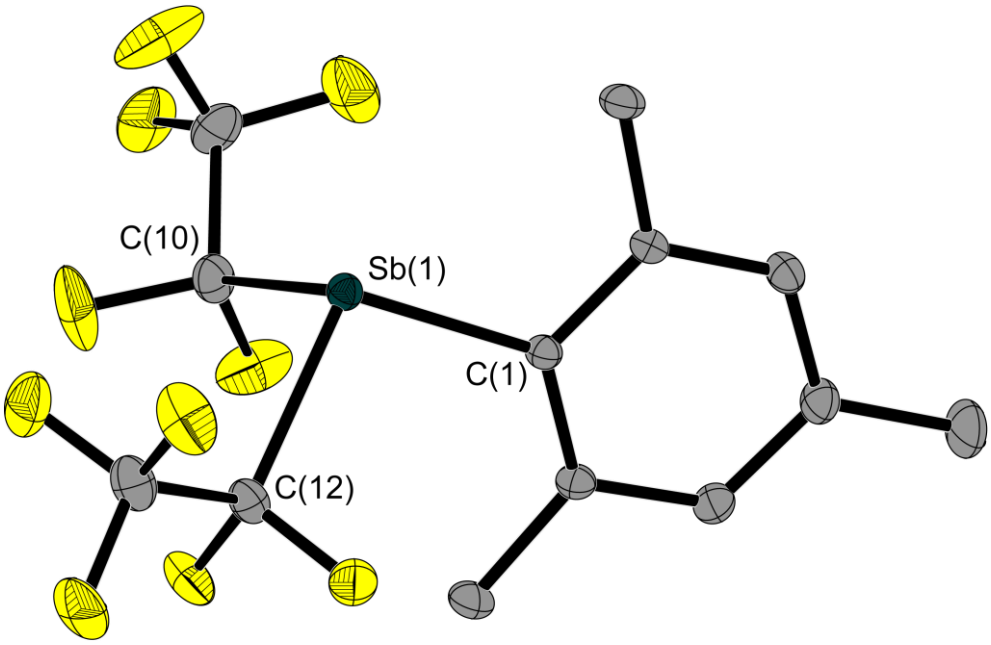

Figure S74 Molecular structure of compound **2** in the solid state. Ellipsoids are set at 50 % probability. The hydrogen atoms are omitted for clarity. Selected bond lengths [Å] and angles [°]: Sb(1)–C(1) 2.152(1), Sb(1)–C(10) 2.240(1), Sb(1)–C(12) 2.246(1); C(1)–Sb(1)–C(10) 98.3(1), C(1)–Sb(1)–C(12) 103.1(1), C(10)–Sb(1)–C(12) 92.7(1).

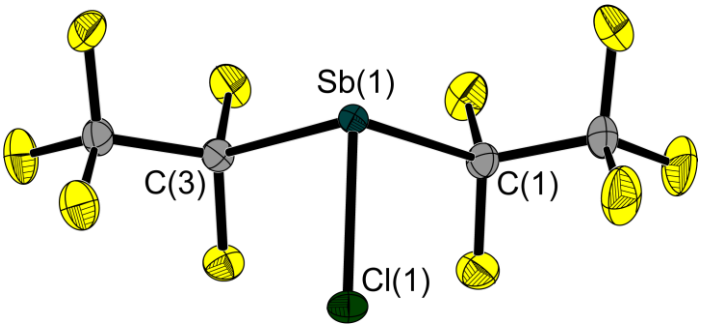

Figure S75 Molecular structure of compound **3** in the solid state. Ellipsoids are set at 50 % probability. Selected bond lengths [Å] and angles [°]: Sb(1)–Cl(1) 2.356(1), Sb(1)–C(1) 2.252(1), Sb(1)–C(3) 2.243(1); C(1)–Sb(1)–Cl(1) 92.8(1), C(3)–Sb(1)–Cl(1) 91.2(1), C(1)–Sb(1)–C(3) 88.5(1).

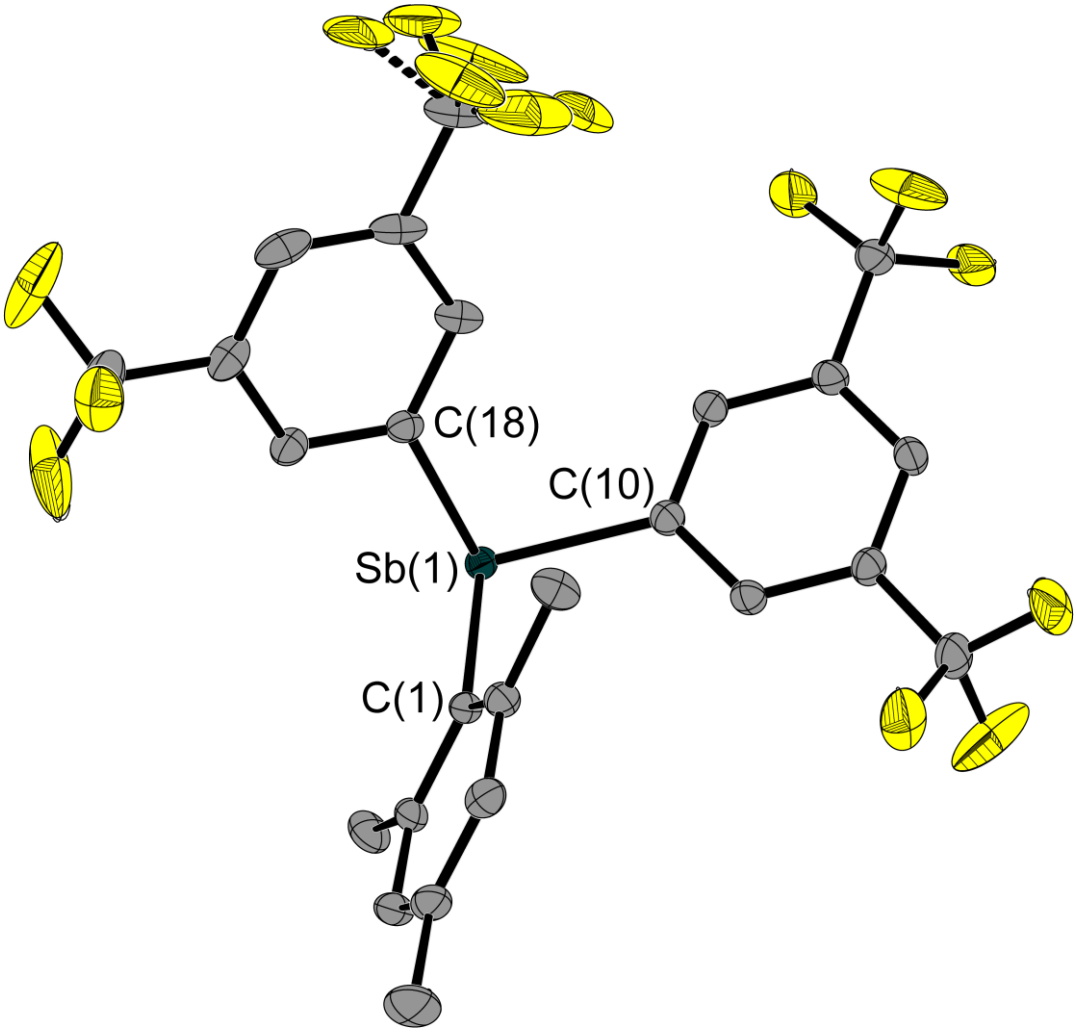

Figure S78 Molecular structure of compound **4** in the solid state. Ellipsoids are set at 50 % probability; hydrogen atoms are omitted for clarity. One trifluoromethyl group [C(25), F(10–12)] is disordered over two sites; ratio 66:34. Selected bond lengths [Å] and angles [°]: Sb(1)–C(1) 2.160(2), Sb(1)–C(10) 2.162(2), Sb(1)–C(18) 2.167(2); C(1)–Sb(1)–C(10) 99.4(1), C(1)–Sb(1)–Cl(18) 96.1(1), C(10)–Sb(1)–C(18) 97.7(1).

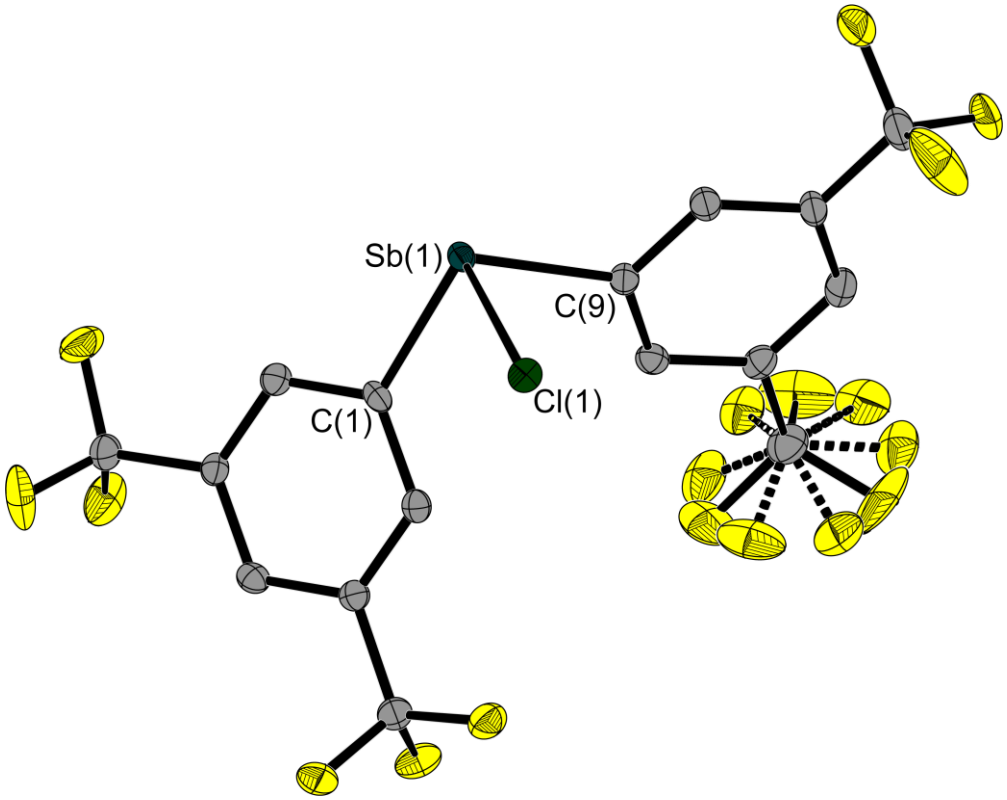

Figure S79 Molecular structure of compound **5** in the solid state. Ellipsoids are set at 50 % probability; hydrogen atoms are omitted for clarity. Disorder of one CF_3-group over three sites (0.613:0.214:0.173). Selected bond lengths [Å] and angles [°]: Sb(1)–Cl(1) 2.504(1), Sb(1)–C(1) 2.151(3), Sb(1)–C(9) 2.152(3); C(1)–Sb(1)–Cl(1) 91.0(1), C(9)–Sb(1)–Cl(1) 87.8(1), C(1)–Sb(1)–C(9) 99.3(1).

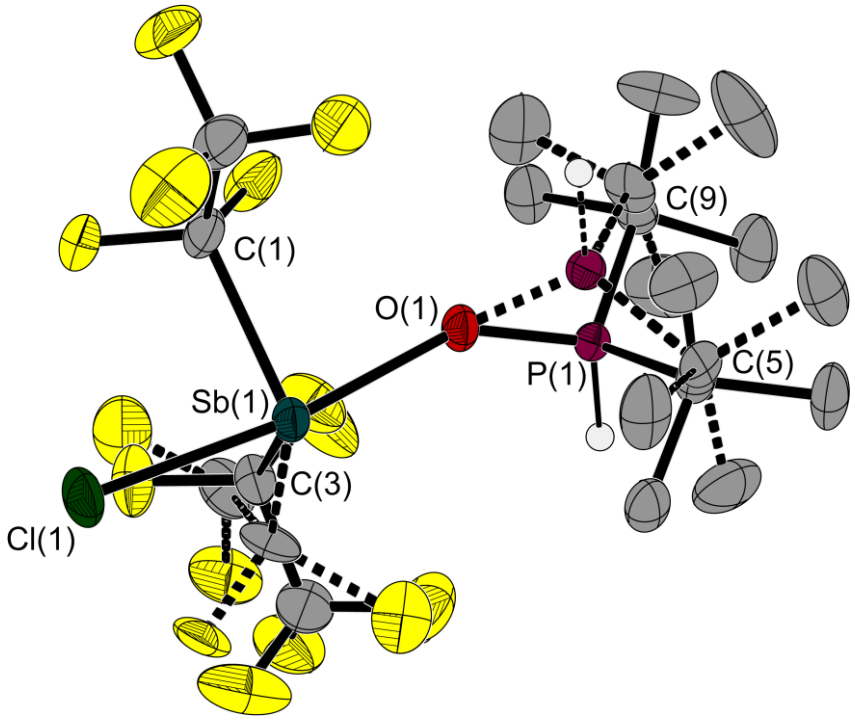

Figure S76 Molecular structure of compound **6** in the solid state. Ellipsoids are set at 30 % probability; most of the hydrogen atoms are omitted for clarity. Disorder with ratio 85:15 of the (tBu)$_2$P(H)–O– and one C_2F_5-group. Selected bond lengths [Å] and angles [°]: Sb(1)–Cl(1) 2.470(1), Sb(1)–O(1) 2.273(2), Sb(1)–C(1) 2.267(3), Sb(1)–C(3) 2.285(4), P(1)–O(1) 1.503(2), P(1)–C(5) 1.821(1), P(1)–C(9) 1.817(1); O(1)–Sb(1)–Cl(1) 167.9(1), O(1)–Sb(1)–C(1) 81.8(1), O(1)–Sb(1)–C(3) 82.2(1), C(1)–Sb(1)–Cl(1) 89.0(1), C(1)–Sb(1)–C(3) 88.6(1), C(3)–Sb(1)–Cl(1) 89.8(1), O(1)–P(1)–C(5) 110.8(3), O(1)–P(1)–C(9) 111.0(3), C(5)–P(1)–C(9) 117.4(4), Sb(1)–O(1)–P(1) 147.5(1).

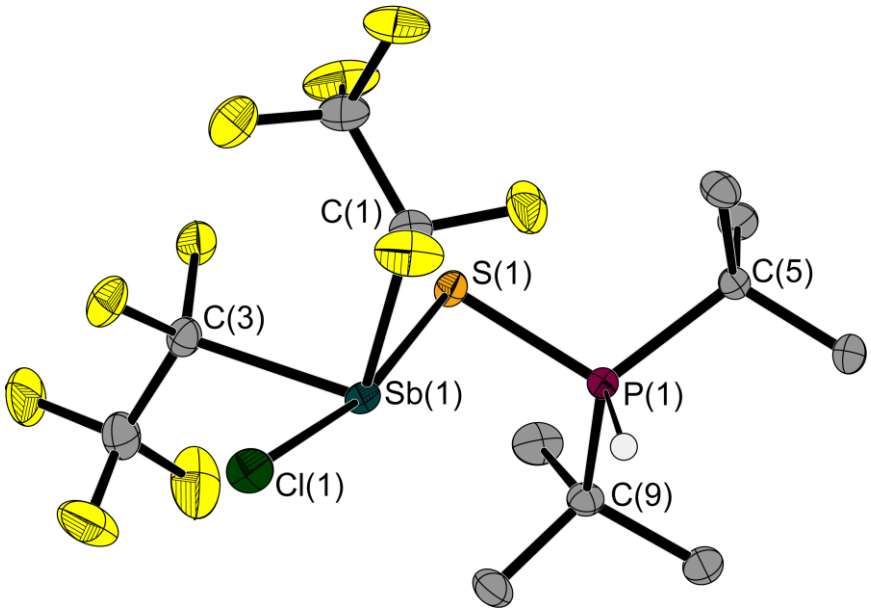

Figure S77 Molecular structure of compound **7** in the solid state. Ellipsoids are set at 50 % probability; most of the hydrogen atoms are omitted for clarity. Selected bond lengths [Å] and angles [°]: Sb(1)–Cl(1) 2.486(1), Sb(1)–S(1) 2.751(1), Sb(1)–C(1) 2.260(1), Sb(1)–C(3) 2.267(1), P(1)–S(1) 2.010(1), P(1)–C(5) 1.852(1), P(1)–C(9) 1.852(1); Cl(1)–Sb(1)–S(1) 169.1(1), C(1)–Sb(1)–Cl(1) 89.6(1), C(1)–Sb(1)–S(1) 87.9(1), C(1)–Sb(1)–C(3) 98.5(1), C(3)–Sb(1)–Cl(1) 86.8(1), C(3)–Sb(1)–S(1) 83.2(1), C(5)–P(1)–S(1) 111.1(1), C(5)–P(1)–C(9) 117.7(1), C(9)–P(1)–S(1) 110.2(1), Sb(1)–S(1)–P(1) 98.5(1).

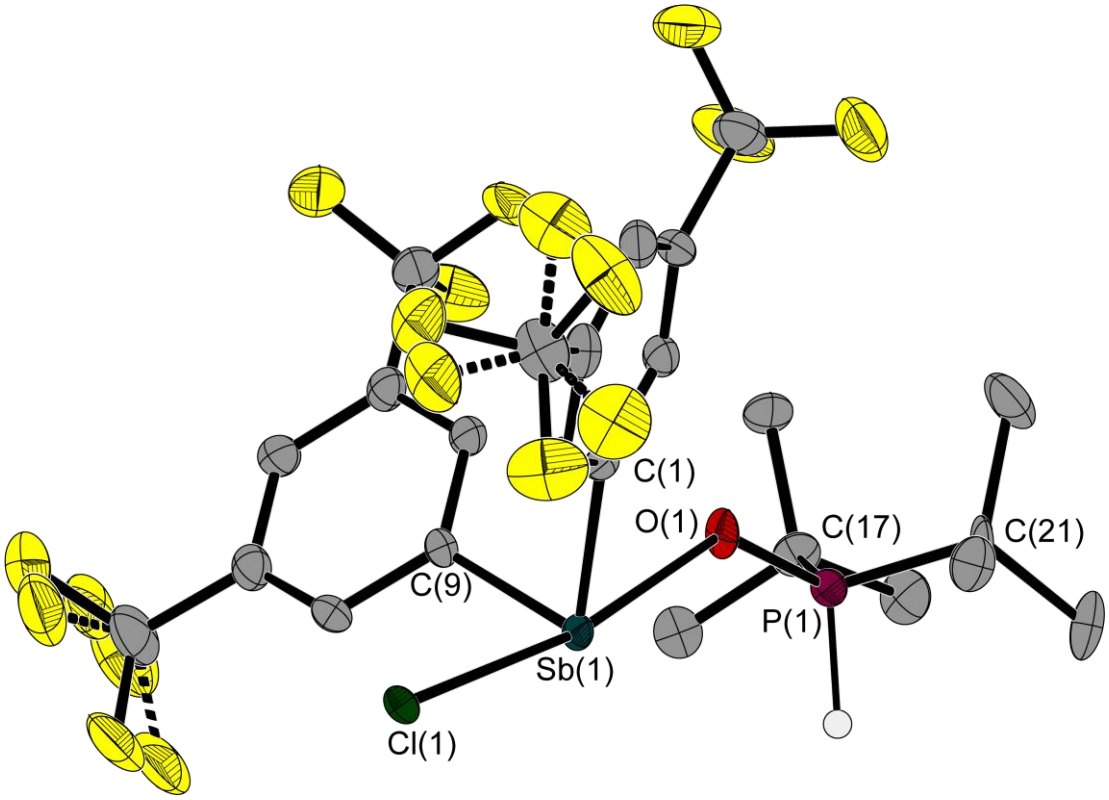

Figure S80 Molecular structure of compound **8** in the solid state. Ellipsoids are set at 50 % probability; most of the hydrogen atoms are omitted for clarity. Disorder of two CF_3-groups over two sites in ratio 74:26 and 79:21. Selected bond lengths [Å] and angles [°]: Sb(1)–Cl(1) 2.505(2), Sb(1)–O(1) 2.348(5), Sb(1)–C(1) 2.168(9), Sb(1)–C(9) 2.183(9), P(1)–O(1) 1.525(6), P(1)–C(17) 1.833(9), P(1)–C(21) 1.828(9); Cl(1)–Sb(1)–O(1) 170.4(2), C(1)–Sb(1)–Cl(1) 90.8(2), C(1)–Sb(1)–O(1) 84.0(3), C(1)–Sb(1)–C(9) 95.0(3), C(9)–Sb(1)–Cl(1) 90.1(2), C(9)–Sb(1)–O(1) 82.3(3), C(17)–P(1)–O(1) 108.6(4), C(17)–P(1)–C(21) 118.4(4), C(21)–P(1)–O(1) 110.5(4), Sb(1)–O(1)–P(1) 131.0(4).

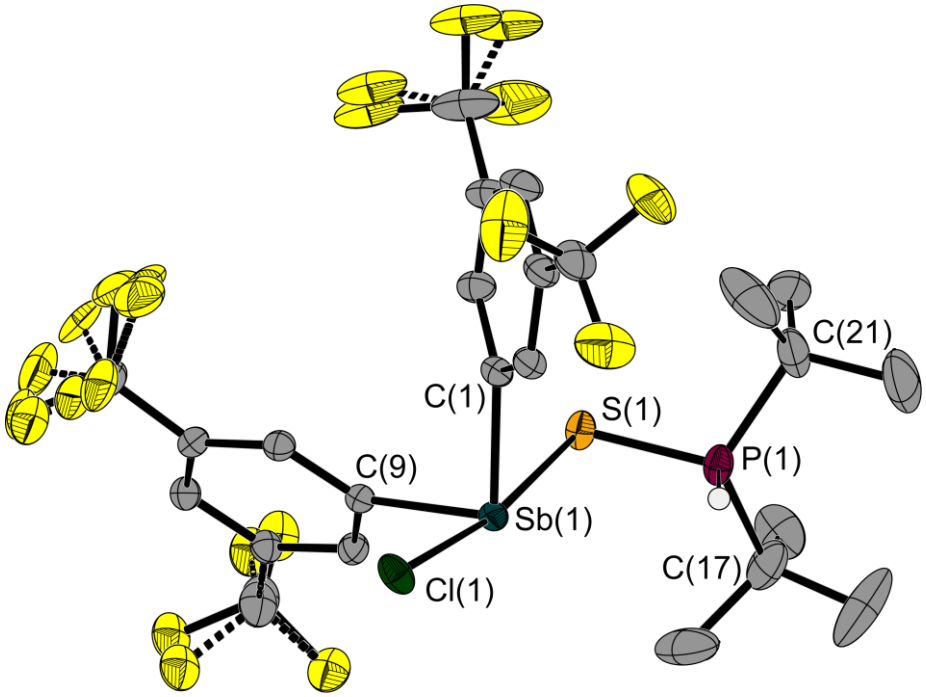

Figure S81 Molecular structure of compound **9** in the solid state. Ellipsoids are set at 50 % probability; most of the hydrogen atoms are omitted for clarity. Disorder of F(4) and F(5) over two sites in ratio 63:37, of F(7) to F(9) over three sites in ratio 68:20:12, and of C(16), F(11), and F(12) over two sites in ratio 73:27. Selected bond lengths [Å] and angles [°]: Sb(1)–Cl(1) 2.520(1), Sb(1)–S(1) 2.829(1), Sb(1)–C(1) 2.157(2), Sb(1)–C(9) 2.147(2), P(1)–S(1) 1.995(1), P(1)–C(17) 1.852(3), P(1)–C(21) 1.841(3); Cl(1)–Sb(1)–S(1) 171.4(1), C(1)–Sb(1)–Cl(1) 88.2(1), C(1)–Sb(1)–S(1) 87.0(1), C(1)–Sb(1)–C(9) 97.4(1), C(9)–Sb(1)–Cl(1) 90.4(1), C(9)–Sb(1)–S(1) 83.3(1), C(17)–P(1)–S(1) 111.3(1), C(17)–P(1)–C(21) 117.7(1), C(21)–P(1)–S(1) 110.8(1), Sb(1)–S(1)–P(1) 95.2(1).

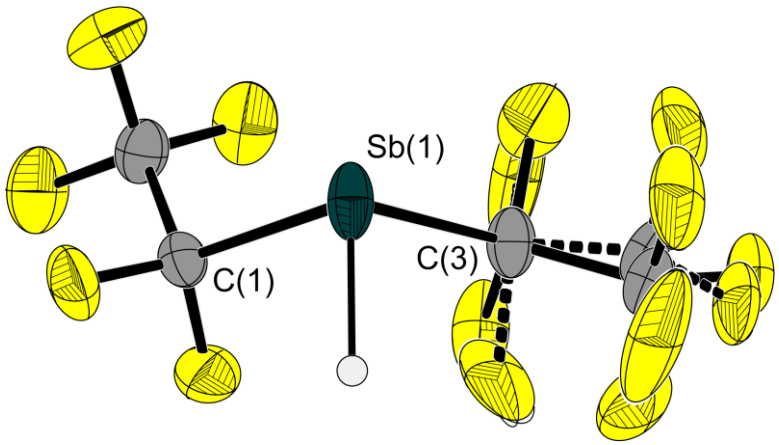

Figure S82 Molecular structure of compound **10** in the solid state. Ellipsoids are set at 50 % probability. One pentafluoroethyl group is disordered over two sites; ratio 72:28. Selected bond lengths [Å] and angles [°]: Sb(1)–C(1) 2.219(1), Sb(1)–C(3) 2.214(1); C(1)–Sb(1)–C(3) 94.4(1).

X-ray Diffraction Studies

Single crystals were examined on a Rigaku Supernova diffractometer. Using Olex2,[11] the structures of **1** and **4–9** were solved with the ShelXT[12] structure solution program using Intrinsic Phasing and were refined with ShelXL[13] refinement package using Least Square minimisation.

The structures of **2** and **10** were solved with the ShelXT[12] structure solution program using Intrinsic Phasing and refined with the olex2.refine[14] refinement package using Gauss-Newton minimisation.

The structure of **3** was solved with the olex2.solve[14] structure solution program using Charge Flipping. **3** and **10** were refined with the olex2.refine[14] refinement package using Gauss-Newton minimisation and NoSpherA2,[15] an implementation of Non-Spherical Atom-form-factors in Olex2. 2021

The crystals obtained by recrystallisation of **1** in *n*-pentane/CH_2Cl_2 were suitable for X-ray diffraction experiments.

The crystal of **2** was grown in situ by freezing the liquid to 266.1 K, establishing a solid-liquid mixture, melting all solid material except one seed with a wire and cooling to 100 K at a rate of 50 K/h.

The crystal of **3** was grown in situ by freezing the liquid to 237 K, establishing a solid-liquid mixture, melting all solid material except one seed with a wire and cooling to 235 K at a rate of 1 K/h and to 100 K with a rate of 100 K/h.

Crystals of **4**, suitable for X-ray diffraction, were obtained due to sublimation.

Single crystals of **5** crystallised from the undercooled melt in the glass tube under ambient temperature.

Recrystallisation of **6**, **7** and **9** in *n*-hexane and **8** in cyclopentane led to single crystals suitable for diffraction experiments.

The crystal of **10** was grown in situ by freezing the liquid to 168.1 K, establishing a solid-liquid mixture, melting all solid material except one seed with a wire and cooling to 166.5 K at a rate of 1 K/h and to 140 K with 100 K/h.

CCDC 2367656-2367665 contain the supplementary crystallographic data for this paper. These data can be obtained free of charge from The Cambridge Crystallographic Data Centre via www.ccdc.cam.ac.uk/conts/retrieving.html.

	1	**2**[a]	**3**	**4**[b]
Empirical formula	$C_9H_{11}Cl_2Sb$	$C_{13}H_{11}F_{10}Sb$	$C_4ClF_{10}Sb$	$C_{25}H_{17}F_{12}Sb$
M_r	311.83	478.98	395.24	667.14
λ [Å]	0.71073	0.71073	0.71073	0.71073
T [K]	200.0(1)	100.0(1)	100.0(1)	100.0(1)
F(000) [e]	900.0	918.559	727.229	1304.0
Crystal system	triclinic	monoclinic	monoclinic	monoclinic
Space group	$P\bar{1}$	$P2_1/n$	$P2_1/c$	$P2_1/c$
a [Å]	8.3946(2)	8.8214(1)	9.9004(2)	17.0987(4)
b [Å]	12.6338(3)	15.6118(2)	10.4822(1)	16.0064(3)
c [Å]	16.1582(5)	11.6490(1)	9.7501(2)	9.2650(2)
α [°]	103.911(2)	90	90	90
β [°]	90.528(2)	94.686(1)	106.183(2)	98.062(2)
γ [°]	93.576(2)	90	90	90
V [Å^3]	1659.65(8)	1598.91(3)	971.75(3)	2510.66(9)
Z	6	4	4	4
$\rho_{calcd.}$ [g cm^{-3}]	1.872	1.990	2.702	1.765
μ [mm^{-1}]	2.923	1.824	3.235	1.201
2Θ range [°]	6.55–69.856	6.58–90.58	7.92–84.38	6.586–69.984
Index ranges h	$-13 \le h \le 12$	$-22 \le h \le 22$	$-18 \le h \le 18$	$-27 \le h \le 26$
Index ranges k	$-19 \le k \le 19$	$-39 \le k \le 40$	$-19 \le k \le 19$	$-24 \le k \le 25$
Index ranges l	$-25 \le l \le 25$	$-29 \le l \le 29$	$-17 \le l \le 18$	$-14 \le l \le 14$
Reflexes collected	55276	182602	99888	77775
Independent reflexes	13754	13368	6841	10677
R_{int}	0.0397	0.0471	0.0387	0.0433
Observed reflexes, $I > 2\sigma(I)$	9642	12391	6474	8897
Data/restrains/ parameters	13754/0/335	13368/0/262	6841/0/146	10677/111/422
R_1/wR_2 [$I > 2\sigma(I)$]	0.0348/0.0668	0.0223/0.0555	0.0185/0.0395	0.0316/0.0672
R_1/wR_2 (all data)	0.0621/0.0784	0.0250/0.0572	0.0201/0.0402	0.0440/0.0729
GoF on F^2	1.030	1.054	1.029	1.044
ρ_{max}/ρ_{min} [e Å^{-3}]	1.38/−1.63	1.00/−0.77	0.88/−0.93	1.28/−0.70
CCDC number	2367656	2367657	2367658	2367661

[a] Hydrogen atoms were refined isotropically. [b] Rotational disorder of one trifluoromethyl group [C(25), F(10–12)] over two sites; ratio 66:34.

	5[c]	**6**[d]	**7**[e]
Empirical formula	$C_{16}H_6ClF_{12}Sb$	$C_{12}H_{19}ClF_{10}OPSb$	$C_{12}H_{19}ClF_{10}PSSb$
M_r	583.41	557.44	573.50
λ [Å]	0.71073	0.71073	0.71073
T [K]	100.0(1)	173.0(1)	173(1)
F(000) [e]	1112.0	1088.0	560.0
Crystal system	orthorhombic	monoclinic	triclinic
Space group	$Pna2_1$	$P2_1/n$	$P\bar{1}$
a [Å]	8.74910(10)	7.7947(3)	8.86178(13)
b [Å]	8.52600(10)	17.4038(7)	10.95308(16)
c [Å]	24.6722(3)	15.4407(6)	11.95144(13)
α [°]	90	90	105.3756(11)
β [°]	90	97.791(4)	102.9282(21)
γ [°]	90	90	108.4462(13)
V [Å^3]	1840.42(4)	2075.31(14)	999.25(3)
Z	4	4	2
$\rho_{calcd.}$ [g cm^{-3}]	2.106	1.784	1.906
μ [mm^{-1}]	1.761	1.620	1.782
2Θ range [°]	3.302–64.29	6.65–60.068	5.146–73.886
Index ranges h	$-12 \le h \le 12$	$-10 \le h \le 10$	$-14 \le h \le 14$
Index ranges k	$-12 \le k \le 12$	$-24 \le k \le 24$	$-18 \le k \le 18$
Index ranges l	$-35 \le l \le 36$	$-21 \le l \le 21$	$-20 \le l \le 19$
Reflexes collected	103347	52993	91566
Independent reflexes	6225	6055	9773
R_{int}	0.0413	0.0468	0.0420
Observed reflexes, $I > 2\sigma(I)$	5800	4754	8844
Data/restrains/ parameters	6225/56/328	6055/689/397	9773/0/245
R_1/wR_2 [$I > 2\sigma(I)$]	0.0211/0.0428	0.0328/0.0711	0.0229/0.0477
R_1/wR_2 (all data)	0.0248/0.0441	0.0488/0.0809	0.0287/0.0500
GoF on F^2	1.087	1.058	1.062
ρ_{max}/ρ_{min} [e Å^{-3}]	0.92/−0.43	0.93/−0.59	0.79/−0.70
Flack parameter	−0.033(6)		
CCDC number	2367662	2367659	2367660

[c] Disorder of one CF_3-group over three sites (0.613:0.214:0.173). [d] Disorder with ratio 85:15 of the (tBu)$_2$P(H)–O– and one C_2F_5-group. Suitable constraints and restraints were applied. [e] H(1) was refined isotropically.

	8[f]	**9**[g]	**10**[h]
Empirical formula	$C_{24}H_{25}ClF_{12}OPSb$	$C_{24}H_{25}ClF_{12}PSSb$	$C_4HF_{10}Sb$
M_r	745.61	761.67	360.80
λ [Å]	0.71073	0.71073	0.71073
T [K]	100.0(1)	100.0(1)	140.0(1)
F(000) [e]	1472.0	1504.0	662.629
Crystal system	monoclinic	monoclinic	monoclinic
Space group	$P2_1/c$	$P2_1/n$	$P2_1/n$
a [Å]	21.3245(12)	12.351(4)	6.5071(3)
b [Å]	14.4630(6)	20.7885(15)	14.7672(5)
c [Å]	9.6209(4)	13.006(3)	9.8826(5)
α [°]	90	90	90
β [°]	101.045(5)	113.50(3)	106.470(5)
γ [°]	90	90	90
V [Å^3]	2912.3(2)	3062.6(14)	910.67(7)
Z	4	4	4
$\rho_{calcd.}$ [g cm^{-3}]	1.701	1.652	2.632
μ [mm^{-1}]	1.188	1.195	3.154
2Θ range [°]	5.152–54.97	5.32–73.98	6.72–75.62
Index ranges h	$-27 \le h \le 27$	$-20 \le h \le 20$	$-10 \le h \le 10$
Index ranges k	$0 \le k \le 18$	$-34 \le k \le 34$	$-25 \le k \le 25$
Index ranges l	$0 \le l \le 12$	$-21 \le l \le 21$	$-16 \le l \le 16$
Reflexes collected	40116	166717	35367
Independent reflexes	6677	15080	4738
R_{int}	0.0971	0.0520	0.0373
Observed reflexes, $I > 2\sigma(I)$	5581	12352	4095
Data/restrains/ parameters	6677/216/428	15080/473/469	4738/0/221
R_1/wR_2 [$I > 2\sigma(I)$]	0.0853/0.1848	0.0398/0.0833	0.0227/0.0459
R_1/wR_2 (all data)	0.0998/0.1924	0.0549/0.0893	0.0285/0.0485
GoF on F^2	1.124	1.132	1.066
ρ_{max}/ρ_{min} [e Å^{-3}]	3.14/−2.38	0.89/−0.74	0.62/−0.40
CCDC number	2367663	2367664	2367665

[f] Twinned crystal, BASF 0.108(2), Matrix: −0.998 0 −0.874 0 −1 0 −0.0050 0.998. Disorder of two CF_3-groups over two sites in ratio 74:26 and 79:21. H(1) was refined isotropically; [g] Disorder of F(4) and F(5) over two sites in ratio 63:37, of F(7) to F(9) over three sites in ratio 68:20:12, and of C(16), F(11), and F(12) over two sites in ratio 73:27. Suitable constraints and restraints were applied. [h] The hydrogen atom was refined isotropically, the thermal motion of Sb1 anisotropically. One C_2F_5 group is disordered with ratio 72:28.

References

1 M. Ates, J. H. Breunig, A. Soltani-Neshan and M. Tegeler, *Z. Naturforsch.*, 1986, **41b**, 321–326.

2 K. A. Smoll, W. Kaminsky and K. I. Goldberg, Organometallics, 2017, 36, 1213; L. Wickemeyer, N. Aders, A.Mix, B. Neumann, H.-G. Stammler, J. J. Cabrera-Trujillo, I. Fernández and N. W. Mitzel, *Chem. Sci.*, 2022, **13**,8088.

3 J. L. Beckmann, J. Krieft, Y. V. Vishnevskiy, B. Neumann, H.-G. Stammler and N. W. Mitzel, *Angew. Chem. Int. Ed.*, 2023, **62**, e202310439

4 (a) R. Mills, *J. Phys. Chem.*, 1973, **77**, 685; (b) W. S. Price, H. Ide and Y. Arata, *J. Phys. Chem. A*, 1999, **103**, 448.

5 A. Macchioni, G. C. Zuccaccia and D. Zuccaccia, *Chem. Soc. Rev.*, 2008, **37**, 479.

6 H.-C. Chen and S.-H. Chen, *J. Phys Chem.* 1984, **88**, 5118.

7 Y. H. Zhao, M. H. Abraham and A. M. Zissimos, *J. Org. Chem.*, 2003, **68**, 7368.

8 S. Alvarez, *Dalton Trans.*,2013, **42**, 8617-8636.

9 http://ddbonline.ddbst.com/DDBSearch/onlineddboverview.exe?submit=Details&systemcomplist=31

10 M. A. Beckett, G. C. Strickland, J. R. Holland and K. S. Varma, *Polymer*, 1996, **37**, 4629–4631; b) U. Mayer, V. Gutmann and W. Gerger, *Monatsh. Chem.*, 1975, **106**, 1235–1257.

11 O. V. Dolomanov, L. J. Bourhis, R. J. Gildea, J. A. K. Howard and H. Puschmann, *J. Appl. Crystallogr.*, 2009, **42**, 339–341.

12 G. M. Sheldrick, *Acta Crystallogr.*, *Sect. A*, 2015, **71**, 3–8.

13 G. M. Sheldrick, *Acta Crystallogr.*, *Sect. C*, 2015, **71**, 3–8

14 L. J. Bourhis, O. V. Dolomanov, R. J. Gildea, J. A. K. Howard and H. Puschmann, *Acta Crystallogr*., 2015, **A71**, 59–75.

15 F. Kleemiss, O. V. Dolomanov, M. Bodensteiner, N. Peyerimhoff, M. Midgley, L. J. Bourhis, A. Genoni, L. A. Malaspina, D. Jayatilaka, J. L. Spencer, F. White, B. Grundkötter-Stock, S. Steinhauer, D. Lentz, H. Puschmann and S. Grabowsky, *Chem. Sci.*, 2021, **12**, 1675–1692.